



Universitetet  
i Stavanger

FACULTY OF SCIENCE AND TECHNOLOGY

## MASTER'S THESIS

Study programme/specialisation:  Petroleum Engineering / Drilling and Well Technology	Spring semester, 2019  Open/ <del>Confidential</del>
Author: <i>Karoline Nyhus</i>	..... (signature of author)
Supervisor(s): <i>Kjell Kåre Fjelde</i>	
Title of master's thesis: <i>A comparison of working stress design and reliability based casing design</i>	
Credits (ECTS): 30	
Keywords: Reliability based casing design Working stress design Casing design Collapse Burst Monte Carlo Simulations	Number of pages: 61  + supplemental material/other: 28 Stavanger,  June 15 <sup>th</sup> , 2019

Title page for Master's Thesis  
Faculty of Science and Technology

## Acknowledgment

This thesis has been written in order to finish my master degree in Well Engineering at the University of Stavanger.

After finishing this thesis, I would like thank my faculty supervisor Kjell Kåre Fjelde for all the support and feedback he has provided. He has been a motivator and helped me understand the topic better and pushed me in the right direction.

I would also thank my friends and family for the support during this semester. Even though all of us have been busy with our own assignments, everyone have contributed to a cheerful work environment.

Karoline Nyhus

June 2019

## Abstract

Working stress design is the most common design method used on the Norwegian continental shelf and its simplicity makes it easy to understand. However, other methods as the reliability based design gives a different view on the casing design and gets more attractive as the wells that are being drilled are getting more complex. Reliability based design gives the opportunity to quantify the risk of the design and one of the outputs from this method is the probability of failure. This means that we get a number on how safe our design is and that makes it possible to do a risk assessment as well. Even though reliability based design is a more complex method and need more input data, compared to the working stress design, the results from the simulations are noticeable.

A casing grade selection was performed for a 13 3/8" intermediate section based on WSD and then on RBD. The loads considered are burst and collapse.

A comparison between the different burst models showed that the API model and the Klever-Stewart rupture limit model had the same spread of data and the API ad-hoc had the largest spread out of the models considered. Since the burst simulation take the rupture limits into account, the Klever-Stewart model was chosen as it seemed to be a the more suitable model for our purposes. Klever-Stewart is also the recommended rupture limit model according to API 5C3 as well.

RBD was performed with the use of Monte Carlo simulations in MATLAB. The simulations showed that RBD4 and RBD5, with Klever-Stewart rupture limit as the strength model, that a casing grade equal to N80 and K55 was sufficient to meet our requirements for a high consequence failure. On the other hand, WSD showed that a grade equal to P110 was necessary when considering the safety factor requirements from NORSOK D-010.

As for the collapse simulation, the API model was used as the strength model. RBD4 and RBD5 showed that K55 was sufficient to meet our target probability both for a low and high consequence failure. However the WSD showed that a grade equal to L80 was necessary to meet the NORSOK requirements regarding the safety factor.

The overall result was that the RBD method gave the opportunity to choose a lower casing grade than the WSD. However, the RBD method is more complex and needs more input data.

As RBD is based on the stochastic nature of the variables, distribution for each variable was taken into account. Parameters as mean and standard deviation for different input parameters like e.g. OD, thickness, yield and model error were found in the API 5C3, however some assumptions were made when data was not available. As for the load calculations, the worst case scenario was considered for the RBD4 and WSD, however subjective assumption was added for the RBD5.

The overall conclusion is that RBD4 allows you to choose a lower casing grade than WSD. RBD5 gives is less conservative than RBD4 and gives an even lower grade, however more relaxed assumptions were made for RBD5 where the uncertainty in the load was included.

# Table of Contents

<b>Acknowledgment</b> .....	<b>II</b>
<b>Abstract</b> .....	<b>III</b>
<b>List of figures</b> .....	<b>VI</b>
<b>List of Tables</b> .....	<b>VII</b>
<b>List of equations</b> .....	<b>VIII</b>
<b>Abbreviations</b> .....	<b>IX</b>
<b>Symbols</b> .....	<b>X</b>
<b>1 Introduction</b> .....	<b>1</b>
1.1 <i>Background</i> .....	2
1.2 <i>Problem definition and objective</i> .....	2
1.3 <i>Structure of thesis</i> .....	3
<b>2 Casing design</b> .....	<b>4</b>
2.1 <i>Loads</i> .....	8
2.1.1 <i>Burst</i> .....	9
2.1.2 <i>Collapse</i> .....	10
2.1.3 <i>Tension loads</i> .....	11
2.1.4 <i>Biaxial and triaxial loads</i> .....	11
2.2 <i>Load scenarios</i> .....	14
2.2.1 <i>Conductor casing</i> .....	14
2.2.2 <i>Surface casing</i> .....	14
2.2.3 <i>Intermediate casing</i> .....	14
2.2.4 <i>Production casing</i> .....	14
2.2.5 <i>Production liner</i> .....	15
2.3 <i>Survival loads and service loads</i> .....	15
2.4 <i>Well integrity</i> .....	16
<b>3 Design methods</b> .....	<b>21</b>
3.1 <i>Working stress design</i> .....	21
3.2 <i>Limit state design</i> .....	23
3.3 <i>Reliability based design</i> .....	23

3.3.1	Monte Carlo simulations .....	25
3.3.2	Basic Statistics .....	25
<b>4</b>	<b>Case study .....</b>	<b>30</b>
4.1	<i>Burst load</i> .....	31
4.1.1	Burst strength models .....	32
4.1.2	Reliability based design .....	37
4.1.3	Working stress design .....	46
4.2	<i>Collapse load</i> .....	47
4.2.1	Collapse models .....	48
4.2.2	Working stress design .....	50
4.2.3	Reliability based design, API .....	51
4.3	<i>Casing selection</i> .....	56
<b>5</b>	<b>Discussion and conclusion .....</b>	<b>58</b>
<b>6</b>	<b>Recommendation for future work .....</b>	<b>61</b>
	<b>References .....</b>	<b>62</b>
<b>A</b>	<b>Appendix .....</b>	<b>I</b>
<b>A.1</b>	<b>Monte Carlo Simulation MATLAB codes .....</b>	<b>I</b>
A.1.1	<i>Comparison of burst strength models</i> .....	<i>I</i>
A.1.2	<i>API ad-hoc burst level 4</i> .....	<i>III</i>
A.1.3	<i>API ad-hoc burst level 5</i> .....	<i>V</i>
A.1.4	<i>Klever-Stewart burst level 4</i> .....	<i>VII</i>
A.1.5	<i>Klever-Stewart burst level 5</i> .....	<i>IX</i>
A.1.6	<i>API collapse level 4</i> .....	<i>XI</i>
A.1.7	<i>API collapse level 5</i> .....	<i>XIV</i>
A.2	<i>Overview of parameters</i> .....	<i>XVII</i>

## List of figures

Figure 2.1 Example of a casing design .....	4
Figure 2.2 Example of a pore pressure plot .....	7
Figure 2.3 Stress-strain diagram.....	8
Figure 2.4 Picture of casing burst (Paslay, Cernocky, & Wink, 1998).....	9
Figure 2.5 Picture of casing collapse (Marx & El-Sayed, 1985) .....	10
Figure 2.6 Stress distribution (Belayneh, 2018).....	12
Figure 2.7 Ellipse of plasticity (Aadnøy, 2010) .....	13
Figure 2.8 Well barrier schematic, drilling (NORSOK, 2013) .....	16
Figure 2.9 Well barrier schematic, production/injection (NORSOK, 2013) .....	17
Figure 2.10 Well barrier schematic, drilling 12 1/4" section(Statoil, 2010).....	18
Figure 2.11 Well barrier schematics, drilling 6" reservoir section (Statoil, 2010) .....	19
Figure 2.12 Example of Bow-Tie diagram (Gouda & Aslam, 2018).....	20
Figure 3.1 Working stress design approach (Suryanarayana & Lewis, 2016).....	22
Figure 3.2 Flowchart, RBD4 design for a survival load (Suryanarayana & Lewis, 2016).....	24
Figure 3.3 Definition of median and P90 .....	26
Figure 3.4 Uniform distribution .....	27
Figure 3.5 Triangular distribution .....	27
Figure 3.6 Normal distribution.....	28
Figure 3.7 Lognormal distribution .....	29
Figure 4.1 Pressure gradient plot.....	30
Figure 4.2 Sketch of formation fluid filled casing .....	31
Figure 4.3 MATLAB plot of each model for the burst strength of the casing, P110.....	36
Figure 4.4 API Burst Scenario RBD4, N80 .....	40
Figure 4.5 API Burst RBD5, L80.....	41
Figure 4.6 Klever-Stewart Burst RBD4, N80 .....	43
Figure 4.7 Klever-Stewart Burst RBD5, K55 .....	45
Figure 4.8 Sketch of loss to thief zone scenario.....	47
Figure 4.9 Collapse pressure vs slenderness for a L-80 tubing (Bellarby, 2009) .....	48
Figure 4.10 API collapse, RBD4.....	54
Figure 4.11 API collapse, RBD5.....	55

## List of Tables

Table 2.1 Typical casing sizes.....	6
Table 4.1 Casing size, setting depth and mud weight for case study.....	31
Table 4.2 Values for n, Klever-Stewart model (API, 2018) .....	34
Table 4.3 Values used in MATLAB simulation .....	34
Table 4.4 Model uncertainty used in the simulations (API, 2018) .....	34
Table 4.5 Distribution parameters used for the burst simulations (API, 2018) .....	35
Table 4.6 Mean, standard deviation, median, P10 and P90 values for each model given in bar.....	37
Table 4.7 Overview of interval spread for strength models.....	37
Table 4.8 Parameters used for API ad-hoc burst simulation.....	38
Table 4.9 Results obtained from simulation, RBD4, N80 .....	39
Table 4.10 Results obtained from simulations RBD5, L80 .....	41
Table 4.11 Parameters used for Klever-Stewart burst simulations .....	42
Table 4.12 Results from RBD4 simulation, burst, N80 .....	43
Table 4.13 Results from RBD5 simulation, burst, K55 .....	44
Table 4.14 Parameters for collapse simulation .....	52
Table 4.15 Distribution parameters used for the collapse simulations (API, 2018) .....	53
Table 4.16 Model error for API collapse strength model (API, 2018) .....	53
Table 4.17 Results from RBD4 simulations, collapse, K55.....	54
Table 4.18 Results from RBD5 simulation, collapse, K55 .....	55
Table 4.19 Summary of casing selection .....	56
Table 5.1 Suggested target probabilities and corresponding safety factors .....	60

## List of equations

(2.1) .....	11
(2.2) .....	12
(2.3) .....	12
(2.4) .....	12
(3.1) .....	21
(3.2) .....	23
(3.3) .....	25
(3.4) .....	26
(3.5) .....	26
(3.6) .....	28
(4.1) .....	32
(4.2) .....	32
(4.3) .....	33
(4.4) .....	33
(4.5) .....	33
(4.6) .....	46
(4.7) .....	46
(4.8) .....	46
(4.9) .....	46
(4.10) .....	49
(4.11) .....	49
(4.12) .....	49
(4.13) .....	49
(4.14) .....	49
(4.15) .....	49
(4.16) .....	50
(4.17) .....	50
(4.18) .....	50



## Abbreviations

API – American Petroleum Institute

BHP – Bottom hole pressure

BOP – Blow out preventer

DDH – Drilling Data Handbook

HPHT – High Pressure High Temperature

ISO – International Organization for Standardization

Ksi – Kilopounds per square inch

LSD – Limit state design

NCS – Norwegian continental shelf

POOH – Pull out of hole

Psi – Pounds per square inch

RBD – Reliability based design

RBD4 – Reliability based design level 4

RBD5 – Reliability based design level5

RIH – Run in hole

s.g. – Specific Gravity

Tol – Wall thickness tolerance

UK – United Kingdom

WCS – Worst Case Scenario

WSD – Working stress design

## Symbols

$\beta$  - Buoyancy factor

$\rho$  - Density

$\mu$  - Expected value

$\sigma$  - Standard deviation

$\sigma_{\theta}$  - Hoop stress

$\sigma_a$  - Axial stress

$\sigma_b$  - Bending stress

$\sigma_r$  - Radial stress

$\sigma_y / \sigma_{yield}$  - Nominal yield strength

A - Cross-sectional area

a - Inner radius

b - Outer radius

cov - Covariance

D / OD - Outer diameter

$F_a$  - Axial force

$F_{ten}$  - Tension load

g - Gravity constant

$K_{dr}$  - Pipe deformation correction factor

n - Number of measurement

$P_a$  - Inner pressure

$P_b$  - Outer pressure

$P_{burst}$  - Burst pressure

$P_{collapse}$  - Collapse pressure

$P_e$  - Elastic collapse

$p_{external}$  - External pressure

$P_i$  - Inner pressure

$p_{internal}$  - Internal pressure

$P_o$  - Outer pressure

$P_p$  - Plastic collapse

$P_t$  - Transitional collapse

$P_y$  - Yield collapse

$\Delta P$  - Differential pressure

r - Radius

$r_i$  - Inner radius

$r_o$  - Outer radius

stdv - Standard deviation

t - Thickness

var - Variance

$x_i$  - Measurement i

$\bar{x}$  - Mean value

# 1 Introduction

As the petroleum industry is constantly looking for new solutions to increase production in an economical matter, the wells that are drilled are getting more and more challenging. One example is the increased activity in both the arctic areas as well as in deep waters. Hence, wells are becoming more and more complex and needs a new mindset when it comes to efficient and affordable designs.

Drilling wells are expensive, and according to Maes et al. (1997) tubular goods represents 16% of the drilling expenses. The expenses are so high, that small changes may result in huge savings. This means that a different casing grade, a change in the safety factor or similar is highly relevant when considering economics.

The traditional approach uses fixed limits when looking at the strength of the material and uses the worst case scenario loads. To be on the safe side of the design, safety factors are applied. These are set due to standards and other regulation in order to account for uncertainties in the assumptions and calculations. One of the biggest challenges regarding this approach is the variation of the safety factor. Companies often develop their own best practice for design which leads to the variation. At the Norwegian continental shelf, the NORSOK D-010 standard are used as reference, however the UK sector uses other standards and regulations. In other words, wells that might only be a few kilometres apart can be considered safe in one sector and not in the other even though they have the same design and are in the same environment.

As mentioned, wells are more complex than ever before. From an economical perspective, the question is whether if it's cheaper to challenge the design and accept a risk of failure or if the consequences of failure is to fatale to be accepted. A cheaper and less strong design may be accepted if the consequence of failure is failed equipment which is easy and cheap to repair or replace.

By the use of conservative methods as for example working stress design, quantification of the risk of failure is not considered. However, other methods as for example reliability based design calculates a probability of failure and thereby makes it easier to make a quantitative risk analysis (Suryanarayana & Lewis, 2016).

It is easier to uphold the safety factor when we are designing "simple" wells due to large margins. However, when looking at more complex wells, the margins we are working with are much smaller. In order to obtain a safe design with the working stress design method, some compromises on the safety factors might be made. To set this in another perspective; when using working stress design, the safest design is obtained in low risk, simple wells and compromises are often made when designing high risk, complex wells where it is even more important to obtain a safe design (Aadnøy et al., 2009).

As mentioned, an alternative to working stress design can be reliability based casing design. This method takes the stochastic nature of each variables into account and calculates a probability of failure (Suryanarayana & Lewis, 2016).

This thesis will provide a comparison of the working stress design method and the reliability based design method considering burst and collapse loads.

## 1.1 Background

The petroleum industry is constantly looking for cost saving options without compromising the safety. Reliability based design calculates a probability of failure based on multiple iterations and available data. The method also makes it possible to do a risk assessment of the design.

The background and motivation for this thesis is the increased interest in the reliability based design as a method for casing design. Further on, this thesis will compare the working stress design method and the reliability based design method.

## 1.2 Problem definition and objective

The goal for this thesis is to make a good comparison of the different methods. The main objectives of this thesis is as follows:

- What is the notable difference between the burst strength models in terms of statistical values?
- How is the choice of casing grade affected by the change of design method?
- How will the probability of failure change between level 4 and level 5 reliability based design?

For this thesis, the focus has been on the 13 3/8" intermediate casing section.

In order to determine a suitable choice of casing grade for this section, burst and collapse calculations have been performed. It is important to note that a proper casing design needs to take more factors into account as for example tension calculations, kick margin and so on. However this has not been taken into consideration in this thesis. Another limitation to note is that this thesis focuses on the casing string and do not consider the strength of the connection when determining a casing grade for the design.

The same casing thickness has been used for all simulation in order to get a better comparison of the different casing design methods. In other words, in order to choose the correct casing, it is only the grade that has been changed.

### 1.3 Structure of thesis

The thesis is built in such way that it should be easy to recreate the results obtained.

Chapter 2 includes theory around the thesis and it starts by introducing the basics behind casing design and the different loads a well might be subjected to. Further on, the thesis will give an overview of the load scenarios for the different casing strings with the main focus on collapse and burst loads. The theory also includes a description of the difference between survival and service loads and will also include the basics of well integrity.

As we continue with chapter 3, the different design methods are explained where the main focus is on working stress design, limit state design and reliability based design. Reliability based design is based on statistics, which is further explained together with presenting Monte Carlo simulations.

For chapter 4, the thesis will consider a constructed case study. A pressure gradient plot for a high pressure high temperature well is provided together with the assumed casing setting depths and other parameters so that the burst and collapse loads can be calculate with the focus on the intermediate casing section. Further on chapter 4 gives a comparison of different burst strength models and finds the most suitable model for our purposes. Using both reliability based design and working stress design, casing grades will be determined and the two methods will be compared. As mentioned, this thesis is only focusing on the collapse and burst scenarios. RBD4 and RBD5 will be performed for both burst and collapse.

The discussion and conclusion is provided in chapter 5.

After the discussion and conclusion, the last chapter of the thesis will provide some recommendations for future work. The Appendix provides all the MATLAB codes developed for the simulations as well as an overview of some collapse parameters and burst strength model error.

## 2 Casing design

After the reservoir has been discovered and the position of the well is determined the next step is to design and drill the well. Designing a well means determining the tubular size, tubular weight and the grade of the material used for the connections and the strings. It also involves determining where the different casings should be placed. In order to have a stable well, tubulars, also known as casings, are installed as a barrier element which will be further explained later.

The drilling process consists of three repeating steps:

- Drilling a hole
- Installing casing
- Cementing

As we get deeper into the well, the casing sizes decreases as the next casing is passing through the previous one similar to a telescope, as shown in the figure 2.1.

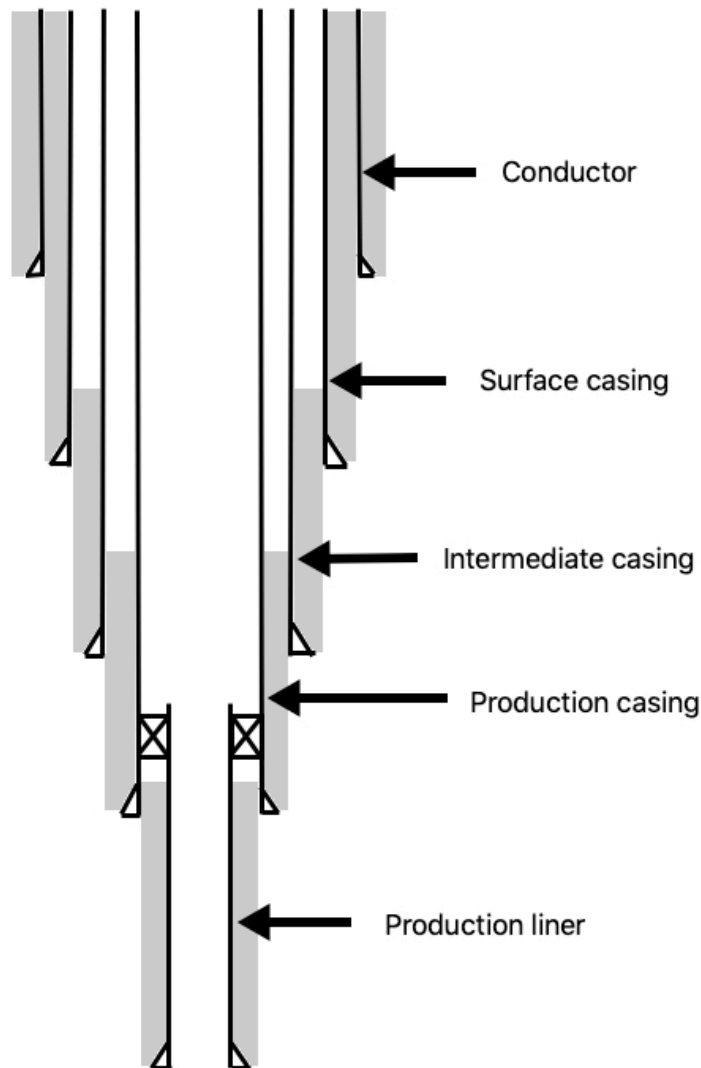


Figure 2.1 Example of a casing design

The different types of casings have different functionalities. The first casing, which is the largest, is called the conductor. The conductor's main functionalities are to isolate unconsolidated formation and to function as a support for other equipment, such as the riser, the wellhead and the surface casing. The conductor is cemented all the way to the seabed (Aadnøy, 2010).

The surface casing is the next casing to be installed. Similarly to the conductor, the surface casing isolates weak formations so that the next section can be drilled safely. This casing is cemented all the way to the seabed, similar to the conductor (Aadnøy, 2010). The wellhead is placed on top of the surface casing and all remaining casings will be hung off this as a foundation. In other words, the other casing strings will be hung off inside the wellhead.

After the surface casing is cemented in place, the intermediate casing is installed. This is set so that the next section can be drilled safely as well. The intermediate casing is required in the design due to pressurized, unstable or weak zones in the formation. When it comes to cementing, this casing is not necessarily cemented to the top, but two hundred meters above the last shoe (Aadnøy, 2010).

As we are getting closer to the reservoir zone, it's time to install the production casing. This casing will be a primary barrier element in the well during production, hence the importance of a proper design. This is often the last casing installed before we enter the reservoir and its main task is to isolate the pay zone. This casing must be able to withstand different types of wear as well as the effect from different chemicals. There are many chemicals that are being used during the lifetime of a well, for example to increase production or to perform intervention activities. Similar to the intermediate casing, the production casing is cemented two hundred meters above the shoe (Aadnøy, 2010).

The production liner is the tubular that is entering the reservoir. The difference between a liner and a casing is that a liner is hung off inside the previous casing that was installed and does not go all the way up to the wellhead as illustrated in figure 2.1. When considering load cases the production liner needs to be designed for full well integrity both during drilling and production while the other casing strings have the opportunity to be designed with reduced well integrity. Full well integrity means that the casing is able to withstand full reservoir pressure. However, the term reduced well integrity implies that the casing cannot withstand a well full of formation fluid when shut in. For the reduced well integrity case one must consider the minimum fracture gradient to reach the next casing setting depth. One must also ensure that the maximum allowable fracture gradient is sufficiently low to ensure that the weak point stays below the casing shoe. One must also determine the maximum allowable kick size which the well can handle without breaking down the formation below the shoe (Aadnøy, 2010).

If it's not possible to design the production liner for a full well integrity case, a tieback line is installed. A tieback line is a section of liners installed from the liner hang off and back to the wellhead. This needs to have the same requirements as the production liner. It may also be installed to increase corrosion resistance (Aadnøy, 2010).

There are variations of the sizes of the casings, but the most common sizes are shown in table 2.1

<b>Casing</b>	<b>Size</b>
Conductor casing	30"
Surface casing	20"
Intermediate casing	13 3/8"
Production casing	9 5/8"
Production liner	7"

*Table 2.1 Typical casing sizes*

The size and setting depth are depending on the well that is being drilled as well as the pore, collapse and fracture pressure. One must always remain within the pressure margin during both drilling and production so that we avoid unwanted situations. During drilling, equilibrium in the well are obtained by choosing the correct mud weight. If the mud weight is too high and exceeds the fracture pressure, one is in danger of fracturing and damaging the formations. On the other hand, if the mud weight is too low one might experience unexpected influx of formation fluids, also known as a kick, or one could experience a collapse situation. These scenarios are undesirable, but needs to be accounted for when doing the design. The casing setting depth are determined so that the shoe is placed at the depth where changes in mud weight are required. In that way, we are able to keep the well stable, avoid kicks and seal off the weaker formations above to avoid fracturing when changing the mud weight.

In order to determine the right mud weight and setting depth, a pressure gradient plot is provided. The pressure gradient plot is obtained from the geologist and it gives estimates for the fracture and pore pressure at the different depths. An example of a pressure gradient plot are shown in figure 2.2. A simple way of determining the mud weight is called the median line principle and is described by Aadnøy (2010). In simple terms, one chooses a mud weight that is in the middle between the pore pressure gradient and the fracture pressure gradient to always ensure a safe drilling environment.



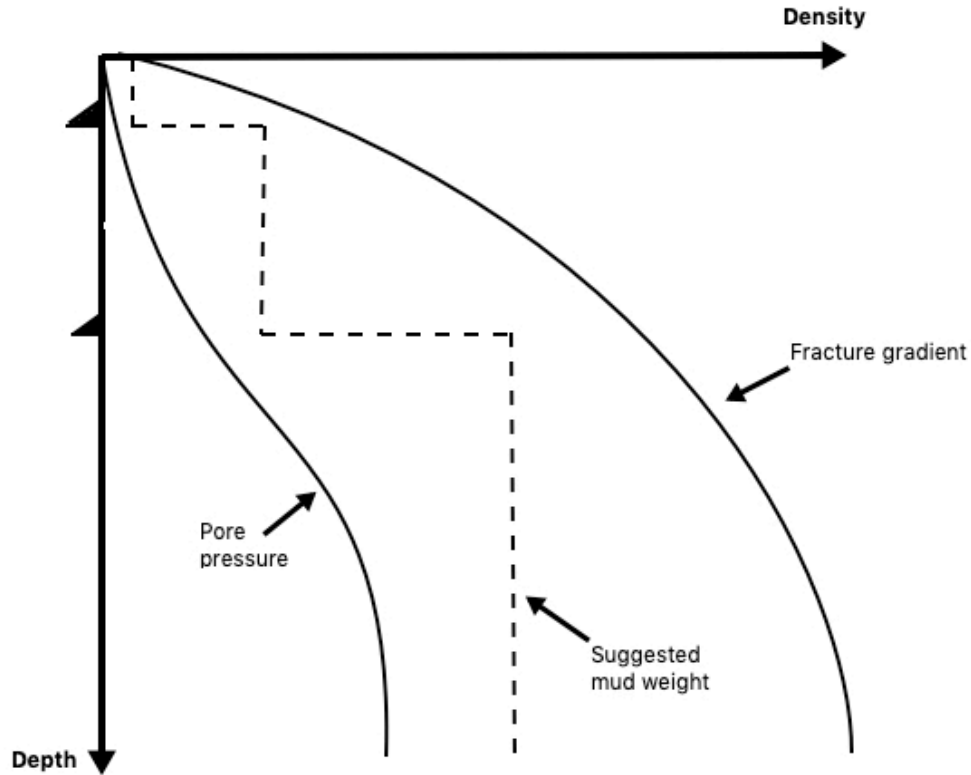


Figure 2.2 Example of a pore pressure plot

Casings are classified based on outer diameter, thickness of the tube and grade of the steel. According to 5CT API (2005), the casing grades are divided into four groups whereas the different groups contain the following

- Group 1: H, J, K and N grades
- Group 2: C, L, M and T grades
- Group 3: P grades
- Group 4: Q grades

Notation of the steel grade is given by one of the letters above followed by a number. The letter is simply to give an unique name to the different steel types and the following number is the nominal yield strength given in ksi. An example of an grade is P110. This is a group 3 type steel with a nominal yield strength of 110 ksi which is the same as 110 000 psi. The term nominal value refers to the value found in tables as for example Drilling Data Handbook. DDH is a highly useful table and provides, among other things, the nominal values for the outer diameter and the casing thickness. It also provides properties as nominal values for burst strength, collapse strength, axial strength as well as nominal yield strength for each casing grade.

As for design purposes, it is also important to note that we have connections in the casing as well. It is important to consider the connection in the design, however this will not be evaluated in this thesis.

As we apply load onto a pipe we create stress and strain in the material. Stress is the load divided by the cross-sectional area and strain is the relative change in length of the steel (Devereux, 1998). As the load increases, the steel will firstly experience elastic deformation. This means that if the load is removed, the material will return to its original shape. However, if we continue to increase the load we will at some point reach plastic deformation of the material, which means permanent deformation. Further on, the material will reach a maximum point before a slight decrease in stress before rupture. The limit between elastic and plastic deformation is known as the yield stress or yield strength. This point may also be known as the yield strength of the material and is one of the key parameters for classification and grading of casings as mentioned earlier. The maximum point we will reach in our material before rupture is called the ultimate yield strength and is shown in figure 2.3. Figure 2.3 is a common way of presenting the material response and is known as a stress-strain diagram.

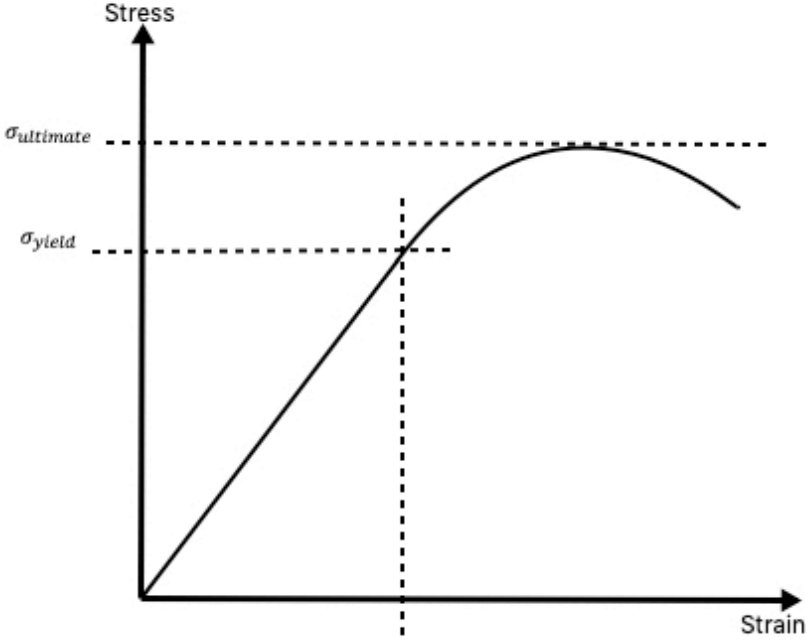


Figure 2.3 Stress-strain diagram

### 2.1 Loads

As wells are drilled, the casings installed will experience different environments depending on the depth and the surrounding pressures. As we get deeper into the formation, the pressure and temperature increases due to the increased amount of overburden and geothermal effects. The variation in pressure and temperature generates different loads on the steel. Different scenarios give different outer and inner pressure and we might have burst load in form of a kick during drilling, collapse load due to loss of fluid to the formation and axial loads due to self-weight of the string.

### 2.1.1 Burst

A burst load is to occur if the pressure inside the casing are larger than the pressure outside the casing. If the inner pressure is to increase in such matters so that it exceeds the casings burst limit, we might experience burst as shown in figure 2.4. This may lead to severe damage on both casing and surrounding equipment.

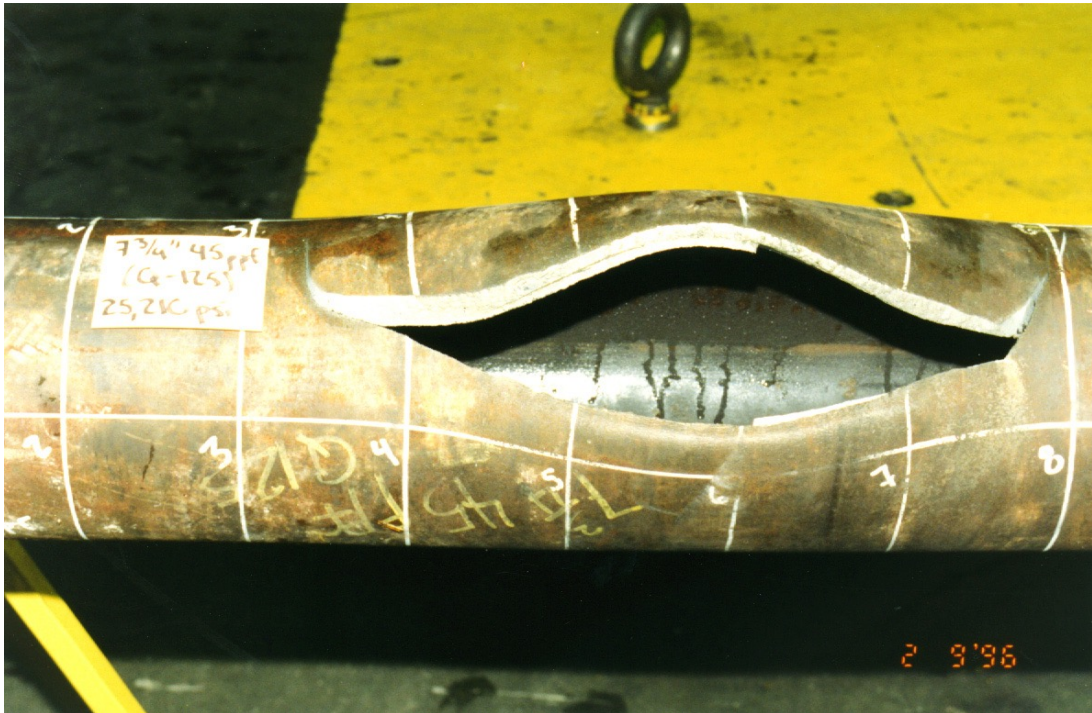


Figure 2.4 Picture of casing burst (Paslay, Cernocky, & Wink, 1998)

Burst load is defined as  $P_{burst} = P_i - P_o$ , where  $P_i$  is the inner pressure and  $P_o$  is the outer pressure. The inner pressure is dependent on the hydrostatic pressure as wells as the surface pressure. The surface pressure might be a planned load, as for example during pressure testing, but also an unplanned load as for example a migrating kick in a closed well (Aadnøy et al., 2009).

Burst strength equations are based on experiments done by multiple scientist and engineers which have resulted in a variety of different equations. API Barlow, API ad-hoc and Klever-Stewart Rupture Limit are burst models that will be used in the simulations for this thesis. Other models for burst modelling can be the von-Mises equation, the Paslay equation, the Moore equation and the Nadai equation. All the burst strength models mentioned above can be found in API 5C3 (API, 2018).

One important parameter for burst strength calculation is the minimum wall thickness. The burst strength will decrease with the decrease of wall thickness. The most common issue for casings is casing wear, due to repeatedly run in hole, pull out of hole during drilling as well as drilling itself. This means that when considering burst strength for a casing, casing wear reduces the burst strength due to the reduction of wall thickness. However when considering a tubing, reduction in wall thickness is more commonly due to corrosion (Bellarby, 2009).

There are multiple burst load scenarios when considering burst, the most common scenarios are listed below:

- Drilling kick
- Pressure test
- Production tubing leak
- Production stimulation

(Aadnøy et al., 2009)

### 2.1.2 Collapse

Similar to burst load, collapse load also considers the differential pressure. This means that if the inner pressure is less than the outer pressure, the casing will experience a collapse load and the collapse load is defined as  $P_{collapse} = P_o - P_i$ . If the load is so high that it exceeds the collapse strength of the casing, we might experience collapse of the casing as shown in figure 2.5. A casing collapse is a situation to avoid as it will result in restricted access in the well. A producing well that has experienced production tubing collapse may still function as normal, however lead to bigger challenges when it comes to intervention work, side-tracking or plugging and abandonment just to mention some.

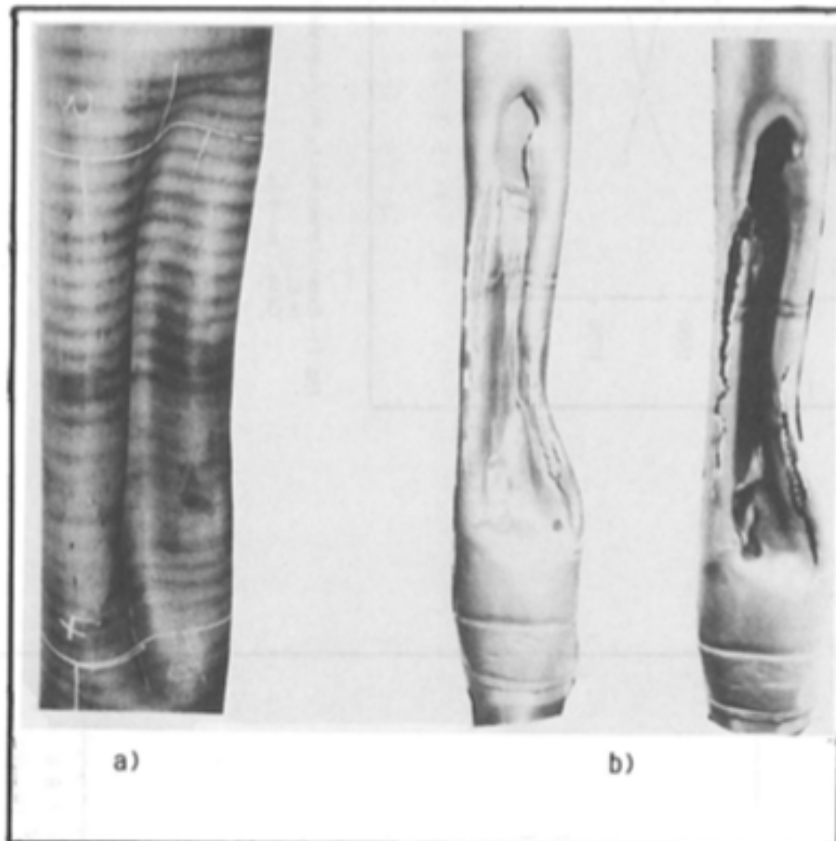


*Figure 2.5 Picture of casing collapse (Marx & El-Sayed, 1985)*

For the collapse strength calculations, one parameter to note is the (D/t) ratio. The outer diameter and casing thickness ratio helps determine the correct equation to use for the collapse strength calculations. One example is the API model. The API model provides four different collapse

equations and by using the table A.2.1 provided in Appendix A.2. These parameters is used so that the most accurate equation can be chosen. The different collapse equations are for yield, plastic, transition and elastic collapse. However, similar to burst strength, there are more models available as for example Klever-Stewart Rupture Limit, Hill's Fully Plastic Burst Limit, Timoshenko collapse and Tamano Collapse (Aadnøy et al., 2009).

This thesis will focus on the API equations for yield, plastic, transition and elastic collapse. During drilling and production, the most common collapse scenarios are listed below

- Collapse during cementing
- Drilling collapse (lost circulation)
- Production casing evacuation collapse
- Salt loading collapse

(Aadnøy et al., 2009)

### 2.1.3 Tension loads

Tension loads will occur in the casing due to static weight of the string itself, shock loads, bending loads, torque and drag, pressure testing or other similar activities. We will always have tension in our casing due to self-weight of the casing, however additional tension may be expected due to overpull while running the casing or bumping the plug during cementing (Aadnøy et al., 2009). Other factor that affect the axial load can be buoyancy, however the buoyancy will reduce the tension load rather than increase it (Bellarby, 2009).

The API equation for axial strength is shown in equation (2.1)

$$F_{ten} = \sigma_y * A \quad (2.1)$$

Where A is the cross-sectional area of the pipe and  $\sigma_y$  is the nominal yield strength of the steel (Aadnøy et al., 2009).

If a tension failure is to occur, the result is a parted pipe or connection. The pipe will as mentioned always be subjected to tension, but failure will occur when the axial load is larger than the mechanical strength of the material (Aadnøy, 2010)

### 2.1.4 Biaxial and triaxial loads

Stress is the load divided by the cross-sectional area and the main stresses acting on our string are axial stress, hoop stress and radial stress. All stresses work simultaneously which means that the string might may start yielding at the inside of the pipe surface when subjected to external load before it may collapse (Aadnøy, 2010). A cross-section of a thin walled cylinder is provided in figure 2.6 together with a visual distribution of axial, hoop and radial stress.

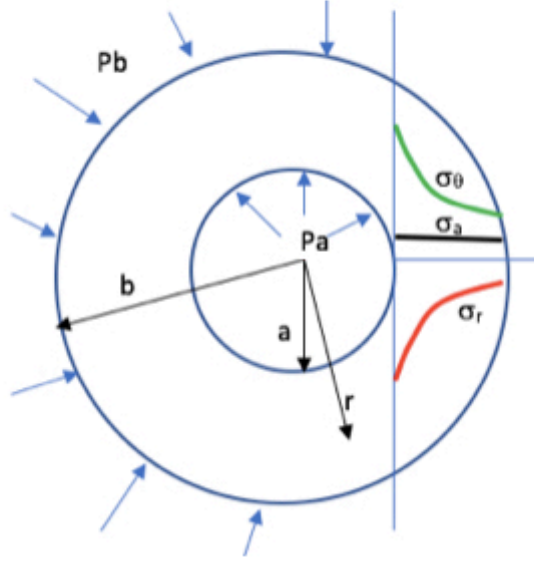


Figure 2.6 Stress distribution (Belayneh, 2018)

Here  $P_b$  is the outer pressure,  $P_a$  is the inner pressure,  $b$  is the outer radius,  $a$  is the inner radius,  $r$  is the radius,  $\sigma_\theta$  is the hoop stress,  $\sigma_a$  is the axial stress and  $\sigma_r$  is the radial stress.

Hencky-von Mises derived a maximum distortion energy theory which says that the critical yield limit exists in the casing regardless of the direction of the load and can be written as in equation (2.2). This equation makes it possible to combine all the stresses into one component.

$$(\sigma_a - \sigma_\theta)^2 + (\sigma_a - \sigma_r)^2 + (\sigma_\theta - \sigma_r)^2 = 2\sigma_{yield}^2 \quad (2.2)$$

Where  $\sigma_a$  is the axial stress,  $\sigma_\theta$  is the hoop stress and  $\sigma_r$  is the radial stress.

For a biaxial analysis, the radial stress is neglected which result in equation (2.3) and the equation is solved for hoop stress in equation (2.4)

$$\begin{aligned} (\sigma_a - \sigma_\theta)^2 + (\sigma_a)^2 + (\sigma_\theta)^2 &= 2\sigma_{yield}^2 \\ \sigma_a^2 - 2\sigma_a\sigma_\theta + \sigma_\theta^2 + \sigma_a^2 + \sigma_\theta^2 &= 2\sigma_{yield}^2 \\ \sigma_\theta^2 - \sigma_\theta\sigma_a + \sigma_a^2 &= \sigma_{yield}^2 \end{aligned} \quad (2.3)$$

(Aadnøy, 2010)

$$\sigma_\theta = \left( \sqrt{1 - \frac{3}{4} \left( \frac{\sigma_a}{\sigma_{yield}} \right)^2} - \frac{1}{2} * \frac{\sigma_a}{\sigma_{yield}} \right) * \sigma_{yield} \quad (2.4)$$

("Drilling Data Handbook, 9th Edition," 2014)

Equation (2.4) is the reduced yield strength due to axial loading, and is based on the von-Mises distortion energy theorem (Bellarby, 2009).

The ellipse of plasticity is a graphical way to do biaxial correction. A biaxial correction is mostly done for collapse strength as axial loading reduced the collapse strength of the material. The ellipse is shown in figure 2.7. In order to use it for biaxial correction for collapse, one needs to calculate the ratio between axial loading and the axial yield strength. As this value is obtained, one can read the amount of reduction of the graph. For example; If we have a load/strength ratio equal to 20%, the value we obtain from the graph is 89%. This means that the collapse strength is reduced by  $100\% - 89\% = 11\%$ .

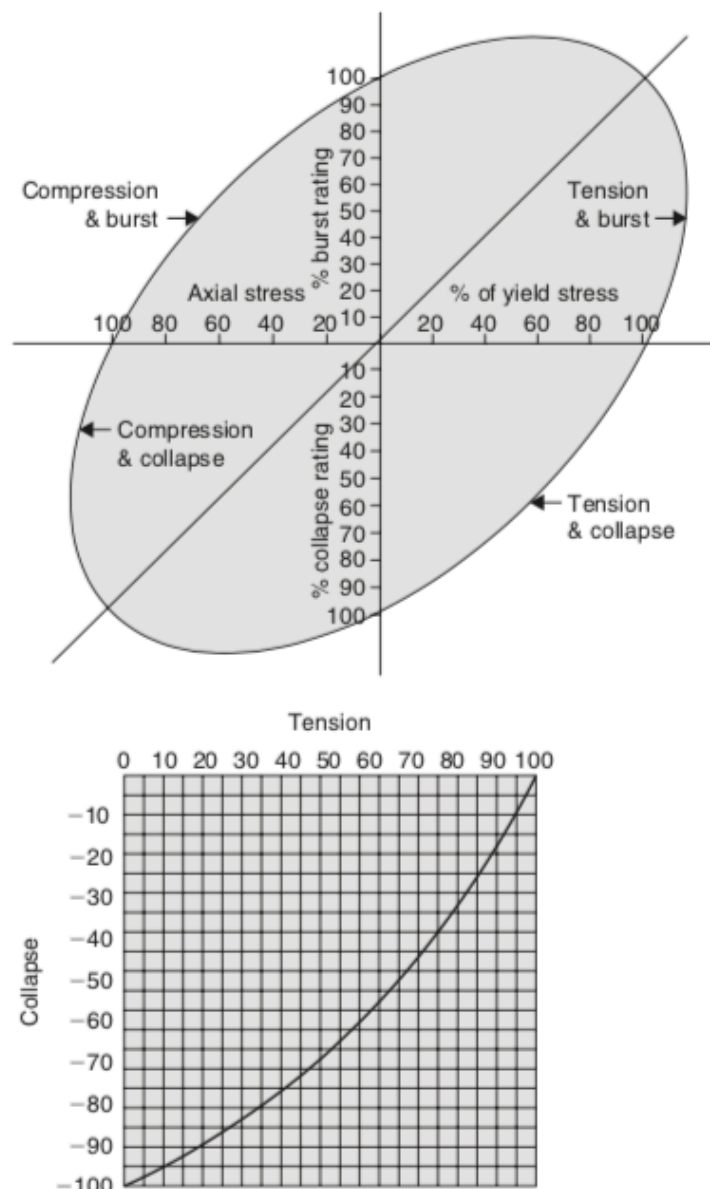


Figure 2.7 Ellipse of plasticity (Aadnøy, 2010)

If we consider the radial stress, we have a triaxial analysis. By using the von-Mises equation given in equation (2.2) one can combine the three stress components into one stress equivalent (Aadnøy, 2010).

## 2.2 Load scenarios

As the different types of casings are installed at different depths in the formation as well as under different conditions, the load scenarios varies from casing to casing. This chapter will give a short overview of possible load scenarios for the different casing strings.

### 2.2.1 Conductor casing

The different load scenarios as collapse, burst, bending and axial tension is usually not considered a problem for the conductor and will therefore not be further discussed. As mentioned earlier, the conductor is set to support the surface casing and wellhead but also to seal off soft and/or unconsolidated formations (Aadnøy, 2010).

### 2.2.2 Surface casing

For the collapse load, the surface casing might experience collapse during cementing. The surface casing is cemented all the way to the wellhead and that will contribute to a high outer pressure. For the worst case scenario we assume that we have cement on the outside of the casing. We also assume that seawater has been used as a displacing fluid which means that we have seawater on the inside of the casing (Aadnøy, 2010). One way of reducing the collapse load when cementing the surface casing is to pump heavier fluid inside the casing so the differential pressure is decreased.

For the burst scenario, there is a possibility of drilling into a shallow gas zone and we might experience a gas leak into our casing and get an increase of the inside pressure (Aadnøy, 2010). The surface casing must also be able to withstand the test pressure at the top of the casing and test pressure plus the hydrostatic pressure at the casing shoe (Devereux, 1998)

### 2.2.3 Intermediate casing

After the surface casing has been drilled and installed, the BOP is set before we continue drilling. There is a possibility that we can get influx of formation fluid also known as a kick. This means that this is considered the worst case scenario regarding burst load for this section. As one might expect, the casing must also be able to withstand the expected test pressure.

The collapse loads for the intermediate casing can be loss to a thief zone or collapse of the casing during cementing (Devereux, 1998). Since the intermediate casing is cemented a couple of hundred meters above the shoe and not to the top, the worst case scenario for this casing is full loss the fluid. In other words, loss of the mud inside the casing to the formation.

### 2.2.4 Production casing

As we proceed to the production casing, the burst scenarios can be unexpected influx of formation fluid or a leaking tubing scenario. As mentioned earlier the production casing must be designed with full well integrity which means it must be able to handle a full string of formation fluid. Since it is a production casing, it must also be able to withstand the loads exerted by injection, artificial gas lift or other production processes.



Similar to the intermediate casing, we might experience collapse during to cementing. However the production casing is cemented a couple of hundred meters above the shoe which means the worst case scenario for collapse will be a loss of fluid inside the casing to the formation during drilling. Losses when perforating or drawdown pressure during production is also collapse loads scenarios that needs to be considered. (Devereux, 1998).

### 2.2.5 Production liner

The production liner will experience the same scenarios as the production casing. For burst, it must be able to withstand a kick and be designed for full well integrity. However, if it is not possible to design with full well integrity, a tie-back string can be installed. A production liner might also experience a tubing leak and must also be able to withstand loads due to injection, artificial lifts or other production processes.

For collapse we look at the possibility for collapse due to cementing as well as loss to a thief zone, with the same assumption as for the production casing. Again, the worst case scenario being complete loss of fluid to the formation (Devereux, 1998).

## 2.3 Survival loads and service loads

From a design point of view, there is a difference between survival loads and service loads. The understanding around survival loads is that they are rarely occurring but with severe consequences. Service loads are the loads that are occurring more frequent and with much lower consequences. Both the survival and service load needs to be considered for the design, however the survival load design takes into account that the event is rare. For design purposes, when considering the extreme and rarely occurring loads, the focus is on survival of the equipment rather than operationality (Suryanarayana & Lewis, 2016).

With the working stress design method, the safety factor can be allowed to be equal to one when we are dealing with survival loads according to API RP 96. In other words, the design challenges the full capacity of the pipe. Further on, it recommends the use of alternative methods when considering survival loads (Suryanarayana & Lewis, 2016).

As briefly mentioned, reliability based design uses Monte Carlo simulations to obtain the probability of failure. However, it is necessary to have a sufficient amount of simulations to obtain a correct probability. If the number of simulations are too low, the result will be misleading. Aadnøy et al. (2009) states that for a target probability of  $10^{-x}$ , a minimum of  $10^{x+2}$  Monte Carlo simulations are necessary. However according to Suryanarayana and Lewis (2016) a minimum of  $10^8$  iterations are sufficient. Suryanarayana and Lewis also give some recommendations regarding the target probability which are listed below

- High consequence failures:  $10^{-6}$  to  $10^{-5}$
- Low consequence failures:  $10^{-3}$  to  $10^{-2}$

Note that these recommendations are based on high magnitude survival loads and the target probabilities are more conservative than for other structural designs.

## 2.4 Well integrity

According to NORSOK (2013) D-010, well integrity is defined as “*application of technical, operational and organisational solutions to reduce risk of uncontrolled release of formation fluids throughout the life cycle of a well*”. In other words, maintenance of the well and its barriers to prevent loss of control.

One key word when talking about well integrity is well barriers. A well barrier is a combination of multiple well barrier elements that together will form a well barrier envelope as shown in figure 2.8 and figure 2.9. When talking about well barriers and well barrier elements we use the terms primary and secondary barrier. This is due to a two barrier philosophy that is also noticeable in our everyday life, as for example in the double isolation of electric cables. The primary barrier is the first barrier and the secondary barrier is the second barrier installed, which also can be viewed as a backup barrier (Gouda & Aslam, 2018).

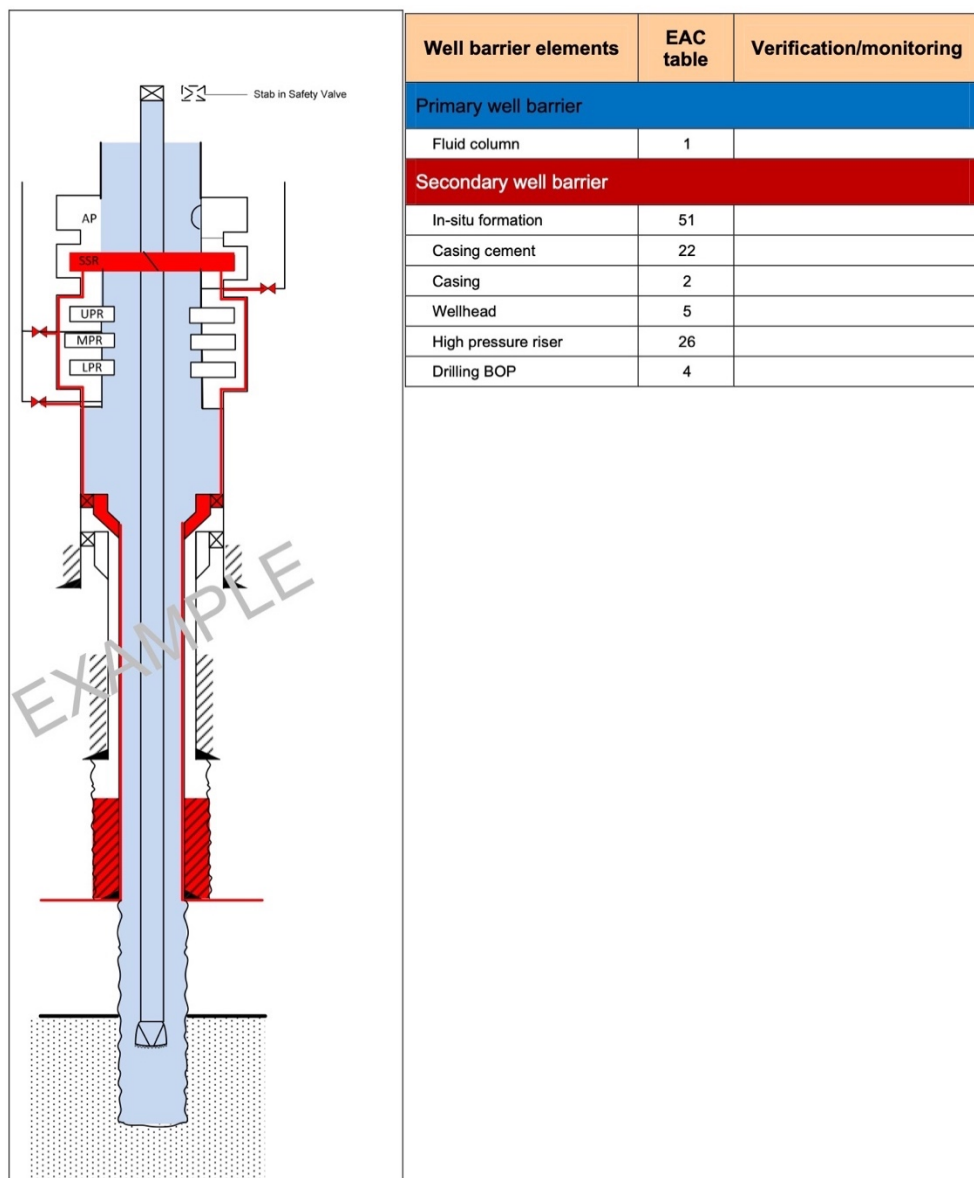
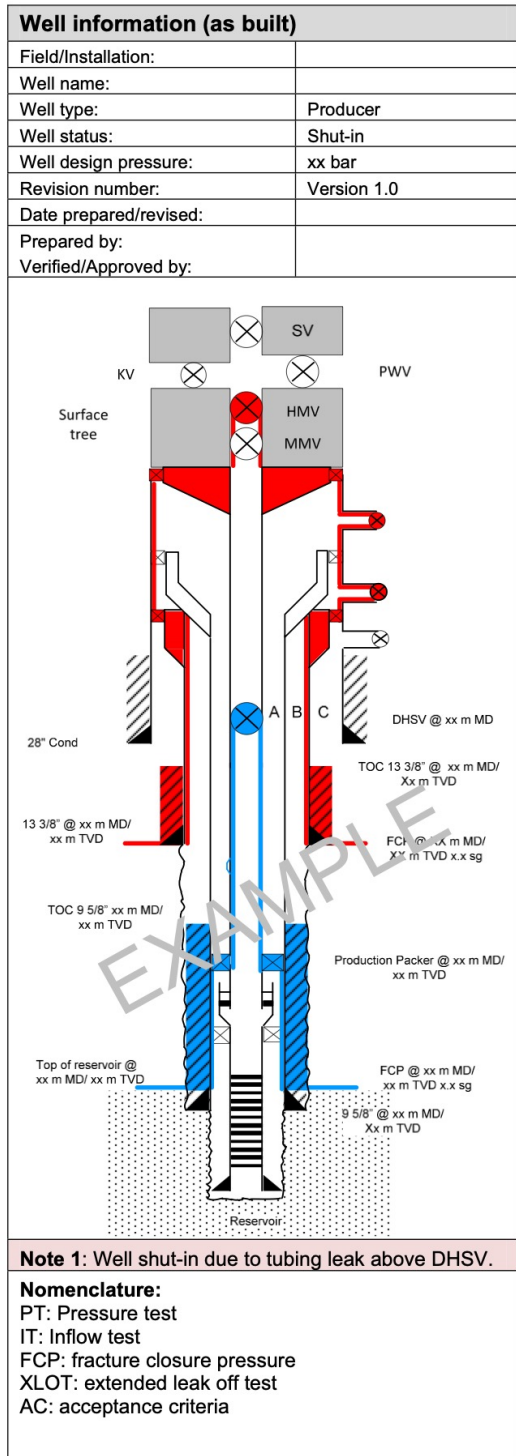


Figure 2.8 Well barrier schematic, drilling (NORSOK, 2013)



Well barrier elements	EAC table	Verification
		Monitoring
<b>Primary well barrier</b>		
In-situ formation (cap rock)	51	FCP: x.x s.g. Based on field model n/a after initial verification
Casing cement (9 5/8")	22	Length: xx mMD Cement bond logs Daily pressure monitoring of B-annulus
Casing (9 5/8")	2	PT: xx bar with x s.g. EMW n/a after initial verification
Production packer	7	PT: xx bar with x s.g. EMW Continuous pressure monitoring of A-annulus
Completion string	25	PT: xx bar with x s.g. EMW Continuous pressure monitoring of A-annulus See Note 1.
Completion string component (Chemical Injection valve)	29	PT: xx bar with x s.g. EMW Periodic leak testing AC DHSV: xx bar/xx min
Downhole safety valve (incl. control line)	8	IT: xx bar (DHSV) PT: xx bar (control line) Periodic leak testing AC DHSV: xx bar/xx min
<b>Secondary well barrier</b>		
In-situ formation (13 3/8" shoe)	51	FCP: x.x s.g. Based on XLOT n/a after initial verification
Casing cement (13 3/8")	22	Length: xx mMD Method: Volume control Daily pressure monitoring of C-annulus
Casing (13 3/8")	2	PT: xx bar with x s.g. EMW Daily pressure monitoring of C-annulus
Wellhead (Casing hanger with seal assembly)	5	PT: xx bar Daily pressure monitoring of C-annulus/ Periodic leak testing
Wellhead / annulus access valves	12	PT: xx bar Periodic leak testing of valve AC: xx bar/xx min.
Tubing hanger (body seals and neck seal)	10	PT: xx bar Periodic leak testing
Wellhead (WH/XT Connector)	5	PT: xx bar Periodic leak testing
Surface tree	33	PT: xx bar Periodic leak testing of valves AC: xx bar/xx min

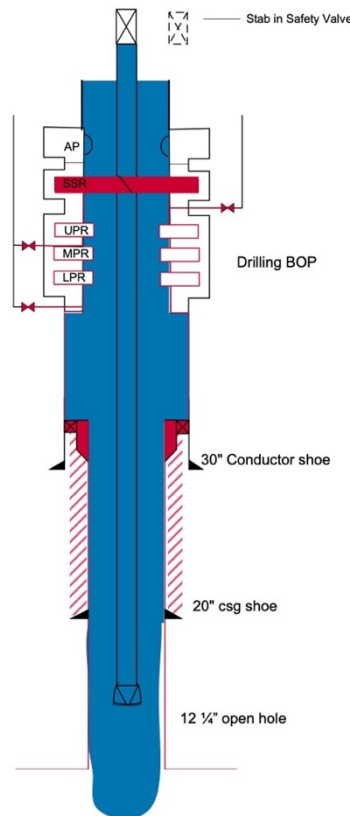
Figure 2.9 Well barrier schematic, production/injection (NORSOK, 2013)

The well barriers are depending on the state of the well. What might be a barrier in a well during drilling of one section may not be a barrier during drilling of another section or during e.g. production. This means that the well barrier schematics are constantly updated during operation so that operators and engineers always know what the current barriers are (Fjågesund, 2015). One example is that the surface and intermediate casing will function as temporary barrier elements during drilling. When the intermediate casing is installed, the surface casing no longer serve as a barrier element. Further on, when the production casing is installed, the intermediate casing no longer serve as a barrier element. The production casing is an example of a permanent barrier element which means that it will be barrier element independent of the state of the well. In figure

2.9, the production casing is listed as a primary barrier element marked in blue as an example. The final well barrier schematic will depend on the type of well completion used and the different components that are installed.

Figure 2.10 shows a well barrier schematic when drilling the 12 ¼” section at Norne (Statoil, 2010). Note that the fluid column is listed as a primary barrier and we see that the 20” casing is listed as a one of the secondary well barrier elements. As mentioned, primary barrier are marked in blue and secondary are marked in red.

**WELL BARRIER SCHEMATIC**  
Drilling 12 ¼” hole section



Well data		
Installation:	Deepsea Bergen	
Well no:	6608/10 K-2 H	
Well type:	Oil Producer	
Revision no	0	Date: 18.09.2009
Prepared:	Linda Brudeli	
Verified:		
Well barrier elements		
Well barrier elements	Ref. WBEAC tables	Verification of barrier elements
<b>PRIMARY</b>		
1. Fluid column	1	1.52 sg OBM
<b>SECONDARY</b>		
1. Casing cement behind 20" casing,	22	
2. 20" Casing	2	Pressure tested to 160 bar with 1.30 sg WBM
3. 18 ¼" Wellhead and seal assembly	5	Pressure tested to 160 bar with 1.30 sg WBM
4. Drilling BOP	4	
Notes:		
<b>BOP Ram configuration, DSB:</b>		
18 ¼" 15k BOP Stack, 11.6 m incl LMRP		
<ul style="list-style-type: none"> <li>• UAP, 18 ¼" 10k</li> <li>• LAP, 18 ¼" 10k</li> <li>• BSR</li> <li>• UPR: Variable ram 3 ½" - 5 1/2"</li> <li>• MPR: Fixed ram element 5 1/2"</li> <li>• LPR: Variable ram 3 ½" - 5 1/2"</li> </ul>		
Disp. no.	Comment	
well integrity issues		
None		

Figure 2.10 Well barrier schematic, drilling 12 ¼" section (Statoil, 2010)

The activity program includes multiple well barrier schematics and figure 2.11 shows the schematics for drilling of the 6" reservoir section. Here we note that the 20" casing no longer serves a secondary barrier element, however the 9 5/8" casing is now listed and included in the secondary well barrier envelope.

Activity Program, Drilling

Rev. No. 0



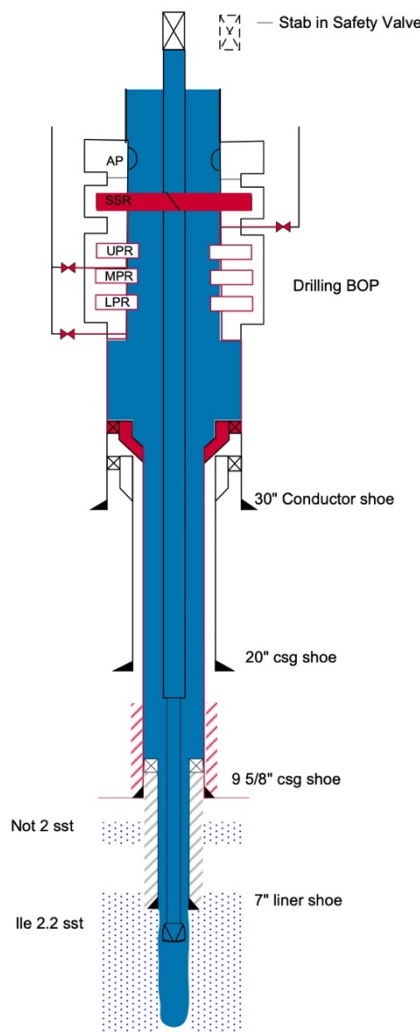
Well 6608/10-K-2 H & AH  
Field Norne

Date 17.02.2010  
Doc. no

Page 120 of 133

### WELL BARRIER SCHEMATIC

Drilling 6" reservoir section



Well data		
Installation:	Deepsea Bergen	
Well no:	6608/10 K-2 AH	
Welltype:	Oil Producer	
Revision no	0	Date: 19.09.2009
Prepared:	Linda Brudeli	
Verified:		
Well barrier elements	Ref. WBEAC tables	Verification of barrier elements
<b>PRIMARY</b>		
1. Fluid column	1	1.30 sg OBM
<b>SECONDARY</b>		
1. Cement behind 9 5/8" casing	22	
2. 9 5/8" casing	2	Pressure tested to 315 bar with 1.52 sg OBM.
3. 10 3/4" casing hanger and seal assembly	5	Pressure tested to 315 bar with 1.52 sg OBM.
4. Drilling BOP	4	
<b>Notes:</b>		
The cemented 7" Liner is not a barrier element, since the 7" liner shoe is placed in a permeable formation (Ile 2.2 sst) and the shoe has been drilled out.		
The 7" Liner is set to isolate the Not Fm due to risk of differential stuck in Not 2 (sst) and hole collapse caused by instability of Not 1 (shale).		
<b>BOP Ram configuration, DSB:</b>		
18 3/4" 15k BOP Stack, 11.6 m incl LMRP		
<ul style="list-style-type: none"> <li>• UAP, 18 3/4" 10k</li> <li>• LAP, 18 3/4" 10k</li> <li>• BSR</li> <li>• UPR: Variable ram 3 1/2" - 5 1/2"</li> <li>• MPR: Fixed ram element 5 1/2"</li> <li>• LPR: Variable ram 3 1/2" - 5 1/2"</li> </ul>		
Disp. no.	Comment	
well integrity issues		
None		



Figure 2.11 Well barrier schematics, drilling 6" reservoir section (Statoil, 2010)

Common for all the schematics provided is the role of one or more of the casing strings as well barrier elements. It is important to note that a well barrier element alone cannot prevent flow but a well barrier envelope which is a combination of multiple well barrier elements do (NORSOK, 2013). This also means that if one of the well barrier elements in the envelope is to fail, the envelope no longer prevents flow.

During the lifetime of a well, a number of different scenarios may happen. Risk is often used to express the combination of probability and the consequence of an unwanted event. A bow-tie diagram is used to document and identify all the incidents, consequences, barriers, escalating factors and as well as controls (Gouda & Aslam, 2018). It is an easy and understandable way of representing the risk to people at every level of competence. The initiating events are listed all the way to the left of the diagram and the green rectangles on the left side are the actions done to prevent the unwanted incident. Figure 2.12 shows a bow tie diagram for a blowout scenario. If a blowout is to occur, the green rectangles on the right side of the diagram represents the actions done and the consequences are listed all the way to the right (Bernsmed, 2016).

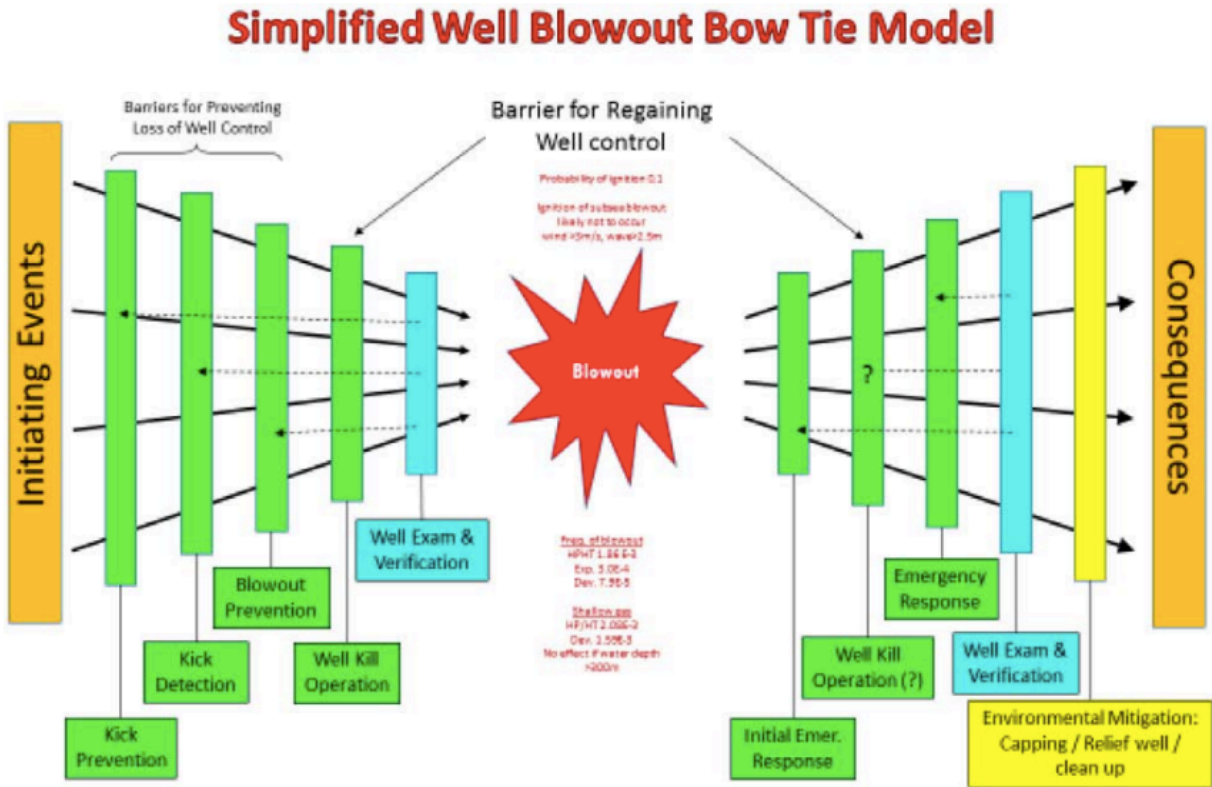


Figure 2.12 Example of Bow-Tie diagram (Gouda & Aslam, 2018)

### 3 Design methods

Some design methods are more used than others, often due to simplicity and acceptance. This chapter will explain the working stress design method, limit state design method and the reliability based design method.

According to Aadnøy et al. (2009) a detailed design requires:

- Pore and fracture gradients
- Temperature profiles
- Mud weights
- Reservoir pressure and depth
- Produced fluid and injection densities
- Packer and completion fluid densities
- Maximum pressure loads

#### 3.1 Working stress design

The traditional approach for casing design today is the working stress design. The basics behind this approach is to assume the worst case load scenario and comparing it to the allowable stresses. If the worst case load scenario do not exceed the allowable stress including a safety factor, the structure is defined as safe (Brand, Whitney, & Lewis, 1995).

Another way of stating the working stress design is shown in equation (3.1)

$$Load \leq \frac{Design\ strength}{Safety\ factor} \quad (3.1)$$

The design strength in WSD is always the minimum yield strength of the material, however since the yield strength is used for the design, exceeding the design strength may lead to deformation rather than failure (Aadnøy et al., 2009). The design strength used in WSD is often collected from Drilling Data Handbook where geometrical characteristic and mechanical properties of casings are listed in section C. The values given in DDH is based on the API models which will be described later in this thesis.

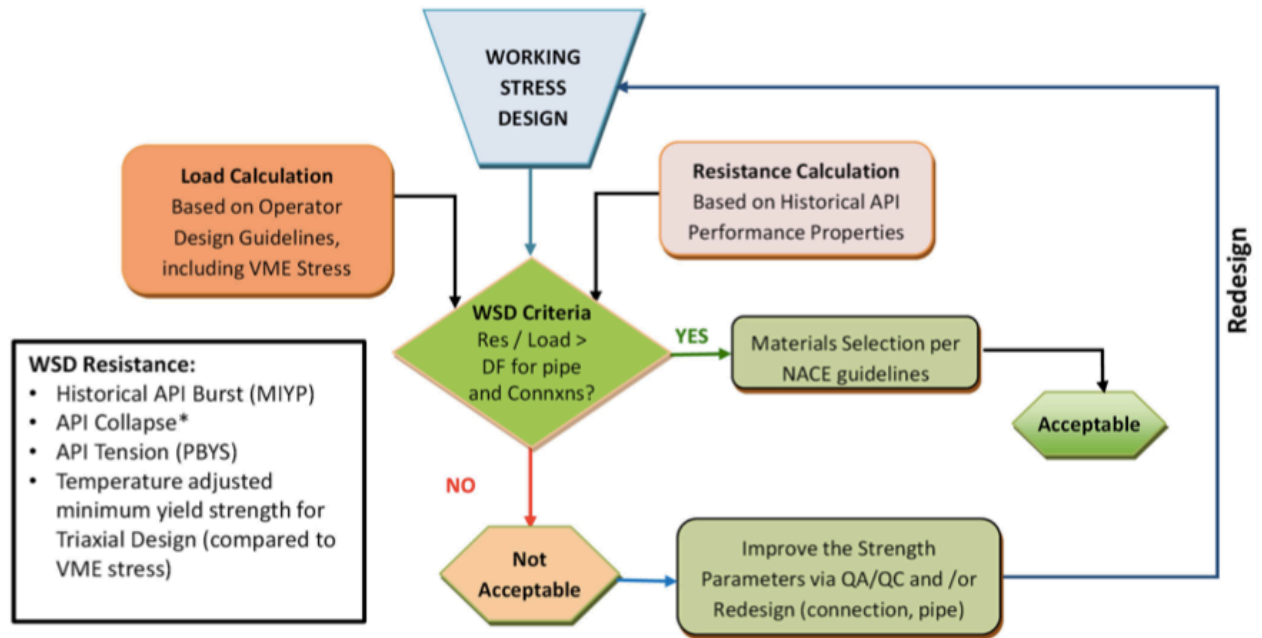
As mentioned, this means that if we are to consider a survival load rather than a service load, the design factor is to be challenged and might approach unity (Suryanarayana & Lewis, 2016).

The safety factors is used so that we account for uncertainties, and these vary between different companies as well as regions. Even though the safety factor vary, the Norwegian Continental shelf follows the NORSOK standard. The safety factors from NORSOK D-010 are given below

Burst:	1.1
Collapse:	1.1
Axial:	1.25
Triaxial:	1.25

(NORSOK, 2013)

If the calculated load including the safety factor is higher than the casing strength, a stronger casing is chosen so that the casing is able to withstand the calculated loads. If the casing strength is sufficient enough and fulfils the standards requirements the design is accepted. A flowchart of the working stress design process are provided in figure 3.1.



\*Strength adjusted for tension, load adjusted for internal pressure. Revision of the API approach so that strength is adjusted for both tension and internal pressure are under way.

Figure 3.1 Working stress design approach (Suryanarayana & Lewis, 2016)

WSD is a simple and widely accepted approach for casing design, but as any design method it has its limitations. Since WSD uses the same safety factor for different load cases, it will always be a safety-factor-consistent design, but not a risk-factor-consistent design. This means that for simple wells we might have overdesign which leads to unnecessary expenses (Aadnøy et al., 2009). An example of this is the safety factor for burst. The burst safety factor is the same for both a kick scenario as well as for a pressure test scenario. The risk of failure will be different for the two cases since the kick scenario do not happen as often as a pressure test scenario. A kick will also have a much higher magnitude than a pressure test, however the design factor stays the same (Aadnøy et al., 2009).

As we design more complex wells with smaller margins, as for example an HPHT well, it might become difficult to obtain the correct safety factor. As mentioned, each casing is decreasingly smaller than the previous one installed. A HPHT is usually deeper than other wells and in order to reach our target depth, the casing strings are becoming smaller and smaller. In other words, it becomes more difficult to obtain a safe design using the recommended safety factors due to the geometrical constrains. This means that the safety factor might be compromised. Reducing the safety factor can be viewed as an equivalent to increasing the risk of failure (Aadnøy et al., 2009).

As implied, the safety factor is an important parameter however it do not take into account every aspect of a load scenario. This means that the risk-consequence evaluation is lost and it becomes



easier to uphold a safety factor for a simple well. However for a more complex well where the margins are much smaller, the risk for compromises the safety factor is greater. In other words, this means that we accept higher risks for wells with a higher consequence of failure (Aadnøy et al., 2009).

### 3.2 Limit state design

In a limit state design, the design is based on the limit load thereby the name. This means that the design strength in equation (3.1) is replaced by the limit state also known as the ultimate yield. Limit state design can be expressed equation (3.2)

$$Load \leq \frac{Limit\ state}{Safety\ factor} \quad (3.2)$$

In limit state we will typically use formulas for the strength calculations that are based on using the ultimate yield strength when considering a survival load scenario.

The limit state, or ultimate yield strength, can be found in the DDH section C1. DDH provides an overview of the most common casing grades and corresponding yield strengths, minimum ultimate yield strengths as well as the maximum yield strength.

Similar to WSD, LSD also uses the safety factor and has the same approach as shown in figure 3.1. Since the API model often takes a basis in yield strength rather than ultimate yield, other models as for example Klever-Stewart Rupture limit, Klever-generalized Tamano or the Hill limit can be used as appropriate models for a limit design (Aadnøy et al., 2009). According to API 5C3, if the API model uses the ultimate strength values, it is referred to as API ad-hoc.

### 3.3 Reliability based design

The parameters used in the casing strength calculations have been determined by theoretical work and multiple experiments. Repeated tests and experiments gives various results which will give a natural spread of the data. Due to this, the parameters are often fitted to a suitable distribution model. Each parameters has its own distribution, which means a range of possible values. For a P110 grade casing, the nominal value for the yield strength is given as 110ksi. The real yield strength can be either higher or lower than the nominal value.

By considering the distribution of each parameter, and repeat the calculation of casing strength multiple times will result in a distribution in the results as well. This is where the reliability based design comes into consideration. As mentioned before, working stress design considers the nominal value of each parameter and considers the worst case scenario. There are different levels of reliability based design and we will focus on level 4 and level 5. In short terms, level 4 means that we have a distribution on the strength calculation and the load scenario is a single value referring to the worst case load scenario. As for level 5, the load scenario is also considered as a distribution (Suryanarayana & Lewis, 2016).

According to Suryanarayana and Lewis (2016), if we are to design for a survival load rather than service load, reliability based design is the recommended approach. The flowchart for a level 4 reliability design for a survival loads is shown in figure 3.2.

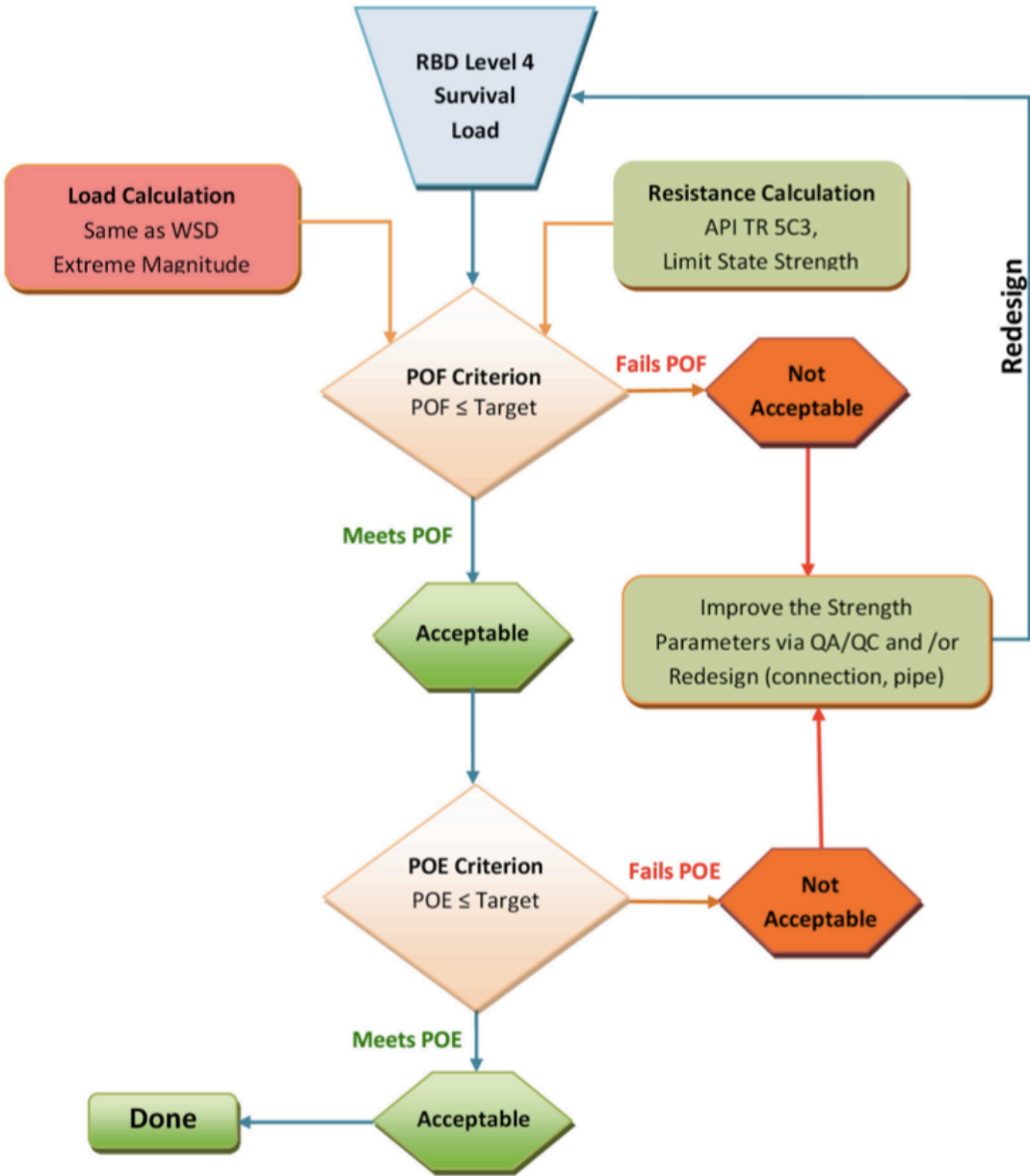


Figure 3.2 Flowchart, RBD4 design for a survival load (Suryanarayana & Lewis, 2016)

Reliability based design provides a probability of failure. This means that it is possible to make a risk assessment of the design and the consequence of the failure may be included as a determining factor in the design. One limitation for the reliability based design to determine the target probability of the design. In other words, how much risk can we accept. Target probabilities has been discusses briefly earlier in this thesis and as we divide between high and low consequence of failure. If the consequence is failure of a type of equipment that are easy to replace, a larger probability of failure can be accepted. This may be seen as a low consequence of failure compared to the consequence of a full blowout. For a full blowout scenario, a lower target probability is required due to a more severe/high consequence (Suryanarayana & Lewis, 2016).

In order to perform the reliability based design, the use of Monte Carlo simulations is recommended. This approach is typically used in quantitative risk analysis.

### 3.3.1 Monte Carlo simulations

Monte Carlo simulations are statistic-based analysis methodology. From a petroleum point of view, the Monte Carlo simulations can be used for estimation of oil and gas reserves, capital exposure, economic values, cost/time estimation of operations and casing design (Williamson, Sawaryn, & Morrison, 2006)

It is relatively easy to use and widely applicable in situation where the relationship between the input and output variable is quite complex (Bratvold, Begg, & Society of Petroleum, 2010).

The procedure for the simulations can be described in the following steps (Bratvold et al., 2010)

1. Have an appropriate model for the problem you are investigating
2. Describe the uncertainty in the input variables in a form of a probability distribution
3. Takes a sample for each distribution and uses them in the model
4. Store the results
5. Repeat step 3 and 4

After repeating step 3 and 4 sufficient amount of times, the output are presented in a histogram and the mean, variance and percentiles can be calculated (Bratvold et al., 2010).

As for the use in reliability based design, the load and/or casing strength are calculated. The number of calculations where the load exceeds the strength are counted and divided by the number of total number of Monte Carlo simulations which provides the probability of failure.

### 3.3.2 Basic Statistics

As statistics plays an important role in Monte Carlo simulations and reliability based design, the following subchapter will provide short explanation of common terms.

#### 3.3.2.1 Mean

The mean value, also known as the average is the sum of n measurements  $x_1, x_2, x_3, \dots, x_n$  divided by n.

$$\bar{x} = \frac{\sum_{i=1}^n x_i}{n} \quad (3.3)$$

(Løvås, 2013)

#### 3.3.2.2 Median

When all the measurements are sorted from smallest to the largest value, we can determine the sample median, also known as the P50 value. This is the value found in the middle of our sorted data.

In order to measure the spread of the data, P10 and P90 values are commonly used. Shortly explained, when the measurements are sorted from minimum to maximum, 10% of the values are

below the P10 value. Similarly 10% of the values are above the P90 value, hence 80% of the values will be in the interval between P90 and P10 (Løvås, 2013).

A graphical definition of median and P90 and the median is shown in figure 3.1 below.

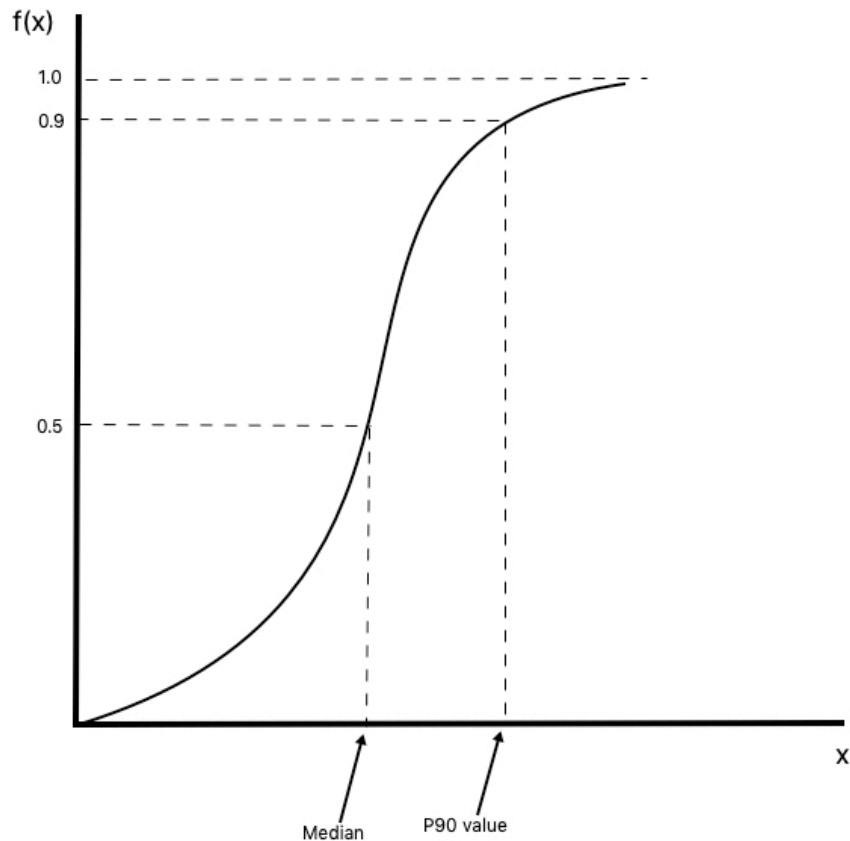


Figure 3.3 Definition of median and P90

### 3.3.2.3 Standard deviation and Variance

The variance is given by equation (3.4). This value is used to determine the standard deviation which is given in equation (3.5).

$$var = \frac{1}{n} \sum_{i=1}^n (x_i - \bar{x})^2 \quad (3.4)$$

$$stdv = \sqrt{\frac{1}{n} \sum_{i=1}^n (x_i - \bar{x})^2} \quad (3.5)$$

One thing to note is that the variance is simply the squared value of the standard deviation. In other words, the variance is most commonly used to determine the standard deviation which is the value of interest. The standard deviation is a way to define the variation of the values compared to the mean value. A large standard deviation means a large spread in the data (Løvås, 2013).

### 3.3.2.4 Distribution models

There are many different distributions models available, and it is important to choose the model that are most suited for your data. One should choose a model that are accurate and simple enough for our purpose (Løvås, 2013). Here, some examples of distribution are provided.

#### 3.3.2.4.1 Uniform distribution

This distribution returns values that are between a given maximum and minimum value. This is a good distribution when there are lack of data, mostly since you are able to include subjective assumptions regarding the maximum and minimum value (Wanke, 2008).

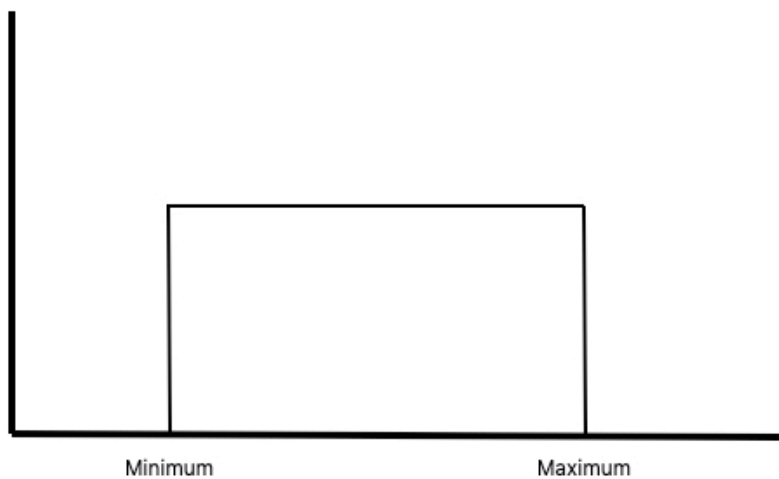


Figure 3.4 Uniform distribution

#### 3.3.2.4.2 Triangular distribution

The triangular distribution is a distribution that is, not surprisingly, shaped like a triangle. It is defined by three values; minimum, maximum value and the most likely value also known as the peak value. This is a good distribution to use in real life situations, when assumptions regarding the parameters needs to me made (Løvås, 2013).

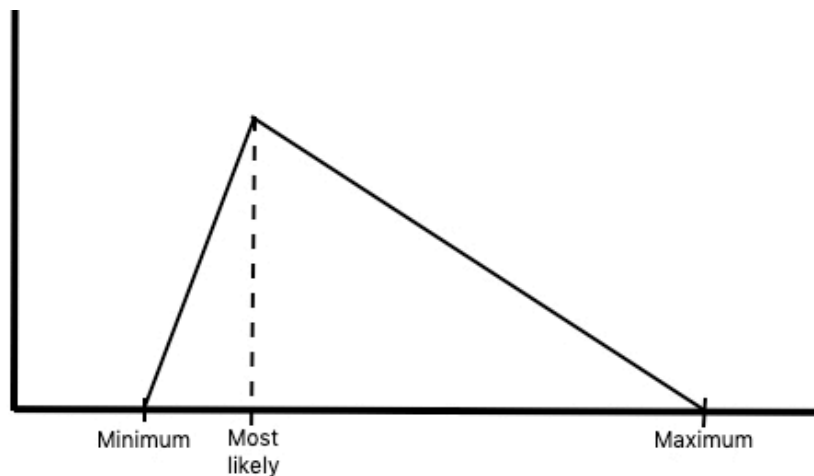


Figure 3.5 Triangular distribution

The notation T(min, most likely, max) is used to describe a triangular distribution. T(0,0.5,1) means that the minimum value possible is 0, the most likely value is 0.5 and maximum value is equal to 1.

### 3.3.2.4.3 Normal distribution

Normal distribution is the most common distribution in statistics. The shape is similar to a clock shape and the distribution is so common that people might think it's the normal way of showing statistics, hence the name.

In a normal distribution the mean and the median has the same value and decreases symmetrically on both sides. The equation for the normal distribution is given in equation (3.6) (Løvås, 2013)

$$f(x) = \frac{1}{\sqrt{2\pi}\sigma} e^{-\frac{(x-\mu)^2}{2\sigma^2}} \quad (3.6)$$

Where  $\sigma$  is the standard deviation and  $\mu$  is the expected value. If the standard deviation is increased, one will obtain a larger spread in the data. In this case, the distribution will become wider.

The notation N(mean, stdv) is used to describe a normal distribution. N(1,0.5) mean that we have an normal distribution with a mean equal to one and a standard deviation equal to 0.5.

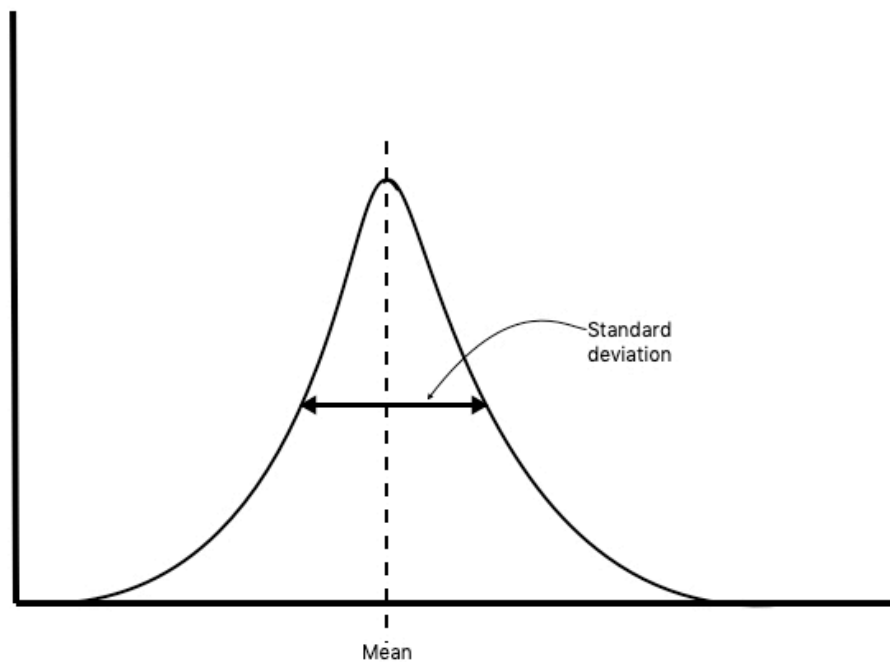
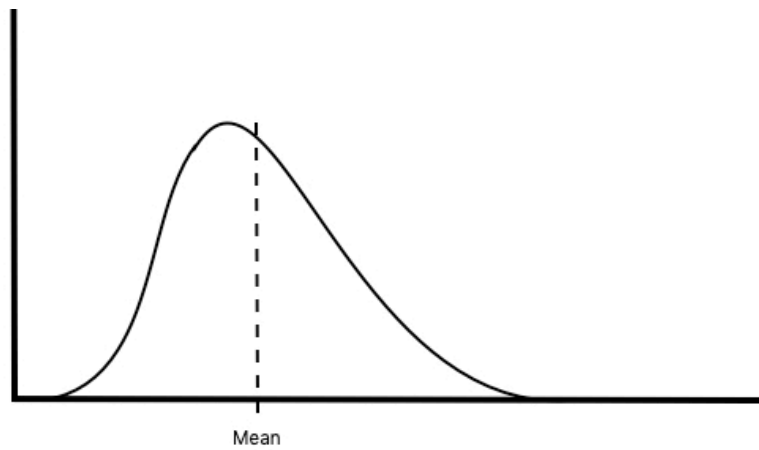


Figure 3.6 Normal distribution

#### 3.3.2.4.4 Lognormal distribution

Lognormal distribution have a normally distributed logarithm. The distribution is determined by the mean and standard deviation similar to a normal distribution. On the other hand, the lognormal distribution has a long “tale” towards the right. However it will become more clock shaped as the variance increases (Aarnes, 2014).



*Figure 3.7 Lognormal distribution*

## 4 Case study

For this case study, we will look further into a high pressure and high temperature well. Per definition, a well is considered HPHT if

- Deeper than 4000 m
- Reservoir pressure exceeds 10 000 psi (690 bar)
- Reservoir temperature above 150°C

(Aadnøy, 2010)

In this simulation study, the pressure gradient plot made up for this case study is shown in figure 4.1.

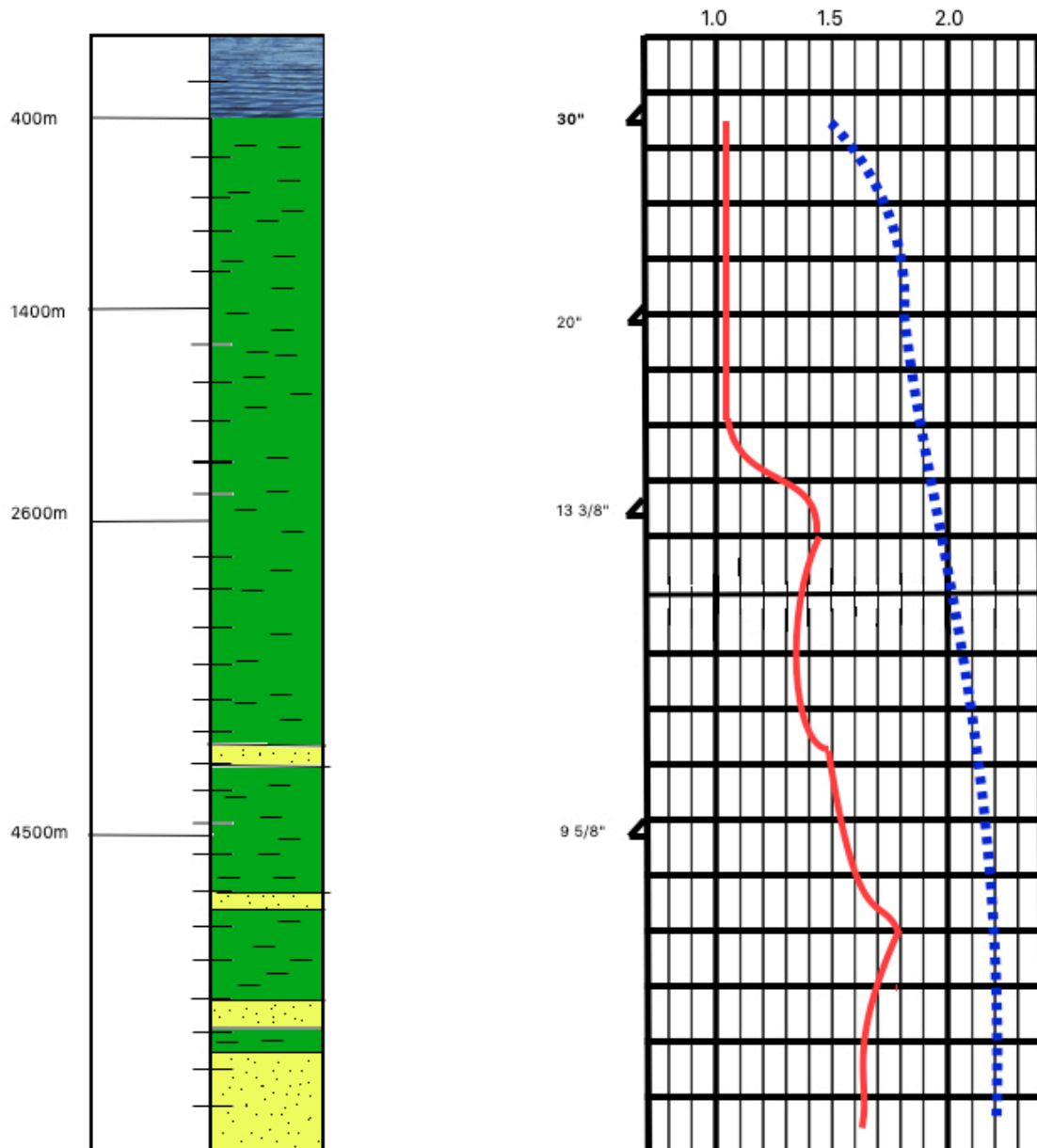


Figure 4.1 Pressure gradient plot



The casing size, setting depths and mud weight are shown in table 4.1.

Casing name	Casing size	Setting depth	Mud weight
Conductor	30"	400m	1.3 s.g
Surface casing	20"	1400m	1.6 s.g
Intermediate casing	13 3/8"	2600m	1.7 s.g
Production casing	9 5/8"	4500m	2.0 s.g

Table 4.1 Casing size, setting depth and mud weight for case study

Further in this case study, the main focus will be on the 13 3/8 intermediate casing. By using burst and collapse calculation with the use of the information above as well as data collected from API 5C3, an appropriate casing grade should be selected for this section.

First, we will consider the burst load and discuss the different burst models available, then the collapse load will be considered and the collapse strength will be calculated by using the API model. Note that only collapse and burst will be considered when determining the design for the 13 3/8" in this thesis.

#### 4.1 Burst load

For the burst load, our worst case scenario will be a gas filled casing. For the burst load scenario, we imagine that a kick is taken at the bottom of the well when drilling the next section as shown in figure 4.2.

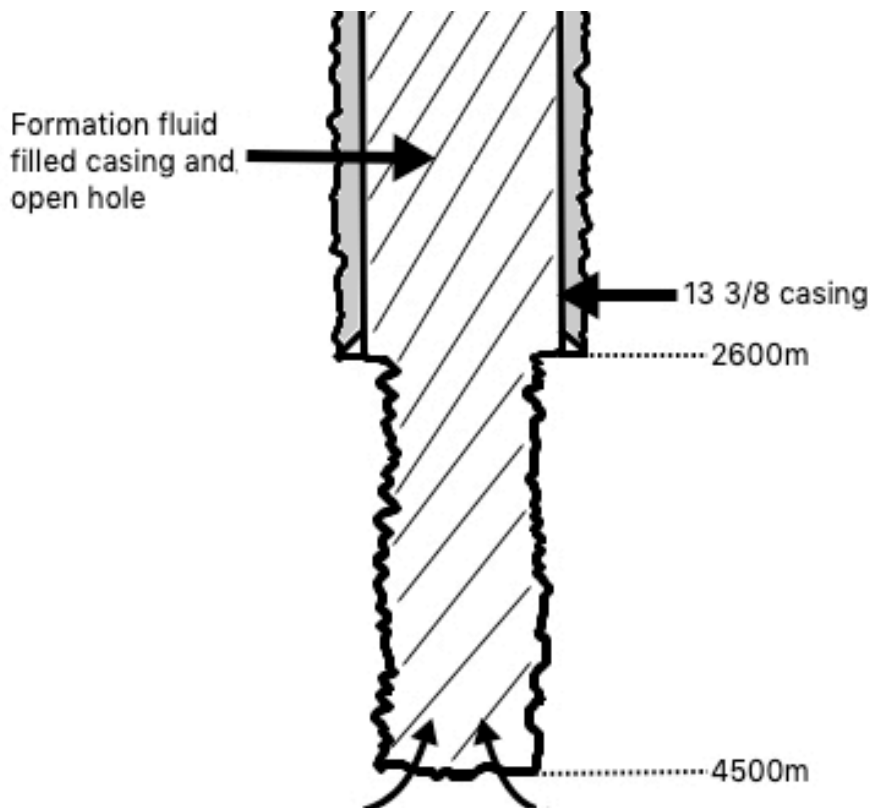


Figure 4.2 Sketch of formation fluid filled casing

Parameters used in the calculation are listed below

Depth of casing: 2600m  
 Depth to seabed: 400m  
 Depth to sea level: 25m  
 Depth of top of cement: 2400m  
 Depth of next hole section: 4500m  
 Pore pressure for next section: 1.5 s.g  
 Fracture gradient at 13 3/8" shoe: 1.95 s.g  
 Formation fluid density: 0.3 s.g  
 Mud density: 1.7 s.g

#### 4.1.1 Burst strength models

There are different models that can be used to calculate burst strength. This subchapter will describe and compare four different models.

Model error for each of the burst strength models listed below can be found in table B.5 in API 5C3.

##### 4.1.1.1 API Classic

The equation that are most commonly used is equation (4.1). This API equation uses the conservative tolerance value of 0.875 as well as the nominal value for yield strength. The nominal value for yield strength can be found in tables as for example DDH.

$$P_{burst,API} = tol * \frac{2 * \sigma_{yield} * t}{OD} \quad (4.1)$$

All parameters used in this equation is the nominal values, and the uncertainties are accounted for in the tolerance (Bellarby, 2009).

##### 4.1.1.2 API Classic with distribution

For this model, the distribution of the different parameters and the model error are taken into account. This means that the stochastic nature of each parameter are taken into consideration and the model becomes more complex. The distributions for each parameter as well as the model error are found in the API 5C3 standard and are listed in table 4.4 and 4.5. Note that the mean and standard deviation is different for each parameter.

The nominal yield strength are used in this equation, and the tolerance is also included.

$$P_{burst,API} = tol * \frac{2 * N(mean_{\sigma}, stdv_{\sigma}) * N(mean_t, stdv_t)}{N(mean_{OD}, stdv_{OD})} * N(mean_{model}, stdv_{model}) \quad (4.2)$$

One example on how the calculation of parameter used in the normal distribution is done as follows.

Standard deviation is equal to COV \* mean and as mentioned, COV and mean values are found in API 5C3 table F.4 and table 4.5.

$$mean_{OD} = OD * 1.0059 = 13.375 \text{ in} * 1.0059 = 13.454 \text{ in}$$

$$stdv_{OD} = mean_{OD} * COV = 13.454 \text{ in} * 0.00181 = 0.02435 \text{ in}$$

$$N(\sigma_{OD}, stdv_{OD}) = N(13.454, 0.02435)$$

#### 4.1.1.3 API ad-hoc

The term ad-hoc means that the ultimate yield strength are used rather than nominal yield strength. The API ad-hoc model can be found in API 5C3 as well as the distribution for the different parameters and the model error. When the distribution for the parameters are taken into account we obtain the expression given in equation (4.3). The mean and standard deviation used in this equation is given in table 4.4 and table 4.5. Note that we assume the same parameters for ultimate yield strength and yield strength.

$$P_{burst,ad-hoc} = \frac{2 * N(mean_{\sigma_{ultimate}}, stdv_{\sigma_{ultimate}}) * N(mean_t, stdv_t)}{N(mean_{OD}, stdv_{OD})} * N(mean_{model}, stdv_{model}) \quad (4.3)$$

Calculations are performed in the same way as for API classic.

#### 4.1.1.4 Klever-Stewart rupture limit

Klever-Stewart is another equation developed to calculate the burst strength. This model is also found in the API 5C3 as well as the model error. This equation uses the minimum wall thickness, however we assume that the minimum wall thickness is equal to the nominal wall thickness for simplicity.

The most noticeable differences between API model and Klever-Stewart model is that the parameter  $K_{dr}$  is added. This is a correction factor based on pipe deformation and material strain hardening (API, 2018) and is given by equation (4.4). Distributions for each parameter as well as the model error is given in table 4.4 and 4.5.

$$K_{dr} = \left(\frac{1}{2}\right)^{n+1} + \left(\frac{1}{\sqrt{3}}\right)^{n+1} \quad (4.4)$$

$$P_{burst,KS} = \frac{2 * K_{dr} * N(mean_{ultimate}, stdv_{ultimate}) * N(mean_t, stdv_t)}{(N(mean_{OD}, stdv_{OD}) - N(mean_t, stdv_t))} * N(mean_{model}, stdv_{model}) \quad (4.5)$$

The n-value used in equation (4.4) is called the stress-strain parameter and is dependent on the API grade of the material. The different n-values are listed in table 4.2. Since the n parameter is a fixed value and do not have a distribution, the  $K_{dr}$  is fixed as well.

API Grade	n
H40	0.137
J55	0.125
K55	0.125
M65	0.117
N80	0.104
L80	0.104
C90	0.096
R95	0.092
T95	0.092
P110	0.080
Q125	0.068

Table 4.2 Values for n, Klever-Stewart model (API, 2018)

#### 4.1.1.5 Comparison of models

In order to further look at the difference between the models, simulations in MATLAB were performed. A P110 13 3/8” casing with a thickness equal to 0.430” will be considered and the following parameters have been used for the simulations.

Parameter	Value
Ultimate yield	125 000 psi
Yield	110 000 psi
Outer Diameter	13 3/8 in
Wall thickness	0.430 in
Tolerance	0.875
n	0.08

Table 4.3 Values used in MATLAB simulation

Model	Name of table in API 5C3	Mean (Predicted/Actual)	COV (Predicted/Actual)	Standard Deviation (Stdv = COV * mean)
API ad-hoc*	B.5	1.08	0.046	0.050
Klever-Stewart	B.5	1.00	0.023	0.023

Table 4.4 Model uncertainty used in the simulations (API, 2018)

\*Assumed same parameters for API and API ad-hoc

Parameter	Name of table in API 5C3	Mean	COV	Standard Deviation (Stdv = COV * mean)
Nominal yield strength for P110	F.3	Nominal yield * 1.1	0.0464	0.0464*mean <sub>nominal yield</sub>
Ultimate yield strength for P110*	F.3	Ultimate yield * 1.1	0.0464	0.0464*mean <sub>ultimate yield</sub>
Nominal yield strength for N80	F.3	Nominal yield * 1.21	0.0511	0.0511*mean <sub>nominal yield</sub>
Ultimate yield strength for N80*	F.3	Ultimate yield * 1.21	0.0511	0.0511*mean <sub>ultimate yield</sub>
Nominal yield strength for L80	F.3	Nominal yield * 1.1	0.0529	0.0529*mean <sub>nominal yield</sub>
Ultimate yield strength for L80*	F.3	Ultimate yield * 1.1	0.0529	0.0529*mean <sub>ultimate yield</sub>
Nominal yield strength for K55	F.3	Nominal yield * 1.23	0.0719	0.0719*mean <sub>nominal yield</sub>
Ultimate yield strength for K55*	F.3	Ultimate yield * 1.23	0.0719	0.0719*mean <sub>ultimate yield</sub>
Outer diameter**	F.4	Outer diameter*1.0059	0.00181	0.00181*mean <sub>outer diameter</sub>
Thickness**	F.4	Thickness*1.0069	0.0259	0.0259*mean <sub>thickness</sub>

Table 4.5 Distribution parameters used for the burst simulations (API, 2018)

\*Assumed same parameters for ultimate yield strength as yield strength, values from CRS ensemble

\*\* Values from ensemble

The first burst strength model considered was the API Classic where no distribution was taken into account. This resulted in the straight vertical line present in our plot shown in figure 4.3. This is the most conservative model out of the four that has been evaluated. For API classic with distribution, we take the distribution of the different input variables into account when calculating the strength and see a noticeable change in the shape of the plot and we obtain the red curve.

The most noticeable effect of API classic with distribution compared to API classic, is the fact that the mean value has changed drastically and we have a noticeable spread in our strength prediction data. The increase in mean is due to the fact that we take the model error into account.

Further on, API ad-hoc was considered as well. As mentioned earlier, ad-hoc means that the ultimate yield is used instead of nominal yield and we can see that this gives a wider spread in the data as well as an increase in the mean value. API ad-hoc gives, according to the simulation, the largest mean and spread in this case.

Klever-Stewart gives approximately the same mean value as API ad-hoc which is expected since both models uses the ultimate yield strength rather than nominal yield. However, compared to the API ad-hoc, Klever-Stewart has a smaller spread.

The MATLAB code is provided in appendix, and the results and output parameters are plotted in figure 4.3 and in table 4.6.

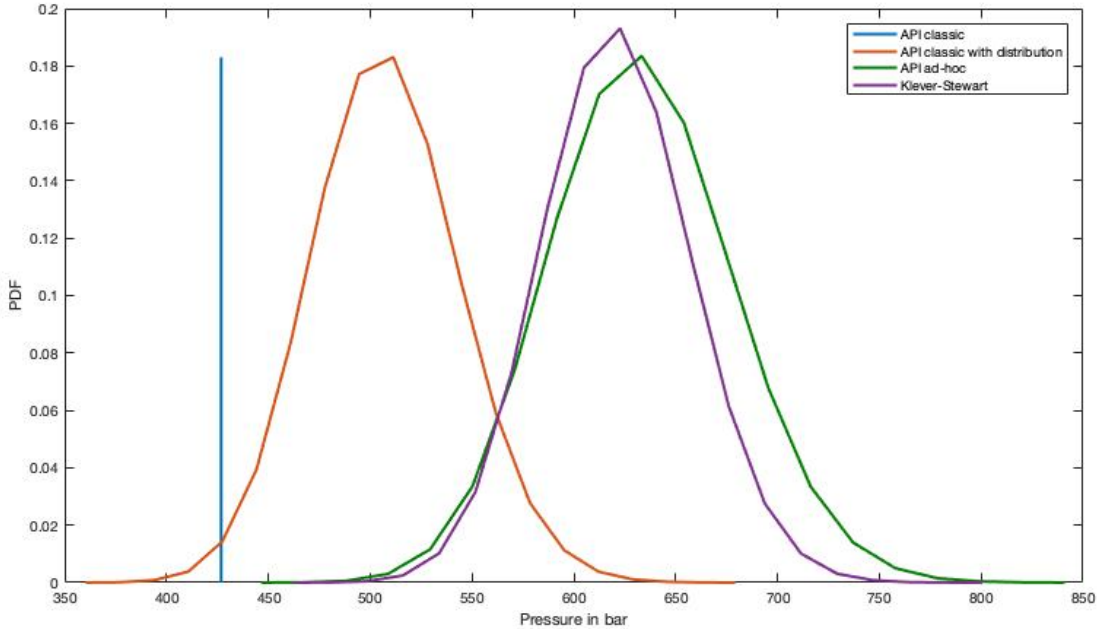


Figure 4.3 MATLAB plot of each model for the burst strength of the casing, P110

	<u>mean</u>	<u>std</u>	<u>P50</u>	<u>P10</u>	<u>P90</u>
<b>API Classic</b>	426.81	0	426.81	426.81	426.81
<b>API classic with distribution</b>	507.57	35.813	506.8	462.18	553.9
<b>API ad-hoc</b>	632.88	45.416	631.88	575.36	691.7
<b>Klever-Stewart</b>	620.88	36.232	620.27	574.8	667.73

*Table 4.6 Mean, standard deviation, median, P10 and P90 values for each model given in bar*

In order to make the difference between the models more clear, the P10 and P90 values have been calculated as well. This means that 80% of the values will be within the interval the given intervals below

<b>Model</b>	<b>Interval</b>	<b>Spread</b>
<i>API</i>	553.9bar – 462.18 bar	92.72bar ≈ 93 bar
<i>API ad-hoc</i>	691.7bar – 575.36 bar	116.34 bar ≈ 116 bar
<i>Klever-Stewart</i>	667.73bar – 574.8 bar	92.93bar ≈ 93 bar

*Table 4.7 Overview of interval spread for strength models*

Based on the simulation and the comparison given above, Klever-Stewart is the most appropriate model to use for reliability based design for burst. It has the same spread of data as the API model, however Klever-Stewart uses the ultimate yield strength and gives a higher mean value. API 5C3 also recommends the use of the Klever-Stewart rupture limit for burst strength limit calculations

The table listed above shows that the API ad-hoc gives a larger spread in the data compared to the API classic model. Due to my earlier assumption regarding the distributions, the standard deviation and the mean for API ad-hoc will be larger due to the increase in yield value. The ultimate yield is higher than the yield strength. This means that we obtain a larger mean value and consequently a larger standard deviation.

Both the API ad-hoc model and Klever-Stewart rupture limit uses the ultimate yield strength rather than the nominal yield strength. Based on this, the preferable model when designing to survival loads and rupture limits is the Klever-Stewart model.

#### 4.1.2 Reliability based design

For the reliability based design, simulation has been performed in MATLAB. The codes that have been used in the simulations are provided in Appendix A.1.

As mentioned, there are different levels of reliability based design. The focus in this thesis will be on level 4 and level 5. RBD4 includes a distribution for the strength calculations, however the load is calculated as a given value. The load in RBD4 is set to be the worst case scenario, however

when considering RBD5, we include the uncertainty in the load parameters as well as the strength calculations. Since RBD4 uses the worst case scenarios and RBD5 includes a distribution of the loads, the results of RBD5 is less conservative than RBD4.

It is important to note that the uncertainties often are higher for the load calculations compared to the strength calculations. Important factors as the assumed pore pressure, worst case kick density and the amount of mud loss are often based on experience and are difficult to determine as a specific value. As we obtain more data, the prediction changes and it is not unusual that the pressure gradient plot that is provided after drilling is quite different from the initial pressure gradient plot.

Despite the earlier recommendations, it was not necessary to have more than  $10^6$  Monte Carlo simulations. The code was run multiple times with  $10^6$  Monte Carlo simulation and some variations in the results were observed. However, the final decision was not affected by the variation since the target probability was set to be  $10^{-6}$  to  $10^{-5}$  and the variation of the results were in the  $10^{-6}$  degree.

#### 4.1.2.1 API ad-hoc burst

The following parameters were used for the API ad-hoc burst simulation. A 13 3/8” casing with a thickness equal to 0.580” was used in these simulations.

Parameter	Value
Number of Monte Carlo simulations	$10^6$
Planned well depth (12 1/4” hole)	4500 m
Seawater depth	400 m
Pore pressure (worst case)	1.5 sg
Triangle distribution for pore pressure for RBD5	T(1.45,1.47,1.5)
Gas density (worst case)	0.3 sg
Triangle distribution for gas density for RBD5	T(0.3,0.4,0.5)
Ultimate yield, N80	100 000 psi
Yield, N80	80 000 psi
Ultimate yield, L80	95 000 psi
Yield, L80	80 000 psi
Outer Diameter	13 3/8 in
Wall thickness	0.580 in

*Table 4.8 Parameters used for API ad-hoc burst simulation*

The values used for distribution of the models as well as the parameters are listed in table 4.4 and table 4.5.

The first model considered for reliability based casing design is the API ad-hoc burst model. The model is called API ad-hoc Barlow in API 5C3. As mentioned, ad-hoc means that the ultimate yield value is used rather than the nominal yield strength. The results obtained from the simulations are the burst load, burst strength mean, burst strength standard deviation, P10 and P90 values which are given in bar. We have also obtained the probability of failure which is given in percentage. N80, L80 and K55 casing grades has been simulated. The strongest casing grade was



simulated first, and then the casing grade was decreased as much as possible so that the requirements for a high consequence of failure was met.

First, reliability based design level 4 will be considered. The plot and the simulation results are shown in figure 4.4 and table 4.9. The MATLAB code for API RBD4 burst simulations are given in Appendix A.1.2. For the RBD4 simulation, the casing grade is chosen to be N80. The load is assumed to be the worst case scenario which means that the gas density is equal to 0.3 s.g as shown in table 4.8.

The burst load is calculated as follows

$$P_{burst\ load} = P_{internal} - P_{external}$$

$$P_{burst\ load} = pore\ pressure * welldepth * 0.0981 - 0.0981 * (welldepth - seawater\ depth) * gasdensity - 0.0981 * 1.03 * seawater\ depth$$

The blue curve represents one single value for the burst load for this case study. According to our simulation using the API ad-hoc equation for burst strength we obtain a probability of failure of 0.0001 % = 10<sup>-6</sup>. This satisfies the recommended target probability for a high consequence scenario.

The burst load is calculated to be 501 bar and the burst strength mean is 782 bar. For our burst strength output data, 80% of the values are between 857 bar and 709 bar which means that we have a spread of data equal to 148 bar.

T =

<b>Burst_load</b>	<b>Burst_strength_mean</b>	<b>Burst_strength_stdv</b>	<b>P10</b>	<b>P90</b>	<b>Probability_of_failure</b>
501.09	782.48	57.672	709.43	857.14	0.0001

Table 4.9 Results obtained from simulation, RBD4, N80

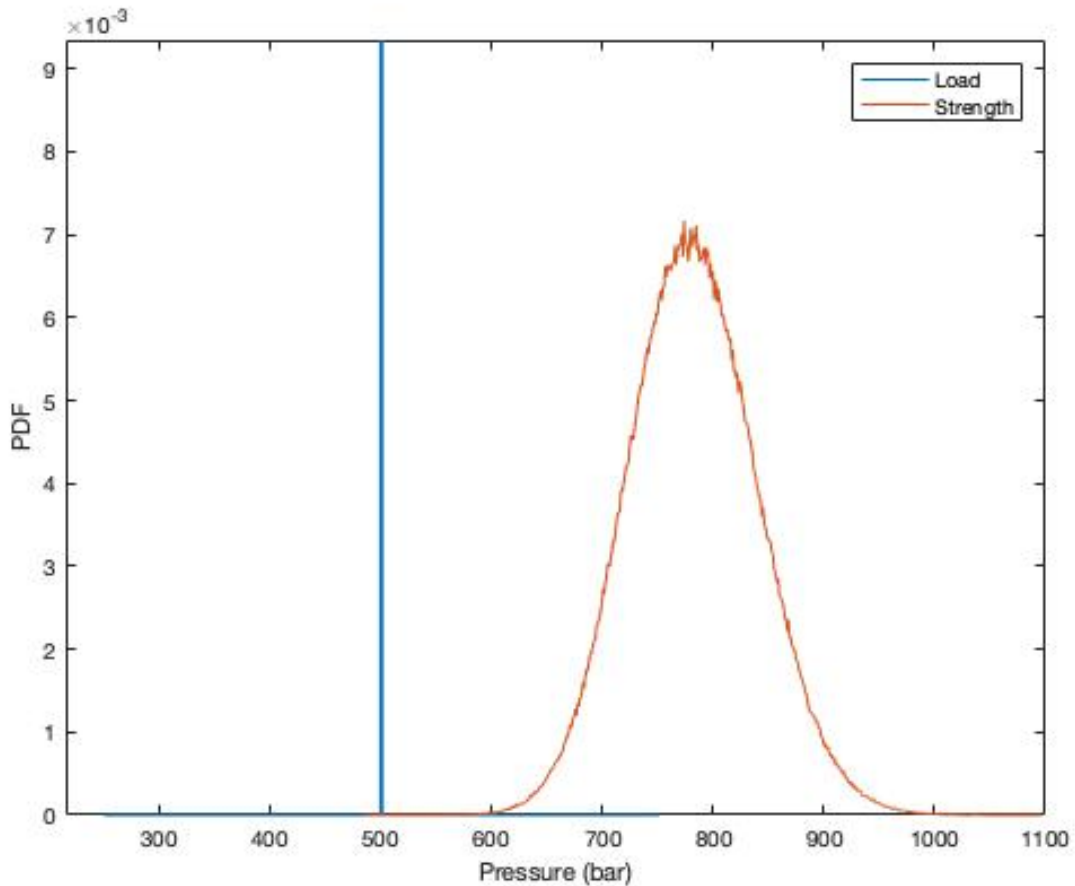


Figure 4.4 API Burst Scenario RBD4, N80

When calculating the burst strength of the casing, distribution for the different input parameters in the API ad-hoc equations were considered as well as a distribution for the model error. As mentioned, these values are given in table 4.4 and 4.5.

Overall, according to the RBD4 analysis a grade equal to N80 can be chosen for this scenario.

The burst strength calculation in RBD5 were performed in the same way as for RBD4, however N80 resulted in a probability of failure equal to 0. Due to this the grade was changed from N80 simulations to L80 for the RBD5 simulation.

The results from RBD5 are shown in table 4.10 and in figure 4.5. The MATLAB code for API RBD5 burst simulations is given in Appendix A.1.3. The load scenario used for the simulation is a gas filled casing, and as mentioned the uncertainty regarding the parameters used for the load calculation is usually higher compared to the strength calculation.

For these simulations, a triangle distribution was added to the gas density as well as in the pore pressure. As mentioned RBD5 is less conservative than RBD4. Due to this, the triangular distribution for the pore pressure in the RBD5 simulation is  $T(1.45, 1.47, 1.5)$ , where 1.5 sg, which is the worst case, is set as the maximum value, 1.47 sg the most likely value and 1.4 as the minimum value. A distribution for the gas density is also included and the triangular distribution is given as  $T(0.3, 0.4, 0.5)$  where the maximum value is set to 0.5 sg, most likely is set to 0.4 sg and the minimum and worst case is set to 0.3 sg.

Similar to the previous simulations, all the values are given in bar with the exception of the probability of failure which is given in percentage.

For the level 5 analysis we obtain a probability of failure equal to  $0.0001\% = 10^{-6}$  and we satisfies our target probability for a high consequence failure. The burst load mean is calculated to be 449 bar and the burst strength mean has a value of 683 bar.

As for the spread of the load data, 80% of the burst load output data are between 472 bar and 426 bar which gives a range of 46 bar. Similarly, 80% of the burst strength output data are between 750 bar and 618 bar which gives a range of 132 bar.

	<b>mean</b>	<b>stdv</b>	<b>P10</b>	<b>P90</b>	<b>Probability_of_failure</b>
<b>Burst load</b>	449.13	17.054	426.29	471.96	0.0001
<b>Burst strength</b>	683.3	51.856	617.57	750.42	0.0001

Table 4.10 Results obtained from simulations RBD5, L80

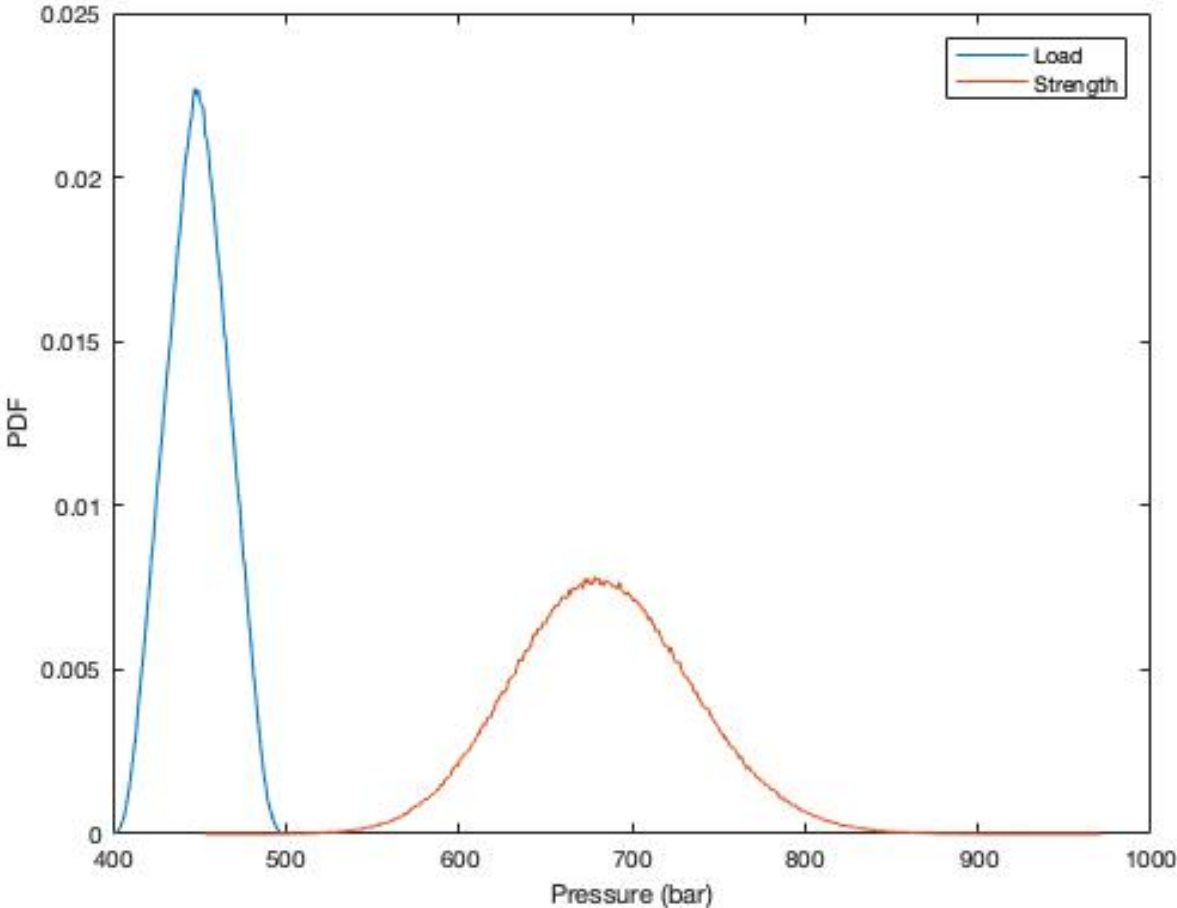


Figure 4.5 API Burst RBD5, L80

According to RBD5 burst simulations with API ad-hoc as the strength model, a 13 3/8” casing with a thickness equal to 0.580” and the grade L80 satisfies our requirements.

#### 4.1.2.2 Klever-Stewart rupture model

The other model used for burst calculations is the Klever-Stewart rupture model. Based on earlier comparison, this model will be a more accurate model due to the smaller spread in strength data. It is also the recommended model for a limit state analysis according to the API 5C3 standard.

The following parameters were used for the Klever-Stewart burst simulations

Parameter	Value
Number of Monte Carlo simulations	10 <sup>6</sup>
Planned well depth (12 ¼" hole)	4500 m
Seawater depth	400 m
Pore pressure	1.5 sg
Triangle distribution for pore pressure	T(1.45,1.47,1.5)
Triangle distribution for gas density	T(0.3,0.4,0.5)
Ultimate yield, N80	100 000 psi
Yield, N80	80 000 psi
Ultimate yield, L80	95 000 psi
Yield, L80	80 000 psi
Ultimate yield, K55	95 000 psi
Yield, K55	55 000 psi
Outer Diameter	13 3/8 in
Wall thickness	0.580 in
n for N80/L80	0.104
n for K55	0.125

*Table 4.11 Parameters used for Klever-Stewart burst simulations*

The following assumption have been made for the Klever-Stewart simulations

- No casing wear
- A smooth pipe
- Minimum wall thickness is equal to nominal wall thickness

Model distribution and parameter distribution used in these simulations are given in table 4.4 and 4.5 and note that the distribution for ultimate yield strength is assumed to be equal to the distribution for nominal yield strength.

First we look at RBD4. The MATLAB code for the simulation is provided in Appendix A.1.4, and the results are presented in figure 4.6 and table 4.12. The casing grade chosen for RBD4 simulations were N80. Simulations for L80 and K55 were performed as well, however the probability of failure did not meet the requirements.

When considering the Klever-Stewart model RBD4, we obtain a burst load equal to 501 bar. Burst strength mean is equal to 765 bar and 80% of the burst strength output data are between 827 bar and 705 bar which give a range of 122 bar.

According to this simulation we obtain a 0 % probability of failure and we satisfy the recommended target probability for a high consequence failure scenario. This is a lower value than what we obtained for the API ad-hoc even though the burst strength for the Klever-Stewart model is lower than for the API ad-hoc model. Simulations were done for grade equal to L80 as well, however the calculated probability of failure was equal to  $0.0025\% = 2.5 \times 10^{-5}$  which is higher than the recommended target probability for a high consequence of failure scenario.

Burst_load	Burst_strenght_mean	Burst_strength_stdv	P10	P90	Probability_of_failure
501.09	765.38	47.663	704.83	826.88	0

Table 4.12 Results from RBD4 simulation, burst, N80

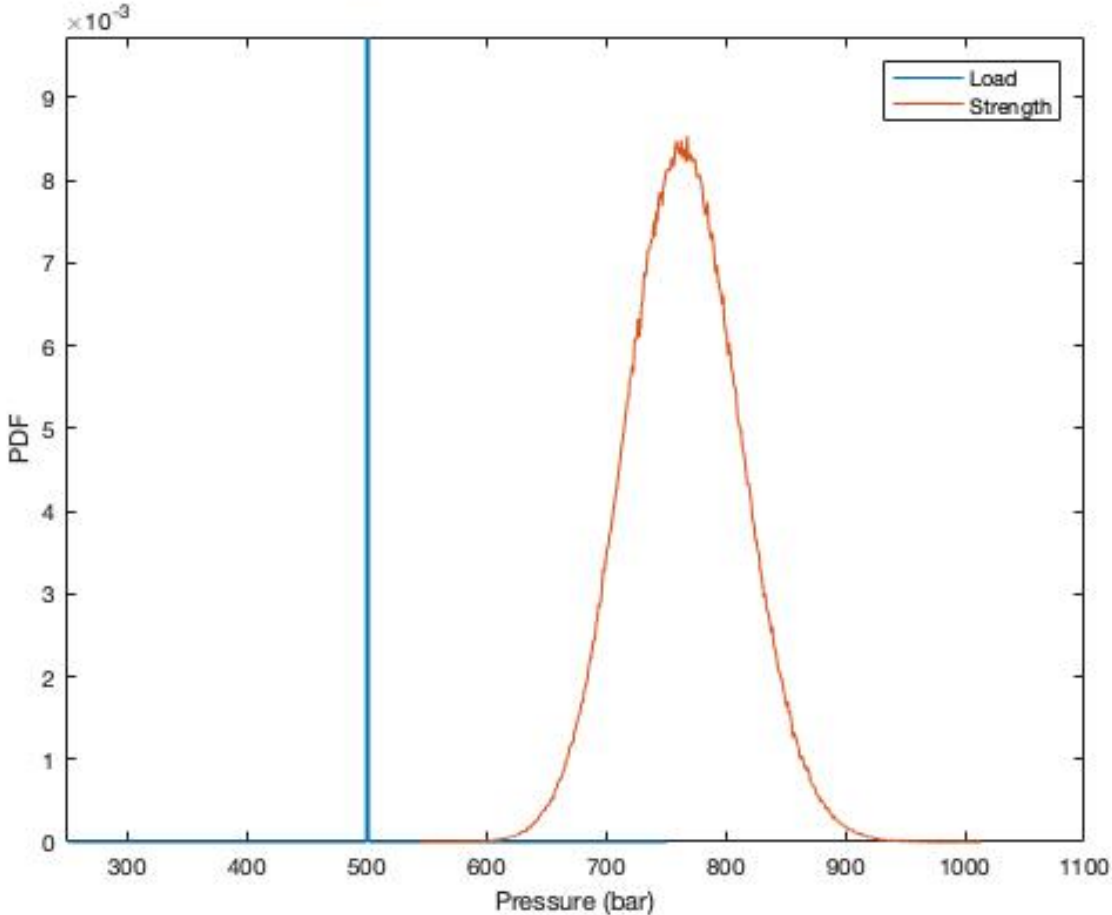


Figure 4.6 Klever-Stewart Burst RBD4, N80

For level 4, Klever-Stewart simulation, N80 grade with a thickness equal to 0.580” for the 13 3/8” casing meets our requirements.

When considering the burst load for the level 5 analysis, an uncertainty in the pore pressure and the gas density was added the same way as for the RBD5 simulation for the API ad hoc model. The MATLAB code for Klever-Stewart RBD5 burst simulations is given in Appendix A.1.5.

The burst load data for RBD5 is calculated the same way as for API ad-hoc. A triangular distribution for the gas density and pore pressure was added as shown in table 4.11. As implied earlier, RBD4 uses worst case scenario loads which means that RBD5 gives a less conservative result.

The result of the simulation is shown in table 4.13 and figure 4.7. Note that for RBD5, the casing grade is changed to K55.

From this simulation, we obtain a probability of failure equal to  $0.0001\% = 10^{-6}$  which again satisfies the recommended target probability. Simulations were performed for L80 as well and the results from that simulation was a probability of failure equal to zero. Both L80 and K55 have the same ultimate yield strength, however a different n – value. As mentioned, the n-value is different for each casing grade and they are listed in table 4.2.

The burst load mean is 449 bar and the burst strength mean is 730 bar. As for the spread of data, 80% of the burst load calculations is between 472 bar and 426 bar, which gives a range equal to 46 bar. Similarly, 80% of the burst strength calculations are between 806 bar and 654 bar which gives a range of 152bar.

	<b>mean</b>	<b>stdv</b>	<b>P10</b>	<b>P90</b>	<b>Probability_of_failure</b>
<b>Burst load</b>	449.12	17.028	426.29	471.93	0.0001
<b>Burst strength</b>	729.51	59.124	654.29	805.8	0.0001

*Table 4.13 Results from RBD5 simulation, burst, K55*

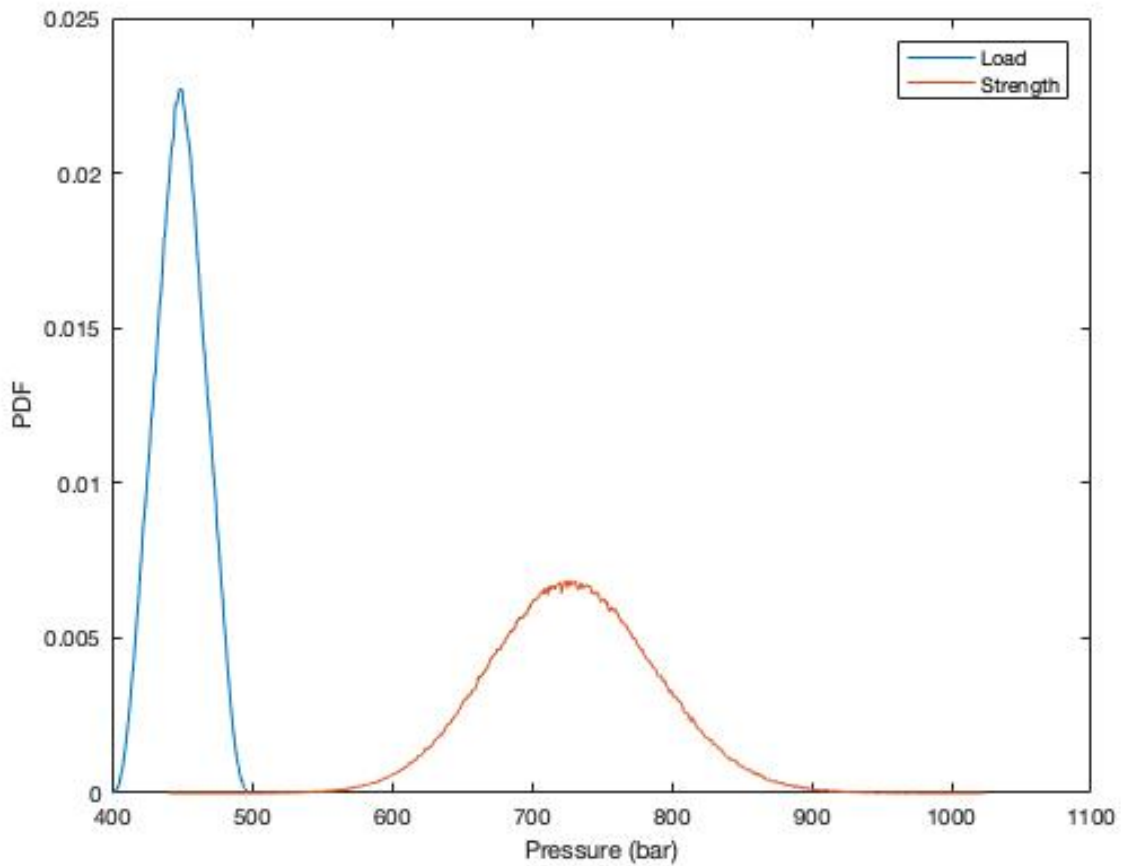


Figure 4.7 Klever-Stewart Burst RBD5, K55

According to these simulations, a 13 3/8” casing with a thickness equal to 0.580” and a grade K55 is sufficient to satisfy our requirements when using the Klever-Stewart Rupture limit model.

To further show the difference between the API ad-hoc model and Klever-Stewart model, simulations using both strength models were performed using the following grades

Burst model	Casing grade	Spread
API ad-hoc	L80	132 bar
	N80	148 bar
	K55	175 bar
Klever-Stewart	L80	108 bar
	N80	122 bar
	K55	152 bar

From these results we see that for the same grade, Klever-Stewart model clearly gives a smaller spread than the API ad-hoc. The overall result from the two models is that Klever-Stewart allows us to choose lower casing grades compared to the API ad-hoc model even though Klever-Stewart gives a lower burst strength mean than API ad-hoc.

### 4.1.3 Working stress design

As for the following calculation, it is assumed that we have seawater behind the 13 3/8” intermediate casing. In order to calculate the burst load, the internal and external pressure at the wellhead is calculated. For the following calculations, we assume a closed well and do not account for casing wear.

To calculate the burst load, we start by calculating the BHP as shown in equation (4.6)

$$\begin{aligned} BHP &= g * \rho_{pore} * \text{depth of the next hole section} \\ &= 0.0981 * 1.5 \text{ s. } g * 4500 \text{ m} = 662 \text{ bar} \end{aligned} \quad (4.6)$$

When the BHP is calculated, we continue to calculate the external pressure at the critical point of the wellbore. For burst load, the depth that will give the highest burst load will occur at the wellhead.

The external pressure at wellhead is shown in equation (4.7).

$$\begin{aligned} P_{External,WH} &= g * \rho_{sw} * \text{depth to seabed} \\ &= 0.0981 * 1.03 \text{ s. } g * 400\text{m} = 40 \text{ bar} \end{aligned} \quad (4.7)$$

A burst load is the pressure difference between the external and internal pressure. In order to further calculate the burst load the internal pressure at the wellhead. Since we are considering a closed well, the calculations are based on the BHP which is already calculated.

The internal pressure at the wellhead is shown in equation (4.10)

$$\begin{aligned} P_{Internal,WH} &= BHP - g * \rho_{ff} * (\text{depth of open hole} - \text{depth to seabed}) \\ &= 662 - 0.0981 * 0.3 \text{ s. } g * (4500\text{m} - 400\text{m}) = 541 \text{ bar} \end{aligned} \quad (4.8)$$

As both the external and internal pressure are calculated, the burst load can be determined. And the calculated burst load is shown in equation(4.11)

$$\Delta P_{burst,WH} = 541 \text{ bar} - 40 \text{ bar} = 501\text{bar} \quad (4.9)$$

The NORSOK safety factor for burst is 1.1 which means that the required burst strength for the 13 3/8” casing becomes

$$501.112 \text{ bar} * 1.1 = 551 \text{ bar}$$

According to this calculations P110 13 3/8” casing, with a thickness equal to 0.580” satisfies our requirements. This is much higher grade compared to what was suggested by RBD where both API ad-hoc and Klever-Stewart suggested lower casing grades.



## 4.2 Collapse load

For the collapse load, we will assume a loss to thief zone scenario. As we did for the burst scenario, the focus will be on the 13 3/8" casing for the collapse load as well. It is assumed that the loss to a thief zone happens when we start drilling the next hole section and a sketch is provided in figure 4.8.

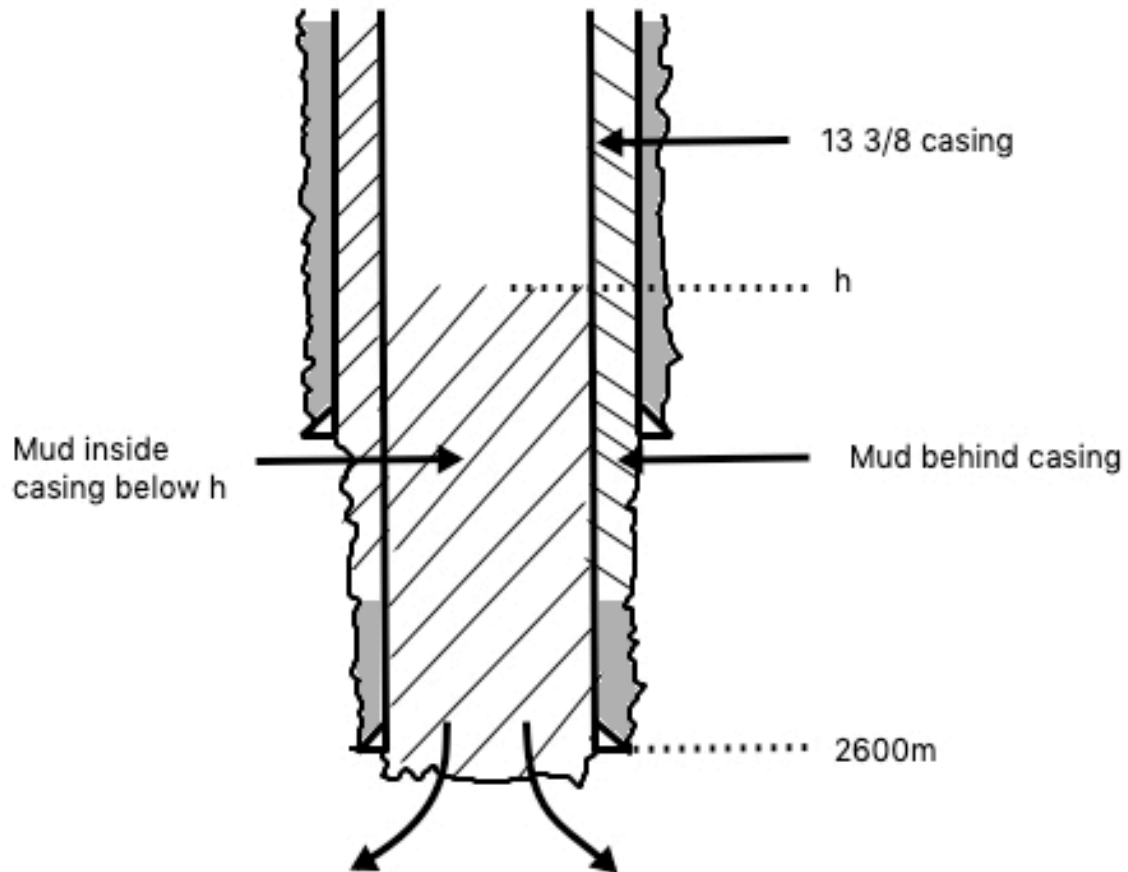


Figure 4.8 Sketch of loss to thief zone scenario

As illustrated, we assume mud both inside and outside the casing. Worst case scenario for loss to thief zone is that the mud level has stabilized at a depth =  $h$  so that the pressure is equal to the seawater gradient.

The parameters used for the collapse calculations are as follows

Depth of 13 3/8" casing shoe: 2600m

Depth to sea level: 25m

Pore pressure for next section: 1.5 s.g

Fracture gradient at 13 3/8" shoe: 1.95 s.g

Mud density: 1.7 s.g

### 4.2.1 Collapse models

For the collapse calculations, the only model considered in this thesis is the API model. The API model can be found in API 5C3 standard.

The API model is divided into four equations which are elastic collapse, transitional collapse, plastic collapse and yield collapse. In order to determine the correct equation, one calculated the  $(D/t)$  ratio. Figure 4.9 shows an illustration of the collapse pressure as a function of the  $(D/t)$  ratio for a L80 tubing.

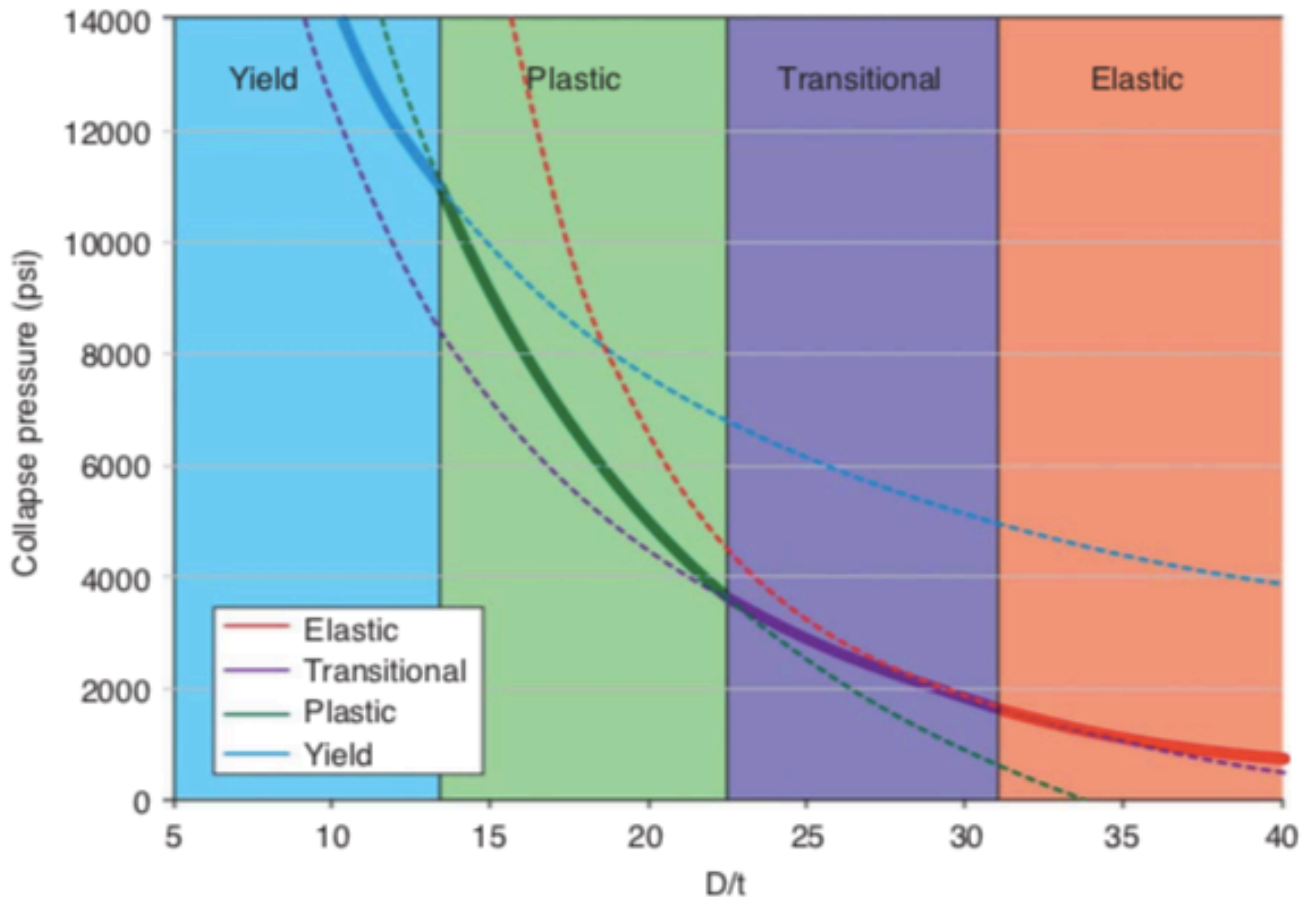


Figure 4.9 Collapse pressure vs slenderness for a L-80 tubing (Bellarby, 2009)

Shortly explained, if one is to use the equation of yield collapse if we are in the elastic collapse ratio, the collapse strength will be overestimated as shown by the blue dotted line. By looking at figure 4.9 one can also see that if one is to use the equation for plastic collapse in a transitional or elastic collapse ratio, the collapse strength will be underestimated as shown by the green dotted line.

The different collapse equations are listed below

Elastic collapse: 
$$P_e = \frac{46.95 * 10^6}{\left(\frac{D}{t}\right) \left[\left(\frac{D}{t}\right) - 1\right]^2} \quad (4.10)$$

Transitional collapse: 
$$P_t = \sigma_y \left( \frac{F}{\left(\frac{D}{t}\right)} - G \right) \quad (4.11)$$

Plastic collapse: 
$$P_p = \sigma_y \left[ \frac{A}{\left(\frac{D}{t}\right)} - B \right] - C \quad (4.12)$$

Yield collapse: 
$$P_y = 2 \sigma_y \left[ \frac{\left(\frac{D}{t}\right) - 1}{\left(\frac{D}{t}\right)^2} \right] \quad (4.13)$$

(API, 2018)

Where D is the outer diameter of the casing, t is the thickness,  $\sigma_y$  is the yield strength and the parameters A, B, C, F and G are found in API 5C3 or Appendix A.2, table A.2.3. The parameters can also be calculated by formulas found in API 5C3. All the equations above are valid for zero axial stress and zero internal pressure (API, 2018)

As mentioned earlier, there are other collapse models as for example Timoshenko and Klever Tamano (Aadnøy et al., 2009). The API model is based on experiments on K55, N80 and P110 specimens with different (D/t) ratios and different material imperfections (Aadnøy et al., 2009). However, when looking at ultimate collapse strength, API 5C3 recommends Klever-Tamano as the most suitable model.

Collapse strength is highly affected by axial load. In order to account for this, the API equation uses an adjusted yield strength which is given in the equation below (Aadnøy et al., 2009)

$$\sigma_{yield_{pa}} = \left( \sqrt{1 - 0.75 \left(\frac{\sigma_a}{\sigma_y}\right)^2} - 0.5 * \frac{\sigma_a}{\sigma_y} \right) * \sigma_y \quad (4.14)$$

Where  $\sigma_a$  is given by

$$\sigma_a = \frac{F_a}{\pi (r_o^2 - r_i^2)} \pm \sigma_b \quad (4.15)$$

Where  $F_a$  is the axial force,  $r_o$  is the outer radius,  $r_i$  the inner radius and  $\sigma_b$  is the bending stress (Aadnøy et al., 2009).

#### 4.2.2 Working stress design

As mentioned, it is assumed that the mud level will stabilize at a depth  $h$ . At this depth, the pressure is equal to the seawater gradient and is calculated as shown below

$$g * \rho_{seawater} * (depth_{casing} - depth_{sea\ level}) = g * \rho_{mud} * (depth_{casing} - h)$$

$$depth_{casing} - h = \frac{\rho_{seawater}}{\rho_{mud}} (depth_{casing} - depth_{sea\ level})$$

$$h = depth_{casing} - \frac{\rho_{seawater}}{\rho_{mud}} (depth_{casing} - depth_{sea\ level}) \quad (4.16)$$

$$h = 2600m - \frac{1.03sg}{1.7sg} * (2600m - 25m) = 1039.9m \approx 1040m$$

The largest differential pressure in the casing is at depth =  $h$ . Here, the internal pressure is equal to 0 since we assume air above the mud. We also assume mud outside the casing which gives an external pressure equal to

$$p_{external} = \rho_{mud} * g * h \quad (4.17)$$

$$p_{external} = 1.7 * 0.0981 * 1040 = 173.44\ bar \approx 173\ bar$$

As mentioned, the internal pressure is equal to zero which means that the collapse load is equal to

$$p_c = p_{external} - p_{internal} = 173\ bar - 0\ bar = 173\ bar \quad (4.18)$$

The collapse resistance of the material is highly effected by axial loading. This means that both the safety factor and a biaxial correction needs to be taken into account.

The collapse load is calculated to 173 bar and according to NORSOK D-10, a safety factor equal to 1.1 must be applied and the collapse load that the casing must be able to withstand is equal to

$$173\ bar * 1.1 = 190.3\ bar$$

To be able to perform a biaxial correction, the axial load/strength ratio is calculated.

For this case we neglect the effect of bending and the axial loading is equal to the weight of the string multiplied with the buoyancy factor. The grade equal to L80 and thickness equal to 0.580"

has been chosen for this design and the axial load calculation are performed below. All data used for the axial load calculation is found in DDH.

$$F_a = weight_{air} * \beta$$

$$F_a = nominal\ weight\ per\ meter * length\ of\ casing * \beta$$

$$F_a = nominal\ weight\ per\ meter * length\ of\ casing * \left(1 - \frac{\rho_{mud}}{\rho_{steel}}\right)$$

$$F_a = 117.8 \frac{daN}{m} * 2600\ m * \left(1 - \frac{1.7sg}{7.8sg}\right) = 239.527 * 10^3 daN$$

Assuming that L80 satisfies our requirements, the load/strength ratio is equal to

$$\frac{Axial\ load}{Axial\ strength} = \frac{239.527 * 10^3 daN}{830 * 10^3 daN} = 0.29$$

The ellipse of plasticity given in figure 2.7 is used to find the collapse resistance reduction factor. In this case, it is equal to 0.83. This gives the new collapse strength equal to

$$Collapse\ strength = 23.8\ MPa * 0.83 = 19.754\ MPa = 197.54\ bar$$

The reduced collapse strength satisfies both our biaxial correction as well as the safety factor and according to this calculations, the choice of casing is 13 3/8", with a thickness equal to 0.580" and grade equal to L80 meets our requirements.

By applying the biaxial correction and assuming that K55 was a suitable choice results in a new collapse strength equal to 146.88 bar = 147 bar. When comparing to our load calculations, the reduced collapse strength is too low to satisfy the criteria for a safety factor equal to 1.1.

### 4.2.3 Reliability based design, API

Due to the complexity of the different collapse models available, the API collapse model was used in this thesis for the reliability based design. The MATLAB code used in these simulations are provided in Appendix A.1.6 and Appendix A.1.7.

Drilling Data Handbook is based on the API equations, which means that if no errors are introduced, the collapse strength calculated by the MATLAB script should be the same as the value provided in the tables in DDH when using single input values. For the verification of this scenario, the single input values were equal to the following

Thickness = 0.580”  
 Outer diameter = 13 3/8”  
 Yield strength = 55 000 psi

For collapse strength calculations, it’s important to choose the correct collapse equation. The MATLAB script calculates A, B, C, F and G and uses an if-else statement in order to determine the correct collapse equation. The equations for the parameters and the different collapse strength equations is found in API 5C3.

When the single values listed above were used in the simulations and the model error was not account for, the burst strength was equal to value found in DDH. DDH is based on API models which means that the script is reliable.

The parameters used for the collapse simulations are given in table 4.14

Parameter	Value
Number of Monte Carlo simulations	10 <sup>6</sup>
13 3/8 casing shoe depth	2600 m
Seawater depth	400 m
Mud density	1.7 sg
Triangular distribution for mud loss in casing	T(0,0.5,1)
Yield, K55	55 000 psi
Outer Diameter	13 3/8 in
Wall thickness	0.580 in
Cross - sectional area	23.31 in <sup>2</sup>
Nominal weight	80.7 lb/ft

*Table 4.14 Parameters for collapse simulation*

A number of 10<sup>6</sup> Monte Carlo simulations was chosen for the collapse simulations. For the collapse case, we use the yield strength rather than the ultimate yield since this is what is used in the API model. This means that the consequence of failure is deformation of the pipe rather than collapse failure. If a collapse failure is to occur, the well might still function as normal however with restricted access. Based on these assumptions, the target probability for the collapse design is set to 10<sup>-3</sup>, a low consequence failure scenario. Similar to burst, some variations in the results were observed. However, in such low degree so that it did not affect the final result in the same way as for burst.

Based on my experience and multiple separate simulations, 10<sup>6</sup> Monte Carlo simulations was sufficient for the collapse scenario.

The values used for model error and input parameters in the model are listed in table 4.15 and 4.16.

Parameter	Name of table in API 5C3	Mean	COV	Standard Deviation (Stdv = COV * mean)
Nominal yield strength for K55	F.3	Nominal yield * 1.23	0.0719	0.0719*mean <sub>nominal yield</sub>
Ultimate yield strength for K55*	F.3	Ultimate yield * 1.23	0.0719	0.0719*mean <sub>ultimate yield</sub>
Outer diameter**	F.4	Outer diameter* 1.0059	0.00181	0.00181*mean <sub>outer diameter</sub>
Thickness**	F.4	Thickness* 1.0069	0.0259	0.0259*mean <sub>thickness</sub>

Table 4.15 Distribution parameters used for the collapse simulations (API, 2018)

\* Assumed same parameters for ultimate yield strength as yield strength, values from CRS ensemble

\*\* Values from ensemble

Model	Name of table in API 5C3	Mean (Predicted/Actual)	COV (Predicted/Actual)	Standard Deviation (Stdv = COV * mean)
API	F.2	1.108*	0.008*	0.0089

Table 4.16 Model error for API collapse strength model (API, 2018)

\* Value from ensemble average

Both RBD4 and RBD5 were performed for the collapse scenario and a casing grade equal to K55 was chosen. First, we look at the level 4 simulations. The MATLAB code for the API collapse simulations is given in Appendix A.1.6.

Similar to RBD4 for burst, RBD4 uses the worst case scenario for its calculations for the collapse scenario as well. In other words, we assume loss of mud inside the casing until its pressure is equal to the sea water gradient. The results of the RBD4 simulation are given in table 4.17 and figure 4.10. The collapse load is calculated to be 173bar. The collapse strength mean is equal to 236 bar with a standard deviation equal to 16 bar. 80% of the strength calculations falls within the interval between 257 bar and 215 bar which gives a spread equal to 42 bar.

As mentioned, the API model uses the yield strength, which means we have a low consequence failure and a probability equal to  $0.0002\% = 2 * 10^{-6}$  which more than satisfies our recommended target probability. If the collapse scenario was a high consequence failure scenario, this probability of failure would satisfy that criteria as well.

<u>Collapse_load</u>	<u>Collapse_strength_mean</u>	<u>Collapse_strength_stdv</u>	<u>P10</u>	<u>P90</u>	<u>Probability_of_failure</u>
173.42	235.97	16.334	215.08	257.09	0.0002

Table 4.17 Results from RBD4 simulations, collapse, K55

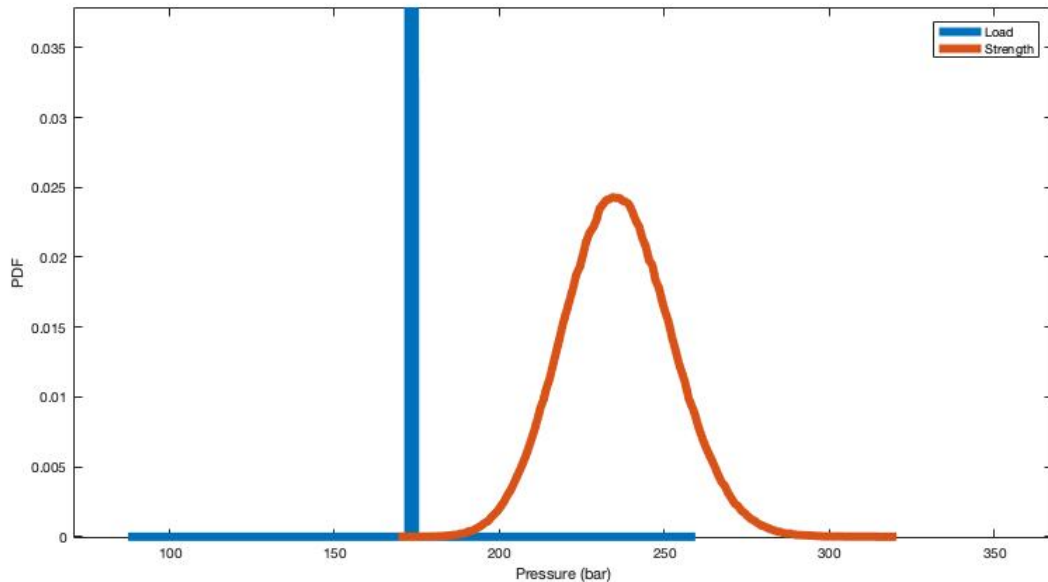


Figure 4.10 API collapse, RBD4

According to the RBD4 simulations, a grade equal to K55 is sufficient to meet our requirements. Simulations were performed for N80 and L80 as well, however they returned a probability of failure equal to zero. RBD4 shows that we are able to choose a lower casing grade according to these simulations compared to the results from the WSD.

The level 5 simulation has added an uncertainty in the amount of mud loss to the formation. The MATLAB code is given in Appendix A.1.7. In RBD4 a worst case scenario was considered which means that the mud level decreased until the pressure is equal to the sea water gradient and can be referred to as a 100% mud loss scenario. In order to add the uncertainty in the amount of mud lost to the formation, a triangular distribution was added. The most likely amount of mud loss is set to 50%, maximum is set to 100% and minimum is set to 0. The triangular distribution for mud loss is described as follows  $T(0,0.5,1) * h$ , where  $h$  is the depth the mud level will drop to if we have a 100% mud loss scenario.

The results from RBD5 are given in table 4.18 and figure 4.11. With the uncertainty added to the calculations, the collapse load is now reduced and the mean is calculated to be 87 bar with a standard deviation equal to 39 bar. 80% of the collapse load calculations are within 135 bar and 39 bar which gives a spread equal to 96 bar which is a quite large spread. This is due to the high uncertainty regarding the amount of mud loss. If the uncertainty regarding the mud loss was lower, the spread of the load data would be smaller.



As for the collapse strength, the mean is calculated to be equal to 236 bar with a standard deviation equal to 16 bar. 80% of the collapse strength values are between 257 bar and 215 bar which gives a spread equal to 42 bar. In other words, the strength calculations are the same as for RBD4. Since we have not changed the casing grade between RBD4 and RBD5 simulations, the only difference between the two levels is a change in the load calculations. When the uncertainty in the load was added, the probability of failure decreased to zero.

	<b>mean</b>	<b>stdv</b>	<b>P10</b>	<b>P90</b>	<b>Probability_of_failure</b>
<b>Collapse load</b>	86.751	35.426	38.769	134.72	0
<b>Collapse strength</b>	235.96	16.336	215.06	257.07	0

Table 4.18 Results from RBD5 simulation, collapse, K55

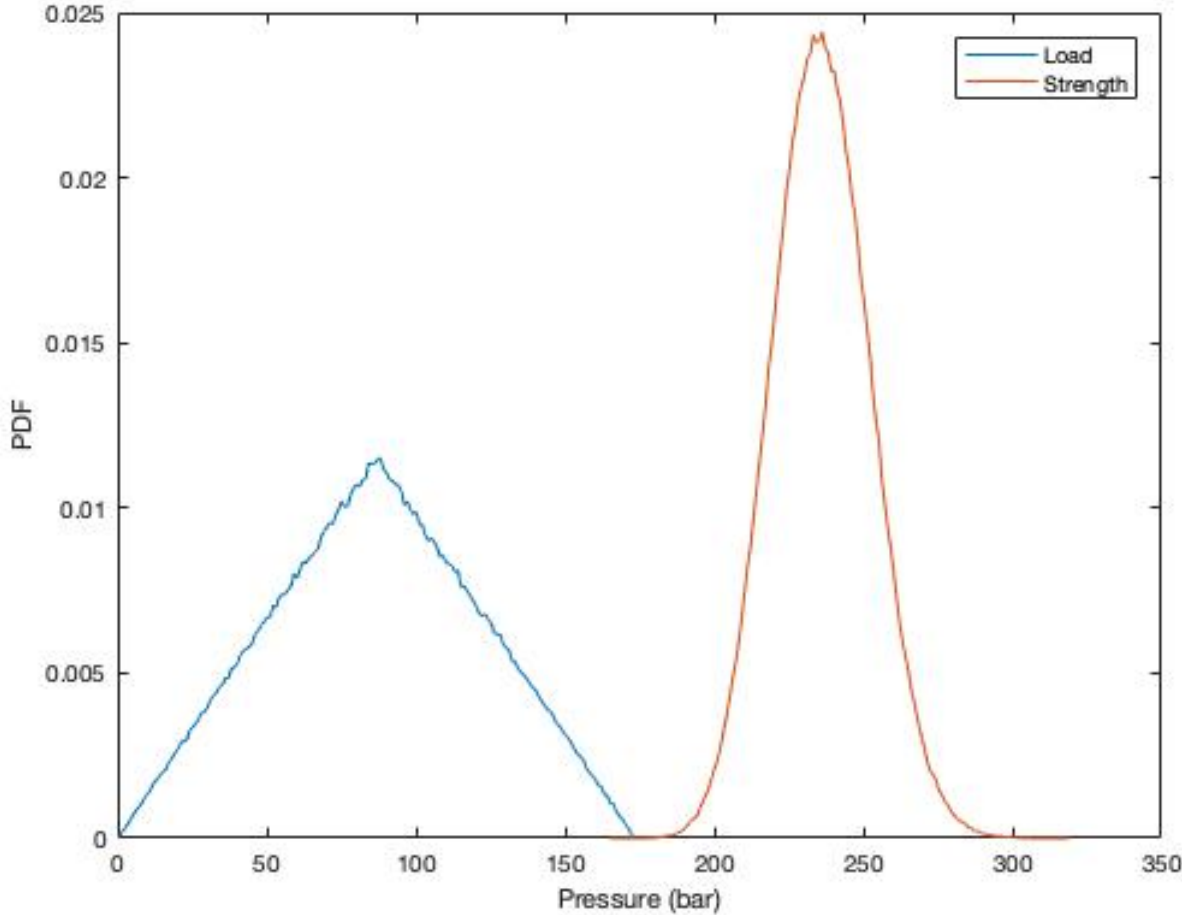


Figure 4.11 API collapse, RBD5

According to these simulations, the 13 3/8” casing with a thickness equal to 0.580” and the grade K55 can be chosen to satisfy our requirements for a RBD5 analysis.

### 4.3 Casing selection

To summarize and compare, the casing selections for each simulation are shown in table 4.19.

	Design method	Casing selection, 13 3/8"	Probability of failure
Burst	API ad-hoc level 4	N80	$10^{-6}$
	API ad-hoc level 5	L80	$10^{-6}$
	Klever-Stewart level 4	N80	0
	Klever-Stewart level 5	K55	$10^{-6}$
	Working stress design	P110	
Collapse	API level 4	K55	$2 * 10^{-6}$
	API level 5	K55	0
	Working stress design	L80	

*Table 4.19 Summary of casing selection*

One thing to note is that the working stress design method considered the yield strength rather than the ultimate yield strength. This means that according to WSD for burst, a grade equal to P110 is necessary to uphold a safety factor of 1.1 and prevent yielding when considering the worst case scenario.

The RBD design for burst considers the ultimate yield strength. RBD4 resulted in casing grade equal to N80 for both API ad-hoc and Klever-Stewart. The results from RBD5 showed that we could choose an even lower casing grade for both models. According to RBD5 with API ad-hoc model, a grade equal to L80 was sufficient, however RBD5 with Klever-Stewart model determined that K55 was sufficient.

For the RBD design, a target probability has been used rather than a safety factor. The target probability was set to  $10^{-6}/10^{-5}$  for a high consequence failure for the burst simulations.

When looking at the collapse design, WSD determined that L80 was necessary in order to uphold the NORSOK safety factor of 1.1. A biaxial correction was taken into account, however bending was neglected.

The reliability based design used the API model when simulating the collapse scenario. When no correction factors or distributions are taken into account the calculated collapse strength using the API model provided the same value that was listed in Drilling Data Handbook. The simulations showed that the casing grade requirement is reduced to K55 for both level 4 and level 5 simulations. The target probability for collapse was set to be  $10^{-3}$  to  $10^{-2}$ , K55 also met the requirements for a high consequence of failure.

For the intermediate section, the determining load scenario is burst. This might change if another case was considered.

The overall overview shows that for both burst and collapse, RBD results in a lower casing grade requirement than WSD.

Klever-Stewart model also seems to give a lower probability of failure than API ad-hoc even though ultimate yield is used in both models and API ad-hoc has a slightly higher mean for the burst strength. This is most likely caused by reduced spread in the Klever-Stewart burst strength distribution.

## 5 Discussion and conclusion

The reliability based design is a well-known design method and widely used in other industries. For the petroleum industry, the method has been used in some scenarios but there is still some scepticism for the method. Working stress design has been the “go to” method and its simplicity makes it easy to understand. As for the results presented in this thesis, the working stress design suggests a higher grade requirement for the casing selection of the 13 3/8” intermediate section than reliability based design for the loads considered in this case study. As shown in the previous chapter, the difference in the suggested casing grade between the two methods are noticeable. For the intermediate section considered here, the burst scenario is the determining factor when it comes to choice of casing grade.

When considering WSD, the choice of casing grade becomes the P110. This is with a design factor equal to 1.1. When using RBD4, both the Klever-Stewart rupture model and API ad-hoc shows that a casing grade equal to N80 is sufficient and we obtain a probability of failure so that the recommended target probability is fulfilled.

RBD4 resulted in a more strict requirement for the casing grade compared to RBD5 for the given probability of failure. For instance, when using Klever-Stewart for the burst calculations, the RBD4 required an N80 casing while RBD5 resulted in a K55 casing. Hence the probability of failure decreased from RBD4 to RBD5 and it was possible to choose an even lower casing grade. The reason for this is that in RBD4, worst case assumption are made for the load calculation. However, when using RBD5 the worst case assumptions are reduced and the load is calculated probabilistically. The input parameters for the load calculations will be distributions which are less conservative than the “extreme” single values used in the RBD4 approach.

In other words, RBD suggests a cheaper design compared to the WSD. One of the outputs from RBD is the probability of failure which makes it possible to make a risk assessment of the design. When using the reliability based design, one have the opportunity to modify the probability of failure and determine how “safe” the design should be. This means that we will have a specific value to work with so that we can determine the degree of safety. As for the working stress design, if the strength of the material is larger than the load including a safety factor, we have a safe design. However, we do not have the possibility to pinpoint how safe the design is. It is important to note that the working stress design uses nominal values which means that the uncertainties of the parameters are not taken into account.

One of the limitation regarding RBD is the amount of data needed in order to do a good design. We have seen in the collapse simulations that when the uncertainty in the load was added (RBD5) we obtained a large spread in the load data due to subjective assumptions. As for the strength calculations, the API 5C3 standard provides mean and COV values for most of the parameters, however some assumptions were made for some parameters due to lack of data. One example of this was as for the ultimate yield strength.

At the beginning of this work, it was difficult to get a full overview over what the API 5C3 standards actually provided in forms of data and a noticeable amount of time was used in order to get a proper overview of the data available and helpful for my purposes.

As mentioned in the introduction, there are a large variety regarding safety factor requirements. On the NCS, the NORSOK D-010 standard is followed and provides set limits for wells there. When determining a target probability, the same variations may occur and decision will be made based on experience and subjective opinions. As mentioned, Suryanarayana and Lewis (2016) gave some recommendations regarding the target probability for a low consequence of failure and a high consequence of failure. They considered the target probabilities from other industries and structures and gave a recommendation based on them. It is mentioned in the paper that the target probabilities for high and low consequence of failure were conservative, however they were used as target probabilities in this thesis.

Overall, my recommendation is to use the reliability based design if the necessary data is available. Here, the challenge when using the reliability based design is to define the limit for when the design is considered safe. As mentioned, the method provides a probability of failure, however the decision whether a probability of failure equal to 0.003% is acceptable rather than 0.0003% is a subjective decision. The NORSOK D-10 standard provided requirements regarding the design factor and the standard should, in a similar way, provide requirements for the probability of failure of the different loads.

Standards as NORSOK D-10 and ISO should have a recommended target probability for the different load cases similar to the requirements regarding the safety factor. As mentioned earlier recommended target probabilities are equal to  $10^{-6}$  for a high consequence failure and  $10^{-3}$  for a low consequence failure. In my perspective, the low consequence failure is designing for a service load where the consequence of failure is yielding of the casing. However, when using the ultimate strength of the casing, the consequence of failure is burst or collapse of the casing string which again can lead to a blow out or severe damage on equipment.

For the burst scenario, the consequence is burst of the casing. This means rupture of the casing and loss of a barrier. This may cause an uncontrolled kick which further can lead to a full blow out and severe human injuries as well as environmental issues. I see this as a high consequence of failure and will therefore place the burst scenario in this category. These assumptions are based on the use of a rupture limit model when doing the strength calculations. For the collapse scenario, a collapse casing can still function as normal. There may be restricted access when intervention work is to be performed and there might also be some restricted flow from a production well, however the casing is still intact and worst case is that it has to be replaced. For the collapse simulations in this thesis, the yield strength was used which means that failure is deformation of the material rather than full collapse. Independent of the model used, I would categorize the collapse failure as a low consequence failure scenario.

This thesis did not focus on the axial strength and axial load other than the biaxial correction when calculating the collapse strength. If the casing is to experience axial failure, the consequence is a parted pipe. This means rupture of the material in the same way as for the burst scenario, and we will lose a barrier element in the same way as for burst. Considering this, I would categorize axial failure as a high consequence failure. This means that the suggested target probabilities and the corresponding safety factors are presented in table 5.1.

Failure	Safety factor according to NORSOK D-010	Suggested target probability
Burst	1.1	$10^{-6}$
Collapse	1.1	$10^{-4}$
Axial	1.25	$10^{-6}$

*Table 5.1 Suggested target probabilities and corresponding safety factors*

The overall conclusion is that reliability based design gives a cheaper design as well as a possibility to do a risk assessment, compared to the working stress design. The determining factor for the intermediate section for the case considered here is the burst load.

There are many assumptions regarding the load calculations including the pore pressure, the gas density and the amount of mud loss to formation just to mention some. These are often a subjective assumption and made by teams and the information available at the time, however my recommendation based on the experience given in this thesis, is to use the reliability based design when it becomes difficult to uphold the safety factor and if the necessary data is available.

For the burst calculations considered performed in this thesis, the API ad hoc had a slightly higher mean for the burst strength compared to Klever-Stewart. Even though it seemed that Klever-Stewart gave a lower probability of failure since it has a more reduced spread. It was seen that for the burst scenario, the Klever-Stewart gave a lower casing grade requirement than API ad-hoc for RBD5. In general, ISO recommends Klever-Stewart and it seems to have advantages compare with API ad-hoc.

## 6 Recommendation for future work

After working with this thesis and doing a comparison of the different methods, I encountered different challenges which brought up ideas for future work regarding reliability based design

One of the challenges during this thesis was how to determine the amount of Monte Carlo simulations necessary. Different literature recommended different numbers of simulations, however I found that the recommend number was so large that each separate simulations took several hours to complete and was not necessary. I therefore chose a smaller number of iterations and when performing several separate Monte Carlo simulations the variations in the failure probability were of such low degree so that it did not affect my choice of casing. Based on this, it would be interesting to see how many Monte Carlo simulations that are necessary before one is able to see a stabilization in the results.

For the collapse simulation, I only looked at the API model. However, it would be interesting to see how different models affects the casing grade selection similar to what was done for the burst strength models. There is a variety of different strength models to choose from, so an extension of this thesis could be to include even more strength models not only for the collapse simulations, but for the burst simulations as well.

As mentioned, one of the limitations of this thesis is that I only looked at the burst and collapse loads and only focusing on the intermediate section. However a casing design have more design criteria's to consider as for example axial loading, kick margins and so on. So another recommendation for future work is to include all the design criteria's in order to do a proper design not only for one section, but for the entire well.

## References

- API. (2005). Specification for Casing and Tubing (Vol. 5TC): American Petroleum Institute.
- API. (2018). Calculating Performance Properties of Pipe Used as Casing or Tubing *API technical report* (7th edition. ed., Vol. 5C3). Washinton, D.C: American Petroleum Institute.
- Belayneh, M. (2018). Advanced Drilling Engineering and Tehcnology, Lecture Note, Chapter 3 Drill String Mechanics, University of Stavanger.
- Bellarby, J. (2009). *Well completion design* Developments in petroleum science, Vol. v. 56.
- Bernsmed, K. (2016, 30.11.2016). Sløyfer og slips i ROS analyser. Retrieved from <https://infosec.sintef.no/informasjonsikkerhet/2016/11/sloyfer-og-slips-i-ros-analyser/>
- Brand, P. R., Whitney, W. S., & Lewis, D. B. (1995). *Load and Resistance Factor Design Case Histories*. Paper presented at the Offshore Technology Conference, Houston, Texas. <https://doi.org/10.4043/7937-MS>
- Bratvold, R. B., Begg, S. H., & Society of Petroleum, E. (2010). *Making good decisions*. Richardson, Tex: Society of Petroleum Engineers.
- Devereux, S. (1998). *Practical well planning and drilling manual* (1st ed ed.). S.l.]: S.l. : PennWell Corporation.
- Drilling Data Handbook, 9th Edition. (2014). *ProtoView*, 1(6-14).
- Fjågesund, T. (2015). Using Schematics for Managing Well Barriers.
- Gouda, M. H., & Aslam, I. (2018). *Well Integrity Life Cycle*. Paper presented at the SPE International Conference and Exhibition on Health, Safety, Security, Environment, and Social Responsibility, Abu Dhabi, UAE. <https://doi.org/10.2118/190504-MS>
- Løvås, G. G. (2013). *Statistikk for universiteter og høgskoler* (3. utg. ed.). Oslo: Universitetsforl.
- Maes, M. A., Gulati, K. C., Brand, P. R., Lewis, D. B., McKenna, D. L., & Johnson, R. C. (1997). Reliability-Based Tubing and Casing Design: Principles and Approach. *Journal of Offshore Mechanics and Arctic Engineering*, 119(4), 257-262. doi:10.1115/1.2829105
- Marx, C., & El-Sayed, A. A. H. (1985). *Evaluation of Collapse Strength of Cemented Pipe-in-Pipe Casing Strings*. Paper presented at the SPE/IADC Drilling Conference, New Orleans, Louisiana. <https://doi.org/10.2118/13432-MS>
- NORSOK. (2013). Well integrity in drilling and well operations (Vol. D-10).
- Paslay, P. R., Cernocky, E. P., & Wink, R. (1998). *Burst Pressure Prediction of Thin-Walled, Ductile Tubulars Subjected to Axial Load*. Paper presented at the SPE Applied Technology Workshop on Risk Based Design of Well Casing and Tubing, The Woodlands, Texas. <https://doi.org/10.2118/48327-MS>
- Statoil. (2010). *Norne Activity Program, Drilling*. Used in the PET505 course, Univeristy of Stavanger 2018
- Suryanarayana, P. V., & Lewis, D. B. (2016). *A Reliability-Based Approach for Survival Design in Deepwater and High Pressure/High Temperature Wells*. Paper presented at the IADC/SPE Drilling Conference and Exhibition, Fort Worth, Texas, USA. <https://doi.org/10.2118/178907-MS>
- Wanke, P. (2008). *The uniform distribution as a first practical approach to new product inventory management* (Vol. 114).
- Williamson, H. S., Sawaryn, S. J., & Morrison, J. W. (2006). Monte Carlo Techniques Applied to Well Forecasting: Some Pitfalls. *SPE Drilling & Completion*, 21(03), 216-227. doi:10.2118/89984-PA
- Aadnøy, B. S. (2010). *Modern well design* (2nd ed. ed.). Boca Raton: CRC Press/Balkema.
- Aadnøy, B. S., Cooper, I., Miska, S. Z., Mitchell, R. F., Payne, M. L., & Society of Petroleum, E. (2009). *Advanced drilling and well technology*. Richardson, Tex: Society of Petroleum Engineers.
- Aarnes, H. (2014). Statistiske sannsynlighetsfordelinger. Retrieved from <https://www.mn.uio.no/ibv/tjenester/kunnskap/plantefys/tall/statfordeling.pdf>



# A Appendix

## A.1 Monte Carlo Simulation MATLAB codes

### A.1.1 Comparison of burst strength models

```
clear
clc
close all

%Chosen the OD = 13 3/8", t = 0.430", P110

yield1 = 110000; %Yield strength, psi
ultimategyield1 = 120000; %Ultimate yield strength, psi
OD1 = 13.375; %Outer diameter, inch
t1 = 0.430; %Thickness, inch
N = 1000000; %Number of Monte Carlo simulations
n=0.08; %n value for P110 grade
Kdr = ((1/2)^(n+1)+(1/(3^(1/2)))^(n+1));

%% API Classic model, no distribution
tol = 0.875;

Pburst1 = ((2*yield1*t1)/OD1)*tol/14.5; %Answer in bar

%% API Classic model, with distribution
for j=1:N

    OD(1,j) = OD1*normrnd((1.0059),(1.0059*0.00181));
    t(1,j) = t1*normrnd((1.0069),(1.0069*0.0259));
    yield(1,j) = yield1*normrnd((1.10),(1.1*0.0464));

Pburst2(1,j) = ((2*yield(1,j)*t(1,j))/OD(1,j))*tol/14.5 * normrnd(1.08,0.05);
%Answer in bar

end

%% API ad-hoc
for j=1:N

    OD(1,j) = OD1*normrnd((1.0059),(1.0059*0.00181));
    t(1,j) = t1*normrnd((1.0069),(1.0069*0.0259));
    ultimategyield(1,j) = ultimategyield1*normrnd((1.10),(1.1*0.0464));

Pburst3(1,j) = (2*ultimategyield(1,j)*t(1,j))/OD(1,j)/14.5 *
normrnd(1.08,0.05); %Answer in bar
end

%% Klever-Stewart
for j=1:N

    OD(1,j) = OD1*normrnd((1.0059),(1.0059*0.00181));
    t(1,j) = t1*normrnd((1.0069),(1.0069*0.0259));
    ultimategyield(1,j) = ultimategyield1*normrnd((1.10),(1.1*0.0464));

Pburst4(1,j) = (2*Kdr*ultimategyield(1,j)*t(1,j))/(OD(1,j)-t(1,j))/14.5 *
normrnd(1,0.023); %Answer in bar
End
```

```

%% PLOT
    s = 20;

[a1,b1]=hist(Pburst1,s);
[a2,b2]=hist(Pburst2,s);
[a3,b3]=hist(Pburst3,s);
[a4,b4]=hist(Pburst4,s);
b1(:)=Pburst1;

figure(1)
plot(b1,a2/N,b2,a2/N,b3,a3/N,b4,a4/N)

legend('API classic','API classic with distribution','API ad-hoc','Klever-
Stewart')
xlabel('Pressure in bar')
ylabel('PDF')

%% Statistics
mean1 = mean(Pburst1);
mean2 = mean(Pburst2(1,:));
mean3 = mean(Pburst3(1,:));
mean4 = mean(Pburst4(1,:));

std1 = std(Pburst1);
std2 = std(Pburst2(1,:));
std3 = std(Pburst3(1,:));
std4 = std(Pburst4(1,:));

p50_1=median(Pburst1);
p10_1=prctile(Pburst1,10);
p90_1=prctile(Pburst1,90);

p50_2=median(Pburst2);
p10_2=prctile(Pburst2,10);
p90_2=prctile(Pburst2,90);

p50_3=median(Pburst3);
p10_3=prctile(Pburst3,10);
p90_3=prctile(Pburst3,90);

p50_4=median(Pburst4);
p10_4=prctile(Pburst4,10);
p90_4=prctile(Pburst4,90);

strenghtmodel = {'API Classic';'API classic with distribution';'API ad-
hoc';'Klever-Stewart'};

mean = [mean1;mean2;mean3;mean4];
std = [std1;std2;std3;std4];
P50 = [p50_1;p50_2;p50_3;p50_4];
P10 = [p10_1;p10_2;p10_3;p10_4];
P90 = [p90_1;p90_2;p90_3;p90_4];
T = table(mean,std,P50,P10,P90,'RowNames',strenghtmodel)

```

## A.1.2 API ad-hoc burst level 4

```
clc
clear
close all
N = 1000000; % Number of Monte Carlo Simulations

%Chosen the OD = 13 3/8", t = 0.580", N80

welldepth = 4500; %Planned TD of next section to be drilled relative RKB,m
seawaterdepth = 400; %m
pp = 1.5; % Assume most likely value of pore pressure, sg
sigmatensile1 = 100000; %minimum ultimate tensile strength from DDH, psi
OD1 = 13.375; %outside diameter, inch
t1 = 0.580; %thickness, inch
sigamean = 1.21; %For grade N80 from API 5C3, table F.4
sigmaCOV = 0.0511; %For grade N80 from API 5C3, table F.4

psurf=zeros(1,N);
pburststrength = zeros(1,N);

counter=0;

for j = 1:N % Start of Monte Carlo loop

    ppore = pp;
    gasdensity = 0.3 ; %Assumed gas density

    sigmatensile(1,j) = sigmatensile1*normrnd(sigamean,(sigamean*sigmaCOV));

    OD(1,j) = OD1*normrnd(1.0059,(1.0059*0.00181));
    %Distribution of outer diameter, mean and COV from API 53C table F.4
    t(1,j) = t1*normrnd(1.0069,(1.0069*0.0259));
    %Distribution of wall thickness, mean and COV from API 53C table F.4

    psurf(1,j)=ppore*welldepth*0.0981-0.0981*(welldepth-
seawaterdepth)*gasdensity;
    psurf(1,j)=psurf(1,j)-0.0981*1.03*seawaterdepth;
    %Returns load calculations in bar

    pburststrength(1,j)=(2*sigmatensile(1,j)*t(1,j))/OD(1,j)*normrnd(1.08,0.050)/1
4.5;
    %Returns strength calculations in bar
    %Mean and COV from API 5C3 table B.5

    % here we count number of times the strength pressure is exceeded
    if(psurf(1,j)>pburststrength(1,j))
        counter=counter+1;
    end

end % End of MonteCarlo loop

prob=counter/N*100 % percentage for having load > strength

% Plot probability density functions

e=min(pburststrength(1,:));
f=max(pburststrength(1,:));
s=[e:1:f];
[c,d]=hist(pburststrength(1,:),s);
```

```

h=min(psurf(1,:));
f=max(psurf(1,:));
w=[h:0.5:f];

[a,b]=hist(psurf(1,:),w);

plot(b,a/N,d,c/N);
legend('Load','Strength')
xlabel('Pressure (bar)')
ylabel('PDF')

%% Table of properties
Burst_load = psurf(1);
Burst_strength_mean = mean(pburststrength(1,:));
Burst_strength_stdv = std(pburststrength(1,:));
P10 = prctile(pburststrength(1,:),10);
P90 = prctile(pburststrength(1,:),90);
Probability_of_failure = prob;

T =
table(Burst_load,Burst_strength_mean,Burst_strength_stdv,P10,P90,Probability_o
f_failure)

```

### A.1.3 API ad-hoc burst level 5

```
clc
clear
close all
N = 1000000; % Number of Montecarlo Simulations

% 13 3/8", t = 0.580" L80

welldepth = 4500; %Planned TD of next section to be drilled relative RKB,m
seawaterdepth = 400; %m
pp = 1.5; % Assume most likely value of pore pressure, sg
deltappore = 0.05; % Uncertainty band to be used in Triangle distribtion
sigmatensile1 = 95000; %minimum ultimate tensile strength from DDH, psi
OD1 = 13.375; %outside diameter, inch
t1 = 0.580; %thickness, inch
sigamean = 1.1; %For grade L80 from API 5C3, table F.4
sigmaCOV = 0.0529; %For grade L80 from API 5C3, table F.4

psurf=zeros(1,N);
pburststrength = zeros(1,N);

counter=0;

for j = 1:N % Start of MonteCarlo loop

    ppore(1,j)=trianglerand(pp-0.05,pp-0.03,pp,1); %WCS, porepressure = 1.5 s.g
    %Triangular distribution in pore pressure
    gasdensity(1,j) = trianglerand(0.3,0.4,0.5,1); %WCS, gasdensity = 0.3 s.g
    %Triangular distriubtion in gas density

    sigmatensile(1,j) = sigmatensile1*normrnd(sigamean,(sigamean*sigmaCOV));

    OD(1,j) = OD1*normrnd(1.0059,(1.0059*0.00181));
    %Distribution of outer diameter, mean and COV from API 53C table F.4
    t(1,j) = t1*normrnd(1.0069,(1.0069*0.0259));
    %Distribution of wall thickness, mean and COV from API 53C table F.4

    psurf(1,j)=ppore(1,j)*welldepth*0.0981-0.0981*(welldepth-
seawaterdepth)*gasdensity(1,j);
    psurf(1,j)=psurf(1,j)-0.0981*1.03*seawaterdepth;
    %Returns load calculations in bar

    pburststrength(1,j)=(2*sigmatensile(1,j)*t(1,j))/OD(1,j)*normrnd(1.092,0.052)/
14.5;
    %Returns strength calculations in bar
    %Mean and COV from API 5C3 table B.5

    % here we count number of times the strength pressure is exceeded
    if(psurf(1,j)>pburststrength(1,j))
        counter=counter+1;
    end

end % End of MonteCarlo loop

prob=counter/N*100; % percentage for having load pressure > strength

% Plot probability density functions
e=min(pburststrength(1,:));
f=max(pburststrength(1,:));
s=[e:1:f];
[c,d]=hist(pburststrength(1,:),s);
```

```

h=min(psurf(1,:));
f=max(psurf(1,:));
w=[h:1:f];

[a,b]=hist(psurf(1,:),w);

plot(b,a/N,d,c/N);
legend('Load','Strength')
xlabel('Pressure (bar)')
ylabel('PDF')

%% Table of properties
mean = [mean(psurf(1,:));mean(pburststrength(1,:))];
stdv = [std(psurf(1,:));std(pburststrength(1,:))];
P10 = [prctile(psurf(1,:),10);prctile(pburststrength(1,:),10)];
P90 = [prctile(psurf(1,:),90);prctile(pburststrength(1,:),90)];
Probability_of_failure =[prob ; prob]

burst = {'Burst load';'Burst strength'};

T = table(mean,stdv,P10,P90,Probability_of_failure,'RowNames',burst)

```

## A.1.4 Klever-Stewart burst level 4

```
clc
clear
close all
N = 1000000; % Number of Montecarlosimulations

% 13 3/8", t = 0.580", N80
welldepth = 4500; %Planned TD of next section to be drilled relative RKB,m
seawaterdepth = 400; %m
pp = 1.5 % Assume most likely value of pore pressure, sg
sigmatensile1 = 100000; %minimum ultimate tensile strength from DDH, psi
OD1 = 13.375; %outside diameter, inch
t1 = 0.580; %thickness, inch
sigmamean = 1.21; %For grade N80 from API 5C3, table F.4
sigmaCOV = 0.0511; %For grade N80 from API 5C3, table F.4

psurf=zeros(1,N);
pburststrength = zeros(1,N);

n = 0.104 %n value for grade of casing N80

counter=0;

for j = 1:N % Start of MonteCarlo loop

    ppore = pp;
    gasdensity = 0.3 ; %Assumed gas density

    sigmatensile(1,j) = sigmatensile1*normrnd(sigmamean,(sigmamean*sigmaCOV));
    %Distribution of ultimate strength, mean and COV from API 53C table F.3
    OD(1,j) = OD1*normrnd(1.0059,(1.0059*0.00181));
    %Distribution of outer diameter, mean and COV from API 53C table F.4
    t(1,j) = t1*normrnd(1.0069,(1.0069*0.0259));
    %Distribution of wall thickness, mean and COV from API 53C table F.4

    Kdr = ((1/2)^(n+1)+(1/(3^(1/2)))^(n+1));

    psurf(1,j)=ppore*welldepth*0.0981-0.0981*(welldepth-
seawaterdepth)*gasdensity;
    psurf(1,j)=psurf(1,j)-0.0981*1.03*seawaterdepth;
    %Returns load calculations in bar
    pburststrength(1,j)=(2*Kdr*sigmatensile(1,j)*t(1,j))/(OD(1,j)-
t(1,j))/14.5*normrnd(1,(1*0.023)); % In psi
    %Returns strength calculations in bar
    %Mean and COV from API 5C3 table B.5

    % here we count number of times the strength pressure is exceeded
    if(psurf(1,j)>pburststrength(1,j))
        counter=counter+1;
    end
end % End of MonteCarlo loop

prob=counter/N*100 % percentage for having load pressure > strength
```

```

% Plot probability density functions
e=min(pburststrength(1,:));
f=max(pburststrength(1,:));
s=[e:1:f];
[c,d]=hist(pburststrength(1,:),s);

h=min(psurf(1,:));
f=max(psurf(1,:));
w=[h:1:f];

[a,b]=hist(psurf(1,:),w);

figure(1)
plot(b,a/N,d,c/N);
legend('Load','Strength')
xlabel('Pressure (bar)')
ylabel('PDF')

%% Table of properties
Burst_load = psurf(1);
Burst_strength_mean = mean(pburststrength(1,:))
Burst_strength_stdv = std(pburststrength(1,:))
P10 = prctile(pburststrength(1,:),10)
P90 = prctile(pburststrength(1,:),90)
Probability_of_failure = prob

T =
table(Burst_load,Burst_strength_mean,Burst_strength_stdv,P10,P90,Probability_o
f_failure)

```



## A.1.5 Klever-Stewart burst level 5

```
clc
clear
close all
N = 1000000; % Number of Monte Carlo Simulations

% K55, 13 3/8", t = 0.580"

welldepth = 4500; %Planned TD of next section to be drilled relative RKB,m
seawaterdepth = 400; %m
pp = 1.5 % Assume most likely value of pore pressure, sg
OD1 = 13.375; %outside diameter, inch
t1 = 0.580; %thickness, inch

psurf=zeros(1,N);
pburststrength = zeros(1,N);

sigmatensile1 = 95000; %minimum ultimate tensile strength from DDH, psi
n = 0.125 %n value for grade of casing K55

sigmamean = 1.23; %K55
sigmaCOV = 0.0729; %K55
sigmastdv = sigmamean*sigmaCOV;
%mean and COV from API 53C table F.3

counter=0;

for j = 1:N % Start of Monte Carlo loop

    ppore(1,j)=trianglerand(pp-0.05,pp-0.03,pp,1);
    %Triangle distribution of pore pressure
    gasdensity(1,j) = trianglerand(0.3,0.4,0.5,1);
    %Triangle distribution of gas density

    sigmatensile(1,j) = sigmatensile1*normrnd(sigmamean,sigmastdv);
    %Distribution of ultimate strength
    OD(1,j) = OD1*normrnd(1.0059,(1.0059*0.00181));
    %Distribution of outer diameter, mean and COV from API 53C table F.4
    t(1,j) = t1*normrnd(1.0069,(1.0069*0.0259));
    %Distribution of wall thickness, mean and COV from API 53C table F.4

    Kdr = ((1/2)^(n+1)+(1/(3^(1/2)))^(n+1));

    psurf(1,j)=ppore(1,j)*welldepth*0.0981-0.0981*(welldepth-
seawaterdepth)*gasdensity(1,j);
    psurf(1,j)=psurf(1,j)-0.0981*1.03*seawaterdepth;
    %Returns load calculations in bar
    pburststrength(1,j)=(2*Kdr*sigmatensile(1,j)*t(1,j))/((OD(1,j)-
t(1,j))/14.5*normrnd(1,(1*0.023))); % In psi
    %Returns strength calculations in bar
    %Mean and COV from API 5C3 table B.5

% here we count number of times the strength pressure is exceeded
if(psurf(1,j)>pburststrength(1,j))
    counter=counter+1;
end
```

```

end % End of MonteCarlo loop

prob=counter/N*100 % percentage for having load pressure > strength

% Plot probability density functions
e=min(pburststrength(1,:));
f=max(pburststrength(1,:));
s=[e:1:f];
[c,d]=hist(pburststrength(1,:),s);

h=min(psurf(1,:));
f=max(psurf(1,:));
w=[h:1:f];

[a,b]=hist(psurf(1,:),w);

figure(1)
plot(b,a/N,d,c/N);
legend('Load','Strength')
xlabel('Pressure (bar)')
ylabel('PDF')

%% Table of properties
mean = [mean(psurf(1,:));mean(pburststrength(1,:))];
stdv = [std(psurf(1,:));std(pburststrength(1,:))];
P10 = [prctile(psurf(1,:),10);prctile(pburststrength(1,:),10)];
P90 = [prctile(psurf(1,:),90);prctile(pburststrength(1,:),90)];
Probability_of_failure = [prob;prob];
burst = {'Burst load';'Burst strength'};

T = table(mean,stdv,P10,P90,Probability_of_failure,'RowNames',burst)

```

## A.1.6 API collapse level 4

```
clear
clc
close all
%Collapse strength

%Input data
yield0 = 55000; %Minimum yield strength, psi
OD0 = 13.375; %outside diameter, inch
t0 = 0.580; %thickness, inch
welldepth = 4500; %Planned TD of next section to be drilled relative RKB, m
seawaterdepth = 400; %m,
pp = 1.45; % Assume most likely value of pore pressure, sg
casingdepth = 2600; %m
seawaterlevel = 25; %m
mud_density = 1.7; %sg
seawater_density = 1.03; %sg
area = 23.31; %cross sectional area, in^2
weight = 80.7; %weight of string, lbs/ft
N = 100000 %Number of MCS

psurf=zeros(1,N);
collapsestrength = zeros(1,N);

tensile_load = weight*casingdepth*3.28/8.05*((1-mud_density)/7.8);
%Calculation of tension load including buoyancy
axialstress = tensile_load/area;
%Calculation of axial stress

counter = 0;

for j = 1:N

    yield(1,j) = yield0 * normrnd(1.10,(1.1*0.0464));
    %Distribution of ultimate strength, mean and COV from API 53C table F.3
    OD(1,j) = OD0*normrnd(1.0059,(1.0059*0.00181));
    %Distribution of outer diameter, mean and COV from API 53C table F.4
    t(1,j) = t0*normrnd(1.0069,(1.0069*0.0259));
    %Distribution of wall thickness, mean and COV from API 53C table F.4

    h = casingdepth - (seawater_density/mud_density)*(casingdepth-seawaterlevel);
    psurf(1,j) = 0.0981*mud_density*h - 0;
    %Load calculations in bar

    yield_a(1,j) = ((1-(3/4)*(axialstress/yield(1,j))^2)^(1/2)-
(1/2)*(axialstress/yield(1,j)))*yield(1,j);
%Biaxial correction
```

```

%Calculation of empirical constants, p36 in API 5C3
A(1,j) = 2.8762 + 0.10679*10^(-5)*yield_a(1,j) + 0.21301*10^(-
10)*yield_a(1,j)^2 - 0.53132*10^(-16)*yield_a(1,j)^3;
B(1,j) = 0.026233 + 0.50609*10^(-6)*yield_a(1,j);
C(1,j) = -465.93 + 0.030867*yield_a(1,j) - 0.10483*10^(-7)*yield_a(1,j)^2 +
0.36989*10^(-13)*yield_a(1,j)^3;
F(1,j) =
46.95*10^(6)*((3*B(1,j)/A(1,j))/(2+B(1,j)/A(1,j)))^3/(yield_a(1,j)*((3*B(1,j)/
A(1,j))/(2+B(1,j)/A(1,j))-B(1,j)/A(1,j))*(1-
(3*B(1,j)/A(1,j))/(2+B(1,j)/A(1,j)))^2);
G(1,j) = F(1,j)*B(1,j)/A(1,j);

%If statement for different regions of collapse and calculation of collapse
%pressure
if (OD(1,j)/t(1,j)) < ((A(1,j)-
2)^2+8*(B(1,j)+C(1,j)/yield_a(1,j)))^(1/2)+(A(1,j)-
2)/(2*(B(1,j)+C(1,j)/yield_a(1,j)));
    collapsestrength(1,j) = (2*yield_a(1,j)*((OD(1,j)/t(1,j))-
1)/(OD(1,j)/t(1,j))^2)*normrnd(1.108,1.108*0.008)/14.5;
elseif (OD(1,j)/t(1,j)) < (yield_a(1,j)*(A(1,j)-
F(1,j)))/(C(1,j)+yield_a(1,j)*(B(1,j)-G(1,j)));
    collapsestrength(1,j) = (yield_a(1,j) * (A(1,j)/(OD(1,j)/t(1,j))-B(1,j))-
C(1,j))*normrnd(1.108,1.108*0.008)/14.5;
elseif (OD(1,j)/t(1,j)) < (2+B(1,j)/A(1,j))/(3*(B(1,j)/A(1,j)));
    collapsestrength(1,j) = (yield_a(1,j)*(F(1,j)/(OD(1,j)/t(1,j))-
G(1,j)))*normrnd(1.108,1.108*0.008)/14.5;
else
    collapsestrength(1,j) = (46.95*10^6 /((OD(1,j)/t(1,j))*((OD(1,j)/t(1,j))-
1)^2 ))/14.5*normrnd(1.108,1.108*0.008)/14.5;
end
% here we count number of times the strength pressure is exceeded
if(psurf(1,j)>collapsestrength(1,j))
    counter=counter+1;
end

end
%%
prob=counter/N*100 % percentage for having load pressure > strength

e=min(collapsestrength(1,:));
f=max(collapsestrength(1,:));
s=[e:1:f];
[c,d]=hist(collapsestrength(1,:),s);

h=min(psurf(1,:));
f=max(psurf(1,:));
w=[h:1:f];

[a,b]=hist(psurf(1,:),w);

figure(1)
plot(b,a/N,d,c/N);
legend('Load','Strength')
xlabel('Pressure (bar)')
ylabel('PDF')

```

```
%% Table of properties
Collapse_load = psurf(1);
Collapse_strength_mean = mean(collapsestrength(1,:))
Collapse_strength_stdv = std(collapsestrength(1,:))
P10 = prctile(collapsestrength(1,:),10)
P90 = prctile(collapsestrength(1,:),90)
Probability_of_failure = prob

T =
table(Collapse_load,Collapse_strength_mean,Collapse_strength_stdv,P10,P90,Probability_of_failure)
```

## A.1.7 API collapse level 5

```
clear
clc
close all
%Collapse strength

%Input data
yield0 = 55000; %Minimum yield strength
OD0 = 13.375; %outside diameter, inch
t0 = 0.580; %thickness, inch

welldepth = 4500; %Planned TD of next section to be drilled relative RKB, m
seawaterdepth = 400; %m,
pp = 1.45 % Assume most likely value of pore pressure
casingdepth = 2600; %m
seawaterlevel = 25; %m
seawater_density = 1.03;%sg
mud_density0 = 1.7; %sg
area = 23.31; %cross-sectional area, in^2
weight = 80.7; % weight of string, lbs/ft
N = 1000000 %Number of MCS

psurf=zeros(1,N);
collapsestrength = zeros(1,N);

counter = 0;

for j = 1:N
    yield(1,j)= yield0 * normrnd(1.10,(1.1*0.0464));
    %Distribution of ultimate strength, mean and COV from API 53C table F.3
    OD(1,j) = OD0*normrnd(1.0059,(1.0059*0.00181));
    %Distribution of outer diameter, mean and COV from API 53C table F.4

    t(1,j) = t0*normrnd(1.0069,(1.0069*0.0259));
    %Distribution of wall thickness, mean and COV from API 53C table F.4

    mud_density(1,j) = trianglerand(mud_density0-
0.2,mud_density0,mud_density0+0.2,1);
    %seawater_density(1,j) = trianglerand(1.03,1.2,1.4,1);

    tensile_load(1,j)=weight*casingdepth*3.28/8.05*((1-mud_density(1,j))/7.8);
    %Calculation of tension load including buoyancy

    axialstress(1,j) = tensile_load(1,j)/area;
    %Calculation of axial stress

    yield_a(1,j) = ((1-(3/4)*(axialstress(1,j)/yield(1,j))^2)^(1/2)-
(1/2)*(axialstress(1,j)/yield(1,j)))*yield(1,j);
    %Biaxial correction

    h(1,j) = casingdepth - (seawater_density/mud_density(1,j)*(casingdepth-
seawaterlevel));
```

```

h(1,j) = h(1,j) * trianglerand(0,0.5,1,1); %Uncertainty of the severity of
the mudloss.
%Most likely amount of mudloss set to 50 %

psurf(1,j) = 0.0981*mud_density(1,j)*h(1,j)-0;
%Load calculations in bar

%Calculation of empirical constants, p36 in API 5C3
A(1,j) = 2.8762 + 0.10679*10^(-5)*yield_a(1,j) + 0.21301*10^(-
10)*yield_a(1,j)^2 - 0.53132*10^(-16)*yield_a(1,j)^3;
B(1,j) = 0.026233 + 0.50609*10^(-6)*yield_a(1,j);
C(1,j) = -465.93 + 0.030867*yield_a(1,j) - 0.10483*10^(-7)*yield_a(1,j)^2 +
0.36989*10^(-13)*yield_a(1,j)^3;
F(1,j) =
46.95*10^(6)*((3*B(1,j)/A(1,j))/(2+B(1,j)/A(1,j)))^3/(yield_a(1,j)*((3*B(1,j)/
A(1,j))/(2+B(1,j)/A(1,j))-B(1,j)/A(1,j))*(1-
(3*B(1,j)/A(1,j))/(2+B(1,j)/A(1,j)))^2);
G(1,j) = F(1,j)*B(1,j)/A(1,j);

%If statement for different regions of collapse and calculation of collapse
%pressure
if (OD(1,j)/t(1,j)) < ((A(1,j)-
2)^2+8*(B(1,j)+C(1,j)/yield_a(1,j)))^(1/2)+(A(1,j)-
2)/(2*(B(1,j)+C(1,j)/yield_a(1,j)));
collapsestrength(1,j) = (2*yield_a(1,j)*((OD(1,j)/t(1,j))-
1)/(OD(1,j)/t(1,j))^2)*normrnd(1.108,1.108*0.008)/14.5;
elseif (OD(1,j)/t(1,j)) < (yield_a(1,j)*(A(1,j)-
F(1,j)))/(C(1,j)+yield_a(1,j)*(B(1,j)-G(1,j)));
collapsestrength(1,j) = (yield_a(1,j) * (A(1,j)/(OD(1,j)/t(1,j))-B(1,j))-
C(1,j))*normrnd(1.108,1.108*0.008)/14.5;
elseif (OD(1,j)/t(1,j)) < (2+B(1,j)/A(1,j))/(3*(B(1,j)/A(1,j)));
collapsestrength(1,j) = (yield_a(1,j)*(F(1,j)/(OD(1,j)/t(1,j))-
G(1,j)))*normrnd(1.108,1.108*0.008)/14.5;
else
collapsestrength(1,j) = (46.95*10^6 /((OD(1,j)/t(1,j))*((OD(1,j)/t(1,j))-
1)^2 ))*normrnd(1.108,1.108*0.008)/14.5;
end

% here we count number of times the strength pressure is exceeded
if(psurf(1,j)>collapsestrength(1,j))
counter=counter+1;
end
end
%%
prob=counter/N*100; % percentage for having load pressure > strength

e=min(collapsestrength(1,:));
f=max(collapsestrength(1,:));
s=[e:1:f];
[c,d]=hist(collapsestrength(1,:),s);

h1=min(psurf(1,:));
f=max(psurf(1,:));
w=[h1:1:f];

```

```

[a,b]=hist(psurf(1,:),w);

figure(1)
plot(b,a/N,d,c/N);
legend('Load','Strength')
xlabel('Pressure (bar)')
ylabel('PDF')

%% Table of properties
mean = [mean(psurf(1,:));mean(collapsestrength(1,:))];
stdv = [std(psurf(1,:));std(collapsestrength(1,:))];
P10 = [prctile(psurf(1,:),10);prctile(collapsestrength(1,:),10)];
P90 = [prctile(psurf(1,:),90);prctile(collapsestrength(1,:),90)];
Probability_of_failure = [prob;prob];
collapse = {'Collapse load';'Collapse strength'};

T = table(mean,stdv,P10,P90,Probability_of_failure,'RowNames',collapse)

```



## A.2 Overview of parameters

Parameter	Ad-hoc Barlow	Ad-hoc Mises	Klevertewart	Paslay	Moore	Nadai
Means of mean	1.08	1.04	1.00	1.02	1.04	1.05
Stdev of means	0.050	0.015	0.023	0.047	0.039	0.063
COV of means	4.6%	1.5%	2.3%	4.6%	3.8%	5.9%

Table A.2.1 Burst strength model error (Table B.5 in API 5C3)

Grade	Elastic Collapse (D/t)	Transitional Collapse (D/t)	Plastic Collapse (D/t)	Yield Collapse (D/t)
K55	> 37.21	25.01 – 37.21	14.81 – 25.01	< 14.81
L80/N80	> 31.02	22.47 – 31.02	13.38 – 22.47	< 13.38
C90	> 29.18	21.69 – 29.18	13.01 – 21.69	< 13.01
T95,	> 28.36	21.33 – 28.36	12.85 – 21.33	< 12.85
P110	> 26.22	20.41 – 26.22	12.44 – 20.41	< 12.44
Q125	> 24.46	19.63 – 24.46	12.11 – 19.63	< 12.11

Table A.2.2 Determination of collapse modes (API, 2018)

Grade	A	B	C	F	G
K55	2.991	0.0541	1206	1.989	0.0360
L80/N80	3.071	0.0667	1955	1.998	0.0434
C90	3.106	0.0718	2254	2.017	0.0466
T95	3.124	0.0743	2404	2.029	0.0482
P110	3.181	0.0819	2852	2.066	0.0532
Q125	3.239	0.0895	3301	2.106	0.0582

Table A.2.3 API collapse parameters from API 5C3